SIMULTANEOUS REMOVAL OF ANTIBIOTIC AND ANTIBIOTIC RESISTANT BACTERIA BY NANOMATERIAL

By

Akser Alam Siddiqua Maya

ID-20MSCHEM015F

A thesis submitted in partial fulfillment of the requirements for the degree of

MASTER of SCIENCE in Chemistry

Department of Chemistry

CHITTAGONG UNIVERSITY OF ENGINEERING AND TECHNOLOGY

DECEMBER 2024

Declaration

I hereby declare that the work contained in this thesis has not been previously submitted to meet the requirements for an award at this or any other higher education institution. To the best of my knowledge and belief, the Thesis contains no material previously published or written by another person except where due reference is cited. Furthermore, the Thesis complies with the PLAGIARISM and ACADEMIC INTEGRITY regulations of CUET.

Akser Alam Siddiqua Maya

Student ID - 20MSCHEM015F

Department of Chemistry

Chittagong University of Engineering & Technology (CUET)

Dedication

To my beloved parents, siblings, teachers, and supportive life partner, and countless others who've contributed to my journey, whether through a kind word, a helping hand, or a moment of inspiration.

List of Publications

Journal Articles

- "A novel interpretable machine learning and metaheuristic-based protocol to predict and optimize ciprofloxacin antibiotic adsorption with nano-adsorbent" Yunus Ahmed, **Akser Alam Siddiqua Maya**, Parul Akhtar, Md Shafiul Alam, Hamad AlMohamadi, Md Nurul Islam, Obaid A. Alharbi, Syed Masiur Rahman, Journal of Environmental Management **(IF: 8.0, Q1)**. DOI: https://doi.org/10.1016/j.jenvman.2024.122614.
- "Advancements and Challenges in Fenton-Based Advanced Oxidation Processes for Antibiotic Removal in Wastewater: From the Laboratory to Practical Applications", Yunus Ahmed, **Akser Alam Siddiqua Maya**, Parul Akhtar, Hamad AlMohamadi, Abdul Wahab Mohammad, S.M. Ashekuzzaman, Agnieszka I. Olbert, Md Galal Uddin, Journal of Environmental Chemical Engineering (Under revision)
- "Degradation Efficiency of Antibiotics in Wastewater by Heterogeneous Fenton-Based Advanced Oxidation Processes: A Study of Morphological Changes of $FeWO_4$ Nanomaterials" **Akser Alam Siddiqua Maya**, Parul Akhtar, Md. Arif Hossen, Md Jahangir Alam, Hamad AlMohamadi, S.M. Ashekuzzaman, Yunus Ahmed, Journal of Environmental Chemical Engineering (Submitted)

Conferences

- "Bangladesh's Strategy for Combating Next Pandemic: Antibiotic Resistance." Yunus Ahmed, **Akser Alam Siddiqua Maya**, Md Mahfujur Rahman, Md Mahbubur Rahman, and Md Jahangir Alam. ICEPSD 2022, 02-04 September 2022.
- "Antibiotic-Resistant Bacteria and its Genes in Urban Water: Making the Invisible Visible." **Akser Alam Siddiqua Maya,** Md. Mahfujur Rahman, Yunus Ahmed. BCSIR Congress 2022, BCSIR, 01-03 December 2022.
- "Synthesis, characterization, and optimization of $FeWO_4@TiO_2$, an efficient nanocatalyst for the degradation of antibiotic and textile dye in neutral solution." **Akser Alam Siddiqua Maya**, Keya Dutta, Md. Mahfujur Rahman, Tahmina Akter and Yunus Ahmed. 7th ICNST, Asian University for Women, 02-03 March 2023.
- "Synthesis, Characterization, Optimization, and Application of $CuWO_4@TiO_2$ Nanoadsorbent for the Removal of Antibiotic from Aqueous Solution." Yunus Ahmed, Md. Mahfujur Rahman, **Akser Alam Siddiqua Maya**, Tahmina Akter, Keya Rani Dutta, Obaide Alharbi. 19th IWA-LET, Essen, Germany, 24-28 June 2024.
- "Efficiency of Antibiotic Degradation in Wastewater: A Study on Different Shapes of $FeWO_4$ Nanomaterials in Fenton Processes." **Akser Alam Siddiqua Maya**, Parul Akhtar, Obaid A. Alharbi, Hamad AlMohamadi, Yunus Ahmed. NANO 2024, Khalifa University, Abu Dhabi, 3-8 November 2024.

Approval/Declaration by the Supervisor(s)

This is to certify that **Akser Alam Siddiqua Maya** has carried out this research work under our supervision and that she has fulfilled the relevant Academic Ordinance of the Chittagong University of Engineering and Technology, so that she is qualified to submit the following Thesis in the application for the degree of MASTER of SCIENCE in Chemistry. Furthermore, the Thesis complies with the PLAGIARISM and ACADEMIC INTEGRITY regulations of CUET.

Dr. Yunus Ahmed (Supervisor)

Associate Professor

Department of Chemistry

Chittagong University of Engineering & Technology

Dr. Saiful Islam (Co-supervisor)

Principle Scientific Officer

Industrial Microbiology and Research Division

Bangladesh Council of Scientific and Industrial Research, Chattogram.

Acknowledgment

All praise to Merciful and Almighty Allah (SWT), who gave me the capability and opportunity to successfully complete the research and submit this thesis for the degree of Master of Science (M.Sc.) in Chemistry.

I am proud to express my heartfelt gratitude, wholehearted indebtedness, sincere appreciation, and profound regard to my honourable teacher and principal supervisor, **Dr. Yunus Ahmed**, Associate Professor, Department of Chemistry, CUET, Chattogram, for his academic guidance, constant untiring supervision, cordial support, endless encouragement, precious advice, guidance, enthusiasm, and helpful discussion throughout the entire period of research work and preparation of this thesis. This achievement would not be possible without his unquenched thrust of research, academic supervision, continuous encouragement, and constructive suggestions.

I want to thank my co-supervisor, Dr. Saiful Islam, Principle Scientific Officer, IMRD, BCSIR, Chattogram, for allowing me to work in the BCSIR microbiology lab and guiding and mentoring me in my research.

I would also like to thank the teachers and staff at CUET's Department of Chemistry for their collaboration, continual inspiration, and encouragement.

I am also grateful to my friends in the Chemistry department, CUET, for their valuable discussion and cooperation, especially **Md. Mahfujur Rahman**, Keya Rani Dutta, Tahmina Akter and Syed Julkar Nine. I am also glad to offer my heartfelt gratitude and appreciation to Jannatul Ferdous, Research Fellow, IMRD, BCSIR, Chattogram, who has provided excellent assistance and attention during my research, and all of my seniors and juniors who helped me with my research at the BCSIR microbiology lab.

I am expressing my heartfelt gratitude to my parents, **Syed Bahadur Alam Siddiqui** and **Mahabuba Alam**; my siblings, **Rokser Alam** and **Arman Alam**; and my beloved husband, **Rabiul Hosen Chowdhury**, for their unwavering support, encouragement, and sacrifices during the tenure of this work.

The author acknowledges funding from BENBAIS ET-20221947 and CUET DRE project-CUET/DRE/2022-23/Chem/021.

CERTIFICATION

The thesis titled **"SIMULTANEOUS REMOVAL OF ANTIBIOTIC AND ANTIBIOTIC RESISTANT BACTERIA BY NANOMATERIAL"** submitted by **Akser Alam Siddiqua Maya** (Student ID: **20MSCHEM015F** of Session: 2020-2021) has been accepted as satisfactory in partial fulfillment of the requirement for the degree of **Master of Science in Chemistry** on 1st December, 2024.

BOARD OF EXAMINERS

1. 1/12/24
Dr. Yunus Ahmed — Chairman (Supervisor)
Associate Professor, Department of Chemistry
Chittagong University of Engineering &Technology
Chattogram-4349.

2. 01.12.24
Dr. Saiful Islam — Member (Co-Supervisor)
Principle Scientific Officer, IMRD
Bangladesh Council of Scientific and Industrial
Research (BCSIR), Chattogram-4220, Bangladesh.

3. 01.12.24
Dr. Mst. Roksana Khatun — Member (Ex-Officio)
Professor & Head, Department of Chemistry
Chittagong University of Engineering &Technology
Chattogram-4349, Bangladesh.

4. 01.12.24
Dr. Md. Rezaul Karim — Member
Professor, Department of Chemistry
Chittagong University of Engineering &Technology
Chattogram-4349, Bangladesh.

5. 01.12.24
Dr. Arup Kumer Roy — Member
Associate Professor, Department of Chemistry
Chittagong University of Engineering &Technology
Chattogram-4349, Bangladesh.

6. 01/12/2024
Prof. Dr. Mohammad Ismail — Member (External)
Department of Applied Chemistry and Chemical
Engineering (ACCE)
University of Dhaka, Bangladesh.

Abstract

The increasing prevalence of antibiotics in water systems poses significant environmental and health concerns, including antibiotic resistance and genotoxicity. This research focuses on synthesizing $FeWO_4$ nanomaterials in three distinct morphologies- nanoparticles, nanorods, and nanofibers via a sustainable hydrothermal process. These nanomaterials were evaluated as heterogeneous catalysts in four different Fenton-based processes: conventional Fenton (CF), photo-Fenton (PF), sono-Fenton (SF), and sono-photo-Fenton (SPF). The performance of each morphology was systematically assessed for the degradation of ciprofloxacin (CIP), a common antibiotic pollutant found in water. The synthesized nanomaterials were characterized using UV-Vis, FESEM, XRD, XPS, EIS, and cyclic voltammetry (CV). The physicochemical analysis also confirmed differences in catalytic performance based on changes in their morphologies. The Response Surface Methodology (RSM) and Central Composite Design (CCD) were used to improve the degradation of CIP by altering three independent variables: solution pH, catalyst dose (mg/L), and reaction time (min). The quadratic model was found to be significant through analysis of variance (ANOVA). This mathematical model fits the experimental data satisfactorily, with $R^2 = 0.9953$ and lack of fit = 0.2441 ($P>0.05$). Almost complete degradation was achieved at the optimum doses of 100 mg/L of $FeWO_4$, pH = 7, and a 40-minute reaction time. Among the Fenton processes, PF and SPF demonstrated higher antibiotic degradation efficiency than CF and SF processes. Notably, $FeWO_4$ nanoparticles exhibited the best performance, achieving complete degradation of CIP under optimized conditions of pH 7, $FeWO_4$ dosage of 100 mg/L, and a reaction time of 40 minutes, with initial concentrations of 10 mg/L for CIP and 2 mM for hydrogen peroxide (H_2O_2). $FeWO_4$ nanoparticles were found to be effective for inactivation of ARB *E. Coli* RP4 by 6.45 log within 20 min. No ARB regrowth occurred after 72 h, which demonstrates the efficacy of this approach in achieving permanent removal of ARB. The synthesized $FeWO_4$ nanoparticles have the potential to degrade demonstrated stability and recyclability, generating potent reactive species such as hydroxyl radicals ($HO^{\bullet}$), superoxide radicals ($O_2^{\bullet-}$), and singlet oxygen ($^1O_2$). These findings underscore the potential of $FeWO_4$ nanoparticles as effective heterogeneous catalysts in advanced oxidation processes for mitigating antibiotics and antibiotic-resistant bacteria in aquatic environments.

বিমূর্ত

জলজ পরিবেশে অ্যান্টিবায়োটিকের ক্রমবর্ধমান উপস্থিতি পরিবেশ ও জনস্বাস্থ্যের জন্য গুরুতর হুমকি তৈরি করছে, যার মধ্যে অ্যান্টিবায়োটিক প্রতিরোধ ক্ষমতা বৃদ্ধি এবং জিনোটক্সিসিটির মতো সমস্যাগুলো উল্লেখযোগ্য। এই গবেষণায় টেকসই হাইড্রোথার্মাল পদ্ধতিতে $FeWO_4$ ন্যানোম্যাটেরিয়ালের তিনটি ভিন্ন গঠন- ন্যানোপার্টিকেল, ন্যানোরড এবং ন্যানোফাইবার আকারে তৈরি করা হয়েছে। এগুলোকে হেটোরোজেনাস ক্যাটালিস্ট হিসেবে ব্যবহার করে চারটি ফেন্টন-ভিত্তিক প্রক্রিয়া, যেমন - কনভেনশনাল ফেন্টন (CF), ফটো-ফেন্টন (PF), সনো-ফেন্টন (SF), এবং সনো-ফটো-ফেন্টন (SPF) এর মাধ্যমে সিপ্রোফ্লোক্সাসিন (CIP) নামক অ্যান্টিবায়োটিক দূষকের অবক্ষয়ে কার্যকারিতা মূল্যায়ন করা হয়েছে। সিন্থেসাইজড ন্যানোম্যাটেরিয়ালগুলোর গুণগত বৈশিষ্ট্য নির্ধারণে UV-Vis, FESEM, XRD, XPS, EIS এবং সাইক্লিক ভোল্টামেট্রি (CV) ব্যবহার করা হয়েছে। গঠনের ভিন্নতার কারণে $FeWO_4$ অনুঘটক এর কার্যকারিতার পরিবর্তন স্পষ্টভাবে লক্ষ্য করা গেছে। রেসপন্স সারফেস মেথডোলজি (RSM) এর সেন্ট্রাল কম্পোজিট ডিজাইন (CCD) ব্যবহার করে pH, অনুঘটক এর ডোজ (mg/L), এবং বিক্রিয়া সময় (মিনিট) পরিবর্তন করে CIP-এর অবক্ষয়কে উন্নত করা হয়েছে। পরীক্ষাগারের ডেটার সাথে কোয়াড্রাটিক মডেলটি অত্যন্ত সামঞ্জস্যপূর্ণ ($R^2 = 0.9953$ এবং ল্যাক অফ ফিট $= 0.2441$; $P>0.05$)। $FeWO_4$ ন্যানোপার্টিকেল ব্যবহার করে $pH = 7$, অনুঘটক ডোজ 100 mg/L এবং 40 মিনিট বিক্রিয়া সময়ে প্রায় সম্পূর্ণ CIP অবক্ষয় অর্জিত হয়েছে। চারটি ফেন্টন প্রক্রিয়ার মধ্যে PF এবং SPF প্রক্রিয়াগুলি সর্বোচ্চ দক্ষতা প্রদর্শন করেছে। $FeWO_4$ ন্যানোপার্টিকেল 20 মিনিটের মধ্যে 6.45 লগ *E. Coli* RP4 অ্যান্টিবায়োটিক-প্রতিরোধী ব্যাকটেরিয়া (ARB) নিস্ক্রিয় করতে সক্ষম হয়েছে এবং 72 ঘণ্টা পর্যন্ত কোনো পুনঃবৃদ্ধি ঘটেনি। $FeWO_4$ ন্যানোম্যাটেরিয়াল শক্তিশালী প্রতিক্রিয়াশীল প্রজাতি যেমন হাইড্রোক্সিল র‍্যাডিকেল ($HO^{\bullet}$), সুপারঅক্সাইড র‍্যাডিকেল ($O_2^{\bullet-}$), এবং সিঙ্গলেট অক্সিজেন ($^1O_2$) উৎপাদনে দক্ষ। এই গবেষণার ফলাফল $FeWO_4$ ন্যানোপার্টিকেলকে অ্যান্টিবায়োটিক এবং অ্যান্টিবায়োটিক-প্রতিরোধী ব্যাকটেরিয়া দূরীকরণের জন্য কার্যকর এবং পুনর্ব্যবহারযোগ্য ক্যাটালিস্ট হিসেবে প্রতিস্থাপনের সম্ভাবনা নির্দেশ করে।

Table of Contents

List of Figures

List of Tables

Nomenclature

Symbols

Symbols	Elaborations
e.g.	For example
etc.	Etcetera
et al.	And Others
Fig.	Figure
nm	Nanometer
λ	Lambda
eV	Electron volt

Acronyms and Abbreviations

ANOVA	Analysis of variance
AOP	Advance oxidation process
ARB	Antibiotic-Resistant Bacteria
BCSIR	Bangladesh Council of Scientific and Industrial Research
CIP	Ciprofloxacin
CCD	Central Composite Design
CF	Conventional Fenton Process
CTAB	Cetyltrimethyl ammonium bromide
CV	Cyclic Voltammetry
E. Coli	*Escherichia coli*
EDDS	Ethylenediamine-N, N'-disuccinic acid
EIS	Electrochemical Impedance Spectroscopy
FE-SEM	Field Emission Scanning Electron Microscopy
IMRD	Industrial Microbiology Research Division
NF	Nanofiber
NP	Nanoparticle
NR	Nanorod
PF	Photo-Fenton
ROS	Reactive Oxygen Species
RSM	Response Surface Methodology
SF	Sono-Fenton
SPF	Sono Photo-Fenton
UV-VIS	Ultraviolet-visible Spectroscopy
WHO	World Health Organization
WWTP	Waste Water Treatment Plant
XRD	X-ray Diffraction
XPS	X-ray Photoelectron Spectroscopy

Chapter 1: INTRODUCTION

1.1 Background

Antibiotics are pharmaceutical agents employed to treat microbial infectious diseases and are extensively used in human and veterinary medicine, as well as in aquaculture and livestock feed [1]. Global antibiotic consumption has surged, with estimates ranging from 100,000 to 200,000 tonnes between 2010 and 2019 [2]. Approximately fifty percent of these antibiotics are used in human medicine, and this figure is projected to rise to 105,596 tonnes by 2030 [3]. The pervasive use and, particularly, the overuse or misuse of antibiotics have generated significant public concern [4]. Recently, antibiotics have been identified as emerging chemical contaminants [5]. Antibiotics excreted by humans and animals may persist in their original form or as active metabolites, leading to their continual presence in soil, surface water, and groundwater [6], posing high toxicity risks to aquatic and human life. It is assessed that 60-80% of prescribed pharmaceuticals are excreted into sewage treatment plants and the environment [7]. In 2018, the European Commission's Science and Knowledge Service released a technical report highlighting concerns about environmental antibiotics [8]. The persistent presence of antibiotics in natural habitats can lead to the development of antibiotic-resistant bacteria (ARBs) and their resistance genes (ARGs), which can accelerate the spread of antibiotic resistance, posing significant risks to human health and ecological systems [9].

To mitigate the environmental impact of antibiotics, various physical, biological, and chemical techniques have been employed [10, 11]. Physical wastewater treatment methods aim to reduce contaminant levels through mechanical separation, relocating rather than degrading the antibiotics [12, 13]. Although biological methods, such as the activated sludge process and biological membrane technologies, are widely used, they face limitations including extended processing times and heat generation that is difficult to recover. Chemical treatments, which include degradation and solid-liquid separation, primarily aim to convert pollutants into non-toxic or non-hazardous compounds.

However, traditional methods are often inadequate for the complete breakdown of antibiotics, as their complex composition and resistance to biodegradation in aquatic environments pose significant challenges [14].

The advanced oxidation process (AOP) represents a more efficient method for removing antibiotics than conventional treatments [15]. AOPs are distinguished by their simplicity, ease of operation, minimal sludge production, and ability to achieve rapid mineralization of pollutants. They are particularly effective in degrading high-strength organic and recalcitrant compounds [16]. In recent years, numerous significant review papers have focused on the removal of antibiotics using AOPs [17, 18]. It includes different treatment methods such as ozonation [19, 20], Ultraviolet (UV/H_2O_2) [21, 22], Fenton (Fe^{2+}, H_2O_2) [23], photo-Fenton ($Fe^{2+}/H_2O_2/UV$) [23, 24], heterogenous photo-Fenton [25, 26], photocatalysis [27, 28], sonication, electrochemical degradation [29, 30], radiation have been effectively used to remove antibiotics from wastewater. AOP gathered potential significant for the simplicity of equipment and easy operation, low cost of construction, no sludge generation, large production of highly reactive oxygen species (ROS) and finally produce mineralized products [31].

Fenton-based AOP processes have emerged as cost-effective, user-friendly, and highly efficient alternatives to traditional wastewater treatment methods, capable of achieving complete mineralization [32]. These methods encompass various Fenton-based reactions, including Fenton [33], photo-Fenton [34], Fenton-like [35, 36], sono-Fenton [37, 38], and electro-Fenton [39, 40], which effectively degrade antibiotics into their mineral components.

Nanomaterials are essential in the degradation of pollutant from WW, because of their large area of surface, which facilitates the efficient removal of contaminants like heavy metals and organic matters. In the field of catalysis, particles which are nano sized such as Ag, Fe, or TiO_2 serve as catalysts by triggering Redox reactions. This procedure deconstructs organic matters or infectious mircoorganism into substances that are less detrimental. In photocatalysis, semiconductor nanomaterials generate reactive oxygen species upon light exposure, facilitating the degradation of organic compounds in wastewater via photocatalytic reactions. A method that has garnered considerable interest is the use of $FeWO_4$ as a promising photocatalyst for the elimination of pollutants

from wastewater. Iron tungstate ($FeWO_4$), a notable wolframite-type metal tungstate, is a low-cost, non-toxic, narrow band gap (2.0 eV), p-type semiconductor material. Many studies have used it as a photocatalyst [41]. It exhibits rapid electron-hole recombination, resulting in low quantum yield as well as inadequate electron and ion transport capacity, and its catalytic effectiveness is not promising [42]. $FeWO_4$ possesses distinctive characteristics that render it a viable option for tackling wastewater contamination issues. In fact, Liu et al. [43] prepared $FeWO_4/WO_3$ photocatalysts with heterostructures that showed higher absorption to visible light and an increasing BET-specific surface area when compared to pure $FeWO_4$ and WO_3 samples. In photocatalytic activity tests, the $FeWO_4$-modified WO_3 composites showed the highest efficiency in the removal of organic pollutants like MB and TC, due to their enhanced adsorption ability, better visible light response, increased surface area, and fast separation and migration of photogenerated carriers. Boudghene et al. [44] conducted a study on $FeWO_4$ as a catalyst for the photocatalytic degradation of malachite green dye in wastewater. The degradation efficiency reached 97.47% under acidic conditions within 3 h. After three consecutive uses, the catalyst maintained stability, and the kinetic model of the degradation reaction followed pseudo-first-order kinetics. $FeWO_4$ nanofibers with single dimension demonstrate remarkable catalytic efficacy for the degradation of Methylene Blue and RhB under neutral circumstances without pH modification, achieving 99.5% elimination of 20 mg/L MB in 14 minutes utilizing trace H_2O_2 and US [45]. After four cycles, the $FeWO_4$ NF maintain their catalytic activity, with h^+ recognized as the principal active species in the degradation process. Notwithstanding its potential, the utilization of $FeWO_4$ in wastewater treatment encounters specific obstacles. A major problem involves adjusting parameters such as pH, temperature, and contact duration. The regeneration and reutilization of $FeWO_4$ nanocatalyst necessitate meticulous attention to preserve their efficacy during several cycles [46]. The prospective application of $FeWO_4$ for the elimination of pollutants from wastewater is promising and bears significant potential.

It is critical for every approach to establish the optimum doses in order to get the highest degradation efficiency. RSM is a statistical multivariate approach [47] for the optimization of variables that requires a limited number of experiments. It is a quick and

effective experimental design for evaluating the effect of variables on targeted responses [48]. The CCD method is among the most widely used RSM techniques. One of the key benefits of this statistical method is that it uses the response surface conditions to estimate the CCD's ideal settings for expressing the effects of each independent variable.

1.2 Aims and Objectives

This study focuses on the following specific objectives

- To synthesize and characterize $FeWO_4$ nanomaterials with different morphologies for effective photocatalytic degradation of Antibiotic and Antibiotic-Resistant Bacteria.
- To assess the efficiency of $FeWO_4$ nanomaterials in degrading antibiotic molecules under four Fenton processes.
- To optimize the photo-Fenton process by Response Surface Methodology (RSM).
- To explore the degradation mechanisms involved in antibiotic degradation and evaluate the stability and reusability of $FeWO_4$ nanomaterial for practical applications.

1.3 Significance of this Study

This study will help educate future researchers on the degradation and removal of antibiotic and ARB in Bangladesh and find environmental remediation. This research will provide an outline of the Heterogeneous PF. The research can also be used to find out the way to inactivate ARB completely by photo-Fenton Process. The study's final phase will involve the mechanism of involved in antibiotic degradation and evaluate the stability and reusability of $FeWO_4$ photocatalysts for practical applications and a sustainable strategy for environmental remediation

1.4 Thesis Outline

Chapter 1 of this thesis focuses on the general introduction of the main topics of this thesis. It mainly describes the context for the research, explains the topic and objectives, and outlines the work.

Chapter 2 of this thesis consists of a brief literature review focusing on wastewater treatment plants, antibiotic resistance, various factors that influence antibiotic removal in the Fenton process, Roles of reactive species for the degradation of antibiotics, lab-scale, and full-scale application of Fenton processes.

Chapter 3 describes the materials and instruments used during the research work and the procedures followed for the range of tests carried out during the work.

Chapter 4 provides a brief description of the characterization of the materials used in the study and its outcomes, such as the degradation of ciprofloxacin by $FeWO_4$ nanomaterials, Parameter optimization by RSM, Degradation of ARB by $FeWO_4$ nanoparticles and other tests carried out to validate the study.

Chapter 5 summarizes the whole study and gives a clear picture and future direction of this study.

Chapter 2: LITERATURE REVIEW

2.1 Background

Antibiotics are pharmaceutical agents employed to treat microbial infectious diseases and are extensively used in human and veterinary medicine, as well as in aquaculture and livestock feed [49, 50]. The excessive use and/or misuse of antibiotics have raised significant public concern. Recently, several studies have reported antibiotics as emerging chemical contaminants for the environment [51, 52]. Usually, antibiotics defecated by humans and animals can persist in their original form or as active metabolites, leading to their continual presence in soil, surface water, and groundwater. This poses significant toxicity risks to the aquatic environment and human health. It is assessed that 60-80% of prescribed pharmaceuticals are excreted into the sewage treatment plants and the environment [53]. The continuous presence of antibiotics in natural environments can contribute to the development of antibiotic-resistant bacteria (ARB) and their resistance genes (ARGs), hastening the spread of antibiotic resistance [54]. Several studies have reported that this situation poses significant risks to human health and ecological systems [55, 56].

To mitigate the environmental impact of antibiotics, various physical, biological, and chemical techniques have been employed [55, 57]. Physical wastewater treatment methods aim to reduce contaminant levels through mechanical separation, relocating rather than degrading the antibiotics [12, 49]. Biological methods such as the activated sludge process and biological membrane technologies, are widely utilized in wastewater treatment [58]. Although recently, these technologies have been criticized due to several limitations, such as extended processing times and heat generation, which are difficult to recover [59]. On the contrary, chemical treatments, including degradation and solid-liquid separation, are widely utilized to convert pollutants into non-toxic or non-hazardous compounds [14, 55]. It should be noted that the traditional approaches are often inadequate for the complete breakdown of antibiotics, as their complex composition and resistance to biodegradation in aquatic environments. Therefore,

antibiotics have been identified in numerous aquatic environments, including rivers, lakes, streams, and groundwater in diverse regions. The concentration of antibiotics in water can range from trace levels to several milligrams per liter (mg/L), contingent upon the nature of the agricultural or industrial practices that often utilize antibiotics [60]. For example, wastewater treatment plants (WWTPs) in certain areas may release effluents containing elevated levels of antibiotics due to incomplete removal during the treatment process [61-63]. Antibiotics such as sulfamethoxazole (SMX), trimethoprim (TMP), ciprofloxacin (CIP), and erythromycin (ERY) are frequently detected in rivers [61]. Antibiotic concentrations tend to be particularly high in Africa and Asia, while the lowest concentrations have been detected in America and Europe, respectively. This could be due to advanced treatment technologies and the successful implementation of various rules and regulations. Li and coworkers (2023) reported the detection of 21 distinct antibiotics across four continents in their WWTPs, as illustrated in Fig. 2.1.

The Advanced Oxidation Process (AOP) is an efficient method for removing antibiotics compared to conventional treatments [18, 64]. AOPs are known for their simplicity, ease of operation, minimal sludge production, and ability to rapidly mineralize pollutants. They are particularly effective in degrading high-strength organic and recalcitrant compounds [16]. In recent years, numerous significant review papers have focused on the removal of antibiotics using AOPs [17, 18, 65]. Most reviews explore specific AOP methods for antibiotic elimination, including hydrogen peroxide-based AOPs [18], UV-based AOPs [66], UV/chlor(am)ine-based AOPs [67], electrochemical-based AOPs (EAOP) [68] as well as graphene-based nanomaterials [69] and photocatalytic degradation process [70]. The previous reviews have particularly focused on AOP reaction mechanisms, analyzing the factors that influence treatment performance. They have also briefly covered lab-based AOP techniques for the removal of antibiotics. Additionally, several studies have provided a concise overview of the reaction kinetics, performance, and practical limitations related to AOPs. These create a gap in understanding the practical limitations of these processes for large-scale commercial treatment.

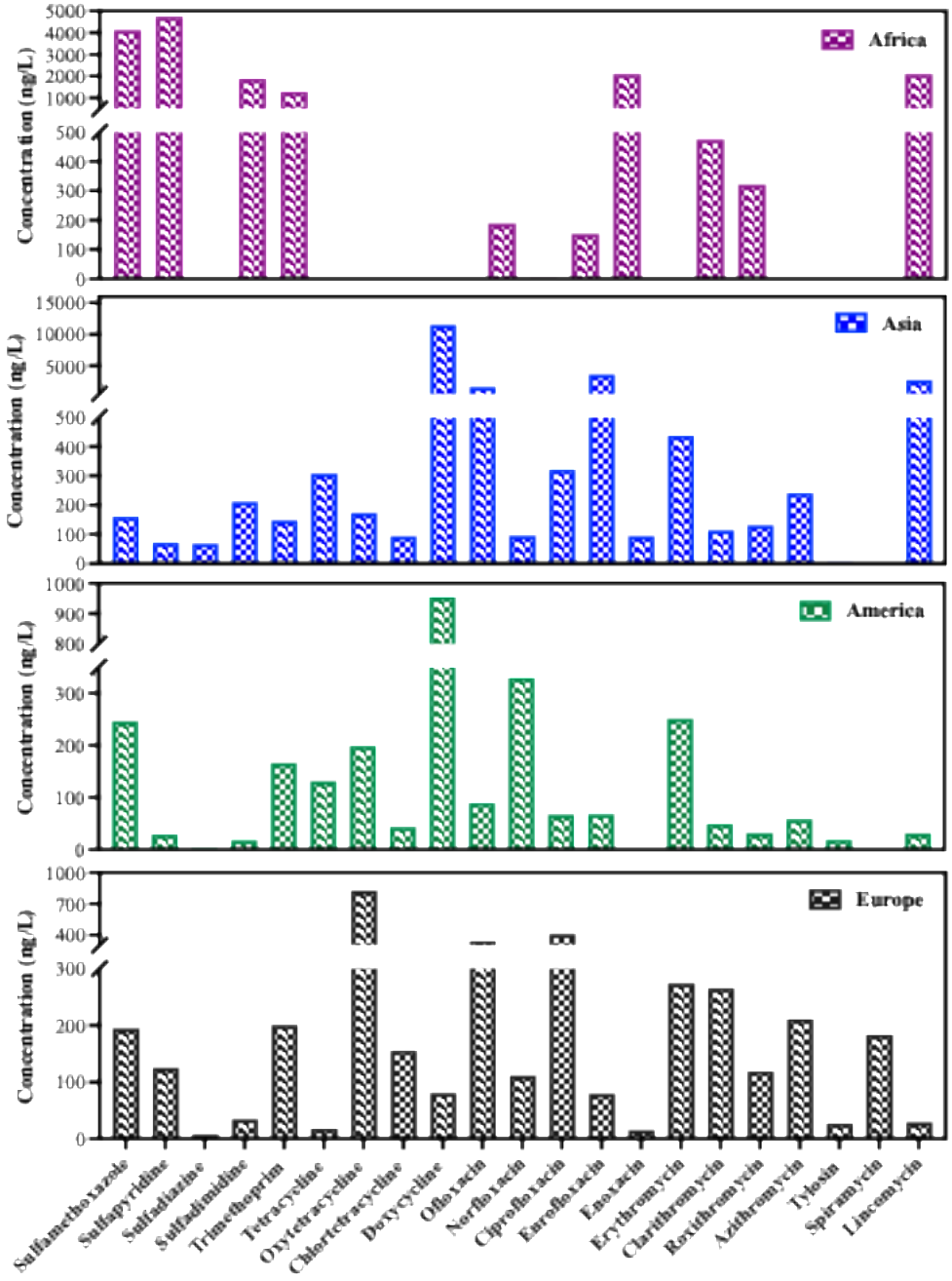

Fig. 2.1 Different typical antibiotic concentrations in wastewater treatment plants (WWTPs) across the four continents.

Fenton-based AOPs are cost-effective, user-friendly, and highly efficient alternatives to traditional wastewater treatment methods. They are capable of achieving complete mineralization of contaminants [24, 71]. These methods including various Fenton processes such as conventional Fenton [33], photo-Fenton [24], Fenton-like [35],

sono-Fenton [38], and electro-Fenton [40], which effectively degrade the antibiotics into their mineral components. While some research has focused on developing and optimizing Fenton processes for lab-scale to real-life applications, there is a lack of comprehensive studies on the detailed mechanisms of each Fenton process, the benefits and drawbacks of scaling up, cost-effectiveness, and sustainability. The existing literature predominantly analyzes Fenton, photo-Fenton, Fenton-like, sono-Fenton, and electro-Fenton processes and their effectiveness against various pollutants. However, there is not much explicit focus on removing antibiotics [72-74]. This review aims to address this gap by discussing critical issues and the key process variables for scaling up these AOP processes. Through a comprehensive review of the literature, this study assesses the progression and significance of Fenton processes over the past three decades, especially in the context of environmental pollution and antibiotic degradation.

The review evaluated the effectiveness of different lab-based Fenton processes in removing antibiotics and also looked at the practical limitations of these processes. It also discussed the environmental impact of antibiotics, the challenges in existing treatment processes, and the factors that can enhance the treatment process. The study seeks to provide readers with an in-depth explanation of the function of reactive species, the mechanisms that govern Fenton reactions, and possible alterations for practical applications. Additionally, it highlights fundamental knowledge gaps and potential future modifications for sustainable wastewater treatment to achieve the goal of protecting the aquatic environment.

2.2 Antibiotic Intrusion into The Environment: Unveiling the Sources

The presence of antibiotics in the environment exerts a significant impact on environmental ecosystems. The primary sources of antibiotics in surface water include animal husbandry and aquaculture, domestic sewage discharges, pharmaceutical manufacturing, and healthcare facilities [75]. Antibiotics in surface water and soil travel to groundwater through the vadose zone via intricate physical, chemical, and biological processes, including leaching, infiltration, and the interactions between underground and surface water. The present study investigates four primary sources of environmental antibiotics, as illustrated in Fig. 2.2 provides a comprehensive analysis of their pathways

and the mechanisms influencing their movement and persistence in groundwater systems.

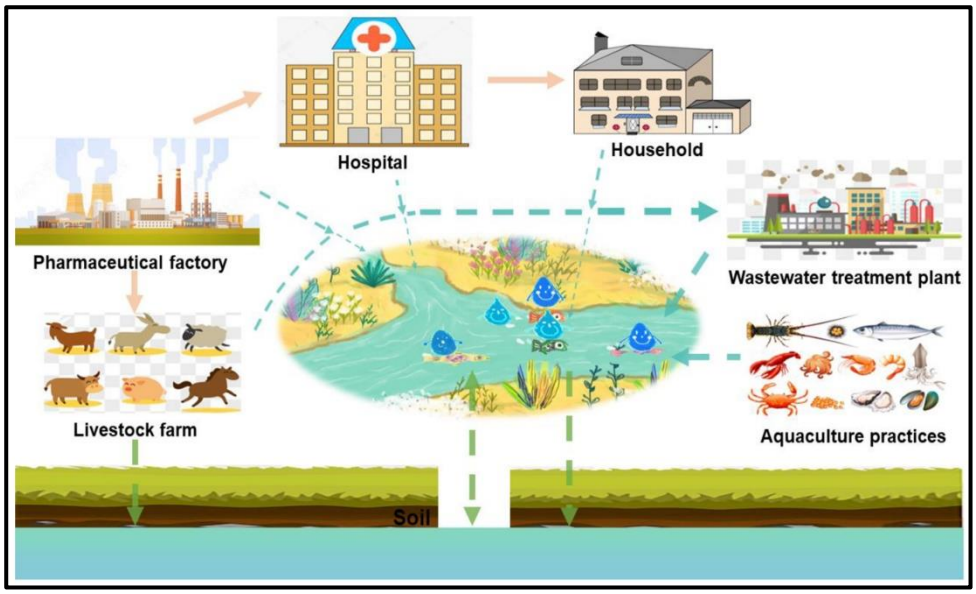

Fig. 2.2 Sources of antibiotics in environmental ecosystems.

2.2.1 Animal Husbandry and Aquaculture

Antibiotics are typically administered to animals through feed or water. In large-scale animal husbandry, antibiotics are added to feed as growth promoters and to prevent and treat infectious diseases in animals [76]. Consequently, animals excrete antibiotic residues in their feces, which can enter the environment through manure application as fertilizer or runoff from animal confinement facilities. Additionally, aquaculture heavily relies on antibiotics. For the low absorption rate, aquatic products can absorb only 20-30% of administered pharmaceuticals [77]. The residual antibiotics are discharged into nearby water bodies or the sediments of the fish farming area via nonpoint source pollution, where they endure and disperse. Antibiotic residues may ultimately pollute urban water sources, threatening environmental and public health.

2.2.2 Discharges From Domestic Sewage

Domestic sewage discharge is a major source of antibiotics in metropolitan water systems [78]. Antibiotics are commonly consumed to treat various infections, but research indicates that only a small percentage of these antibiotics are absorbed and

utilized by the human body. The remaining 40%–90% are excreted as active drugs or metabolites in feces and urine [79]. Consequently, these antibiotics enter wastewater treatment plants or septic systems, where they may not be completely removed. Treated wastewater or septic effluent containing residual antibiotics can then be discharged into nearby water bodies [80]. The types and concentrations of antibiotics in the effluents of sewage treatment plants vary significantly due to the differing types and concentrations of antibiotics used across various regions and countries, leading to variable antibiotic-containing wastewater treatment processes.

2.2.3 Pharmaceutical Manufacturing

Antibiotics can enter urban water systems as a result of industrial and production processes. Pharmaceutical companies produce, handle, and dispose of substantial quantities of antibiotics during manufacturing. Improper disposal methods, such as inadequate treatment or accidental spillage, can lead to the release of antibiotics into water bodies. A study revealed that antibiotic concentrations in water sources downstream of pharmaceutical production plants were significantly higher than those upstream. Furthermore, the researchers found that antibiotic concentrations were highest in water sources closest to pharmaceutical manufacturing facilities. The levels of antibiotics in the wastewater were sufficient to contribute to the development of antibiotic resistance in downstream water sources [81].

2.2.4 Hospital and Healthcare Facilities

Hospitals and healthcare facilities are significant contributors of antibiotics to urban water systems [82]. These settings utilize large doses of antibiotics for patient treatment, leading to the excretion of antibiotic residues into wastewater. Additionally, improper disposal of expired or unused drugs by healthcare facilities can result in antibiotic contamination of water sources. The incineration of medical waste is another primary source of antibiotic emissions, potentially facilitating the proliferation of antibiotic resistance. A study found that antibiotic concentrations in hospital wastewater were substantially higher than those in domestic sewage [83].

2.3 Key Factors Influencing Antibiotic Removal in Fenton Processes

Multiple factors affect the efficacy of antibiotic elimination via Fenton processes. It utilizes highly reactive oxidants to degrade antibiotics in the environment. Key factors impacting the removal efficacy of antibiotics include the concentration of hydrogen peroxide and ferrous ions, pH levels, temperature, and coexisting organic and inorganic substances. Additionally, the initial concentration of antibiotics, reaction time, and the specific characteristics of the antibiotics being treated play crucial roles in determining the effectiveness of the Fenton processes. Understanding these factors is essential for optimizing the conditions and maximizing the efficiency of antibiotic removal in environmental applications.

2.3.1 Antibiotic Properties

The physicochemical properties of antibiotics are crucial factors influencing their removal from water by Fenton processes. These properties include chemical structure, stability, functional groups, electron density, solubility, and complexity in environmental samples. The stability of an antibiotic molecule significantly affects its removal efficiency. Certain antibiotics, such as tetracyclines, macrolides, sulfonamides, cephalosporins, and carbapenems, exhibit high chemical stability, making them resistant to oxidative degradation due to their complex structures, which include multiple aromatic rings and macrolide ring structures [84]. However, Fenton processes can still degrade these stable antibiotics under specific reaction conditions, extended treatment times, or higher oxidant concentrations. Antibiotics with susceptible functional groups are more easily oxidized; for example, those containing hydroxyl (OH), amine (NH_2), and carbonyl (C=O) groups have high electron densities, making them more likely to undergo oxidative reactions [85]. Additionally, the solubility of antibiotics in water impacts their distribution within the treatment system. Poorly soluble antibiotics may not be as effectively treated in Fenton processes as they may not adequately interact with reactive species [86]. Studies have demonstrated that the effectiveness of degradation decreases as the concentration of pollutants surpasses a specific threshold. When the concentration of antibiotics increases, the availability of active radicals necessary for breaking down pollutant molecules diminishes, resulting in a reduced degradation rate

[57]. Furthermore, elevated levels of antibiotics can obstruct catalytic sites, impacting the generation of active radicals [87].

2.3.2 Catalyst or Iron Concentrations

The concentration of the catalyst in the Fenton process significantly impacts the removal efficiency of antibiotics and other contaminants by playing a crucial role in activating oxidants such as H_2O_2. The amount of catalyst used directly affects the rate at which antibiotics decompose [86]. Generally, the efficiency of degrading antibiotics tends to increase with higher iron or catalyst dosages up to a certain point [86, 88]. For instance, a study by Ouyang et al. (2019), using iron-based catalysts ($GFe_{0.5}$) for the Fenton oxidation of lincomycin showed that adding 0.01 g/L of $GFe_{0.5}$ catalyst resulted in a 93.85% reduction in lincomycin after 90 minutes of reaction time. Increasing catalyst dosages to 0.05 and 0.1 g/L resulted in the complete removal of lincomycin within 10 minutes [89]. However, excessive catalyst dosages can have adverse effects. They not only led to higher operational expenses and increased production of iron sludge but also intensified the scavenging action of hydroxyl radicals ($HO^{\bullet}$), negatively impacting the degradation of antibiotics [74]. However, the optimal catalyst concentration required for maximum degradation of organic contaminants must be determined through experimentation. For example, in the case of sulfamethazine, the removal efficiency increased from 67% to 82% when the Fe^0/Ce^0 catalyst concentration increased from 0.1 to 0.5 g/L, but efficiency decreased from 67% to 45% when the catalyst amount rose from 1.0 to 1.5 g/L due to the scavenging of $HO^{\bullet}$ by excess ferrous ions [90]. Additionally, the release of excess catalysts into the environment can have ecological impacts, affecting the sustainability of the Fenton process. Therefore, it is critical to evaluate the potential influence of discharging catalysts and unreacted H_2O_2 into the environment.

2.3.3 Oxidant Dosage

Hydrogen peroxide (H_2O_2) serves as the primary oxidant in the Fenton process. Adding it to the Fenton process improves the breakdown of antibiotics by helping to produce different ROS that can efficiently oxidize and degrade the molecular structure of antibiotics into less harmful substances [91]. However, the efficacy of the Fenton

process is intricately linked to the dosage of H_2O_2 utilized. Insufficient amounts of H_2O_2 may result in incomplete removal of contaminants, while excessive concentrations may not necessarily enhance antibiotic degradation and can even lead to undesirable outcomes [18]. This phenomenon is attributed to the potential formation of less reactive species through the reaction of $HO^{\bullet}$ radicals with each other, diminishing the oxidative capacity. Additionally, higher concentrations of H_2O_2 can lead to side reactions with other water matrix compounds, generating harmful substances that persist in the environment. For instance, researchers observed an increase in the elimination efficiency of sulfamethazine (SMT) from 40% to 74% as the concentration of H_2O_2 increased from 4 mM to 12 mM. However, a subsequent rise in H_2O_2 concentration from 12 mM to 16 mM resulted in a gradual decline in SMT elimination efficiency to 54%, attributed to H_2O_2 excess consumption of $HO^{\bullet}$ radicals [90].

2.3.4 pH of the Solution

The pH of the reaction medium significantly influences the degradation of antibiotics in Fenton processes. Changes in pH impact the reaction rate and efficiency [57]. Fenton reactions typically occurred under acidic conditions, ranging between 2.0 and 3.0, which is the optimal condition for achieving the highest efficiency. The study also reported that the free Fe(III) concentration have decreased significantly at pH level of approximately 1, leading to the generation of $FeOH^{2+}$ and $Fe(OH)_2^{+}$ aqua-complexes [92], as depicted in Fig. 2.3. The formation of the aqua-complex $[Fe(H_2O)_6]^{2+}$ occurs at pH values below 2.0 [72], with the subsequent reaction between this complex and H_2O_2 characterized by a slower rate. Moreover, this reaction facilitates the formation of $[Fe(O_2H)]^{2+}$, which exhibits weak oxidizing ability [72, 92]. In extremely acidic conditions, the abundance of H^{+} ions can neutralize $HO^{\bullet}$ radicals, rendering H_2O_2 unstable and forming $H_3O_2^{+}$. This process impedes the synthesis of $HO^{\bullet}$ radicals and the regeneration of Fe^{2+} ions [93]. At acidic pH levels (2 to 3), $FeOH^{2+}$ is the predominant form, ensuring maximum system reactivity. However, as the pH exceeds 3.0, system reactivity diminishes due to decreased concentration of photoactive $FeOH^{2+}$ and dissolved iron. When the pH exceeds 5 to 12 (Fig. 2.3), the degradation efficiency decreases due to the precipitation of dissolved iron as ferric hydroxide ($Fe(OH)_3$),

hindering ferrous ion regeneration and resulting in the production of sludge with a high iron concentration [72, 92]. Furthermore, when the pH level goes beyond its optimal range, the breakdown of H_2O_2 happens, causing a decrease in the generation of $HO^{\bullet}$ radicals, which then leads to reduced antibiotic degradation. Baran and Adamek [94] demonstrated the effective degradation of ampicillin, doxycycline, and tylosin at pH 3.5, underscoring the influence of pH.

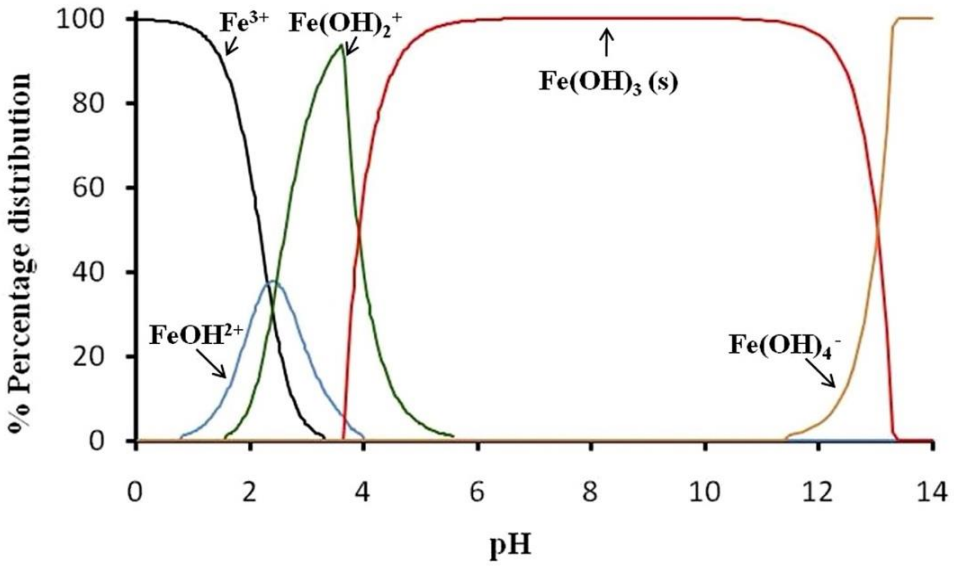

Fig. 2.3 Illustration of the relationship between the different forms of ferric species and the pH containing Fe(III) at 25 °C.

Numerous studies have investigated the use of ligands in the Fenton process, such as citrate, oxalate, nitrilotriacetic acid (NTA), tetra amido macrocyclic (TAML), ethylenediamine-tetra acetic acid (EDTA), and ethylenediamine succinic acid (EDDS). When Fe(III) is dissolved in an aqueous solution with ligands, soluble Fe(III)-containing compounds are generated at a pH exceeding 3.0 due to the production of soluble complexes (Fe-L), which can be adjusted to basic pH levels without precipitating Fe(III) [24, 57]. The addition of citrate, NTA, oxalate, and EDDS can sustain Fe(III) availability at near-neutral pH by creating soluble complexes. In this modified Fenton process, we observed higher efficiency of antibiotic removal. However, TOC and COD tend to increase after the process, which represents a common limitation in practical application.

2.3.5 Matrices of Water

Water matrices are essential for the elimination of antibiotics from water.. Within the Fenton process, both organic and inorganic substances present in water matrices can act as scavengers, competing with target contaminants such as antibiotics for ROS generated during oxidation [95]. Complex matrices, such as municipal or industrial effluents, may harbor a diverse array of interfering substances capable of adversely affecting antibiotic removal efficiency. Natural organic matter (NOM), a complex amalgamation of naturally occurring organic compounds derived from decaying plant and animal materials, constitutes a significant component. The variability of NOM in water sources holds paramount importance in water treatment and the application of the Fenton process for antibiotic elimination. Moreover, water hardness, determined by the levels of calcium and magnesium ions, can exert a profound influence on antibiotic removal efficiency. Elevated water hardness can precipitate the formation of insoluble metal hydroxides, potentially disrupting the efficacy of the Fenton process [96]. Additionally, it may contribute to scaling and fouling in equipment, leading to decreased heat transmission and hindering the efficiency of the photo-Fenton process.

2.3.6 Radiation Sources and Irradiation

UV-visible assisted advanced oxidation processes can be categorized into two types according to the characteristics of the radiation source: (1) linear sources and (2) continuous sources that emit radiation across a range of wavelengths [97]. The first category encompasses mercury vapor arc lamps, which can be further categorized into low-pressure and high-pressure lamps, as well as incoherent excimers. The second category includes xenon arc lamps, which can operate in either pulsed wave mode or continuous wave mode [72]. One source of UV-visible radiation is thought to be the sun. Photocatalyzed Fenton reactions can transpire at multiple wavelengths, including UV-A, UV-B, UV-C ($\lambda < 285$ nm), and visible light ($\lambda > 400$ nm). The efficiency of deterioration is affected by photon wavelength, as photons with larger wavelengths have reduced energy [72]. For instance, the heterogeneous Fe-POM/BMO-3 catalyst exhibited an impressive removal efficiency of 99.79% for tetracycline after 18 minutes of exposure to 5 W light [98]. Another study noted that the degradation rate of ciprofloxacin increased

by 94.7% when exposed to visible light. The rate constant exhibited an 11.7-fold increase compared to the Fenton system, indicating that visible light can significantly enhance the Fenton system [99]. Two events are frequently linked to light's impact on the Fenton process: (1) the breakdown of the aqua complex $Fe(OH)^{2+}$ through photolysis, resulting in the regeneration of Fe^{2+} and the generation of $HO^{\bullet}$ radicals. This process also prevents the accumulation of Fe^{3+} (2) The decomposition of H_2O_2 by a light source, which produces two $HO^{\bullet}$ radicals [72, 100].

2.3.7 Reaction Time

The duration of treatment or reaction time is a critical factor influencing the efficiency of antibiotic removal in the Fenton process. Longer reaction times typically allow for more extensive contact between the ROS and the antibiotics, resulting in a higher degradation rate. If complete mineralization is the objective, an extended reaction time becomes essential to ensure thorough removal [101]. For instance, Qin and colleagues observed that the $MnFe_2O_4$@C-NH_2 catalyst can degrade ofloxacin, amoxicillin, and tetracycline by approximately 52.8%, 64.8%, and 38.4%, respectively, after 30 minutes of reaction time [102]. In contrast, the degradation efficacy reaches 100% after 180 minutes of reaction. This phenomenon is attributed to the prolonged reaction time allowing for the generation of more $HO^{\bullet}$ radicals, facilitating the degradation of additional antibiotic molecules [102]. However, some researchers noted a negative impact on degradation efficiency with increasing reaction time. When assessing removal methods, optimizing reaction time is crucial. Determining the ideal reaction time is essential to any chemical reaction, as exceeding the equilibrium state renders the procedure no longer cost-effective [103].

2.3.8 Temperatures

In the Fenton process, temperature has a major impact on the rate of reaction. Elevated temperatures enhance oxidation rates, resulting in accelerated reactions and more rapid removal of antibiotics [104]. For instance, a rise in temperature from 15 to 45°C leads to faster degradation of CIP, with higher reaction kinetics ranging from 0.0055 to 0.0105 min^{-1} [105]. Higher temperatures can reduce the activation energy required for

chemical reactions, facilitating the initiation of oxidation reactions by ROS, thereby increasing antibiotic degradation. Tetracycline, for example, was completely degraded after 60, 90, and 120 minutes of reaction at 65°C, 55°C, and 45°C, respectively. In contrast, lower temperatures such as 15°C, 25°C, and 35°C necessitated a longer reaction time for the removal of acetaminophen and naproxen [106]. The positive impact of temperature rise on antibiotic degradation through sonochemistry has been frequently observed [107]. Temperatures above 35°C require a higher frequency (1000 kHz) to achieve complete degradation [106]. Moreover, the increase in reaction temperature enhances the deterioration of sulfadiazine in the US/Fe^0/PS system. Increasing the reaction temperature from 10 to 50°C led to an increase in the observed rate constant from 3.56 to 27.39 h^{-1}. Elevated temperatures ranging from 22 to 50°C enhanced the rate constant (k) for tetracycline removal in the sono/Fe_3O_4/H_2O_2 system. Furthermore, the temperature is crucial in affecting the stability and behavior of oxidants like H_2O_2. Lower temperatures generally promote greater stability, while higher temperatures can accelerate decomposition, leading to a loss of oxidizing capability.

2.3.9 Irradiation Sources and Cost Constraints

Energy consumption and cost-effectiveness are critical considerations in implementing the Fenton process for antibiotic removal in water treatment systems. The Fenton reaction uses energy to operate lights or ultrasonic devices. Hence, it is essential to optimize energy use for efficient treatment [108]. Determining the light intensity requirement in the Fenton process at specific H_2O_2 concentrations is crucial, as exceeding this point may not significantly enhance treatment efficiency. Energy consumption can be reduced without compromising treatment effectiveness by optimizing Fenton factors such as reactant amount, treatment duration, and process conditions. Utilizing renewable energy sources like solar energy instead of UV or visible light can reduce the cost of energy usage [109]. In the sono-Fenton process, ultrasound irradiation plays a pivotal role by influencing cavitation, which involves the formation, growth, and collapse of bubbles in the liquid. At optimal ultrasonic power, cavitation bubbles reach their resonant size and collapse violently, producing $HO^{\bullet}$ that drives the degradation of antibiotics [37]. Increasing ultrasonic power enhances cavitation by lowering the

threshold limit and increasing the number and size of cavitation bubbles, thereby generating more active radicals. This improvement also enhances the mass transfer of pollutants and breaks up catalysts, increasing the reactive surface area and boosting degradation efficiency [110]. Karaca et al. (2023) observed that increasing ultrasonic irradiation power from 300 W to 450 W enhanced tetracycline degradation efficiency from 59.76% to 92.85%. Another study demonstrated that the degradation rate of metronidazole increased from 82.8% to 89% as ultrasonication power was raised from 40 W to 60 W, but a subsequent increase to 70 W reduced the degradation rate to 88.4% [38]. However, excessively high ultrasonic power can cause a scattering effect, reducing cavitation effectiveness and the overall degradation process [110]. Similarly, in the electro-Fenton reaction, current flow increases the generation of ROS, but excessive current can stimulate undesirable side reactions [40]. Yang et al. (2023) observed that the mineralization efficiency of ofloxacin increased from 69 % to 100 % as the current density rose from 4.2 to 16.6 mA/cm² [111]. Achieving a balance between treatment efficiency and energy consumption is critical, considering factors such as catalyst and oxidant costs. High concentrations of costly catalysts may not be economically viable, highlighting the need for a cost-benefit analysis to assess the economic viability of Fenton implementation for antibiotic removal, considering both implementation costs and improved water quality benefits. Conducting life cycle and cost-benefit analyses provides comprehensive insights into Fenton process costs and resource utilization, aiding in informed decision-making for sustainable water treatment solutions.

2.4 Roles of Reactive Species for The Degradation of Antibiotic

The Fenton process is a highly efficient technique for degrading antibiotics from contaminated water by generating diverse reactive species (RSs) through a series of cyclic reactions that break down antibiotic molecules [112, 113]. In the conventional Fenton process, hydroxyl ($HO^{\bullet}$) radicals are primarily produced by the decomposition of H_2O_2 with iron (Eq. 2.1). The catalyst, typically iron, undergoes a redox reaction in which it is reduced from Fe^{3+} to Fe^{2+} (Eq. 2.2) in the presence of oxidant (H_2O_2) in an acidic environment. This process produces hydroperoxy radicals ($HO_2^{\bullet}$). Subsequently, these $HO_2^{\bullet}$ generate $HO^{\bullet}$ radicals through the oxidation by other H_2O_2 molecules (Eq. 2.3). At

pH 7, $HO_2^{\bullet}$ is predominantly present as the radical anionic form ($O_2^{\bullet-}$), with only 0.6% existing in its protonated form. $O_2^{\bullet-}$ have a strong reduction capacity, facilitating the conversion of Fe^{3+} to Fe^{2+} (Eq. 2.4) [57]. Ultimately, the $O_2^{\bullet-}$ radical is converted into $HO^{\bullet}$ through the Haber–Weiss reaction (Eq. 2.5) [114, 115]. Additionally, the disproportionation of $HO^{\bullet}$ radicals leads to the generation of singlet oxygen ($^1O_2$) (Eq. 2.6) [115]. The conventional Fenton process typically produces three types of ROS as $HO^{\bullet}$, $O_2^{\bullet-}$ and $^1O_2$. However, the precise percentage of these ROS in a reaction varies depending on the process parameters [57, 93]. The Fe^{2+} ion acts as the primary catalyst in the traditional Fenton process, whereas the Fenton-like process can utilize a variety of multivalent metal ions, including Cu, Co, Mn, Ce, Ag, Cr, Ru, W, Mo, V, and Ti. These metal ions exhibit both oxidation and reduction properties, allowing them to activate H_2O_2 and produce different ROS [116]. The flexibility in using different metal ions broadens the applicability and efficiency of the Fenton and Fenton-like processes in treating wastewater containing antibiotics.

In the homogeneous Fenton process, exposure of the reaction system to light significantly boosts the production of $HO^{\bullet}$ radicals by facilitating the conversion of Fe^{3+} to Fe^{2+}. This light-assisted process enables the simultaneous reduction of Fe^{3+} and the generation of $HO^{\bullet}$ radicals (as shown in Eq. 2.7) [57]. In a heterogeneous system, the process begins when photons with energy greater than the semiconductor's band gap are adsorbed. This adsorption triggers a catalytic reaction that generates charge carriers including electrons (e^-) and holes (h^+) (Eq. 2.8). These charge carriers can be trapped on the catalyst surface in the presence of oxidants such as oxygen or H_2O_2, leading to the formation of ROS like $HO^{\bullet}$, $O_2^{\bullet-}$ and $^1O_2$. The presence of light enhances this process by generating additional photoinduced electrons, which reduce Fe^{3+} to Fe^{2+} (Eq. 2.9) and further catalyze the reduction of dissolved oxygen (Eq. 2.10) and H_2O_2 (Eq. 2.11) to produce $O_2^{\bullet-}$ and $HO^{\bullet}$, respectively. The holes generated during this process have a strong oxidation potential (2.53 V versus NHE) [117], which allows them to oxidize hydroxyl groups or water molecules to generate more $HO^{\bullet}$ radicals (Eq. 2.12). In the CF process, it is important to avoid the formation of Fe^{3+} hydroxy complexes such as $Fe(OH)^{2+}$ and $Fe_2(OH)_2^{4+}$, especially under acidic conditions. When exposed to light, these complexes undergo photoreduction, producing additional $HO^{\bullet}$ and Fe^{2+} (Eq. 2.13),

thus enhancing the catalytic activity. Conversely, the Fenton process occurs in absence of light, and the Fe^{3+} hydroxy complexes present in the system slow the reaction rate. The production of $HO^{\bullet}$ radicals initiate the degradation of antibiotic molecules through two primary chemical pathways: (a) the abstraction of a hydrogen atom from the antibiotic molecule (R-H), leading to the formation of a free radical intermediate (Eq. 2.14), and (b) the addition of an oxygen atom to the antibiotic molecule, resulting in the creation of an oxygenated intermediate (Eq. 2.15). These intermediates can react further with $HO^{\bullet}$ radicals or other reactive species. This may lead to additional hydrogen abstraction, oxygen addition, or bond cleavage, leading to antibiotics degradation.

The combination of simultaneous Fenton oxidation and photo-reduction in the PF process presents a distinct advantage. When $HO^{\bullet}$ radicals are exposed to light, a significant portion of them is converted into other ROS, thereby broadening the available pathways for antibiotic removal. Moreover, the addition of US to the Fenton processes harnesses acoustic cavitation. This phenomenon involves ultrasonic waves generating localized hot spots with intense pressure fluctuations and high temperatures, reaching up to 5000 K and approximately 1000 atm. As a result, microbubbles form and rapidly collapse, leading to the dissociation of water and oxygen molecules and the generation of reactive radicals such as $HO^{\bullet}$, $H^{\bullet}$, $HOO^{\bullet}$, and $O^{\bullet}$. These radicals are instrumental in oxidizing and decomposing the chemical structures of antibiotics, ultimately breaking them down into harmless by-products (Eq. 2.16).

$$Fe^{2+} + H_2O_2 \rightarrow Fe^{3+} + HO^{\bullet} + OH^{-} \quad \text{Eq. 2.1}$$

$$Fe^{3+} + H_2O_2 \rightarrow Fe^{2+} + HO_2^{\bullet} + H^{+} \quad \text{Eq. 2.2}$$

$$H_2O_2 + HO_2^{\bullet} \rightarrow HO^{\bullet} + O_2 \quad \text{Eq. 2.3}$$

$$Fe^{3+} + HO_2^{\bullet} \rightarrow Fe^{2+} + H^{+} + O_2 \quad \text{Eq. 2.4}$$

$$O_2^{\bullet-} + H_2O_2 \rightarrow HO^{\bullet} + HO^{-} + O_2 \quad \text{Eq. 2.5}$$

$$4HO^{\bullet} \rightarrow 2H_2O + {}^1O_2 \quad \text{Eq. 2.6}$$

$$Fe^{3+} + H_2O + h\nu \rightarrow Fe^{2+} + HO^{\bullet} + H^{+} \quad \text{Eq. 2.7}$$

$$\text{Catalysts} + h\nu \rightarrow e^{-} + h^{+} \quad \text{Eq. 2.8}$$

$$Fe^{3+} + e^- \rightarrow Fe^{2+} \quad \text{Eq. 2.9}$$

$$O_2 + e^- \rightarrow O_2^{\bullet -} \quad \text{Eq. 2.10}$$

$$H_2O_2 + e^- \rightarrow HO^{\bullet} + OH^- \quad \text{Eq. 2.11}$$

$$h^+ + H_2O \rightarrow H^+ + HO^{\bullet} \quad \text{Eq. 2.12}$$

$$Fe(HO)^{2+} + h\nu \rightarrow Fe^{2+} + HO^{\bullet} \quad \text{Eq. 2.13}$$

$$HO^{\bullet} + R\text{-}H \rightarrow R^{\bullet} + H_2O \quad \text{Eq. 2.14}$$

$$HO^{\bullet} + R\text{-}H \rightarrow R\text{-}OH \quad \text{Eq. 2.15}$$

$$\text{Antibiotics} + HO^{\bullet} \rightarrow H_2O + \text{Degradation products} \rightarrow CO_2 + H_2O \quad \text{Eq. 2.16}$$

2.5 Laboratory-Based Fenton Processes

Antibiotics and other organic pollutants can be efficiently eliminated from wastewater using the Fenton procedures. Developed in the 19th century, the Fenton processes utilize iron salts (Fe^{2+}) and H_2O_2 to generate various ROS, which are powerful oxidants capable of degrading organic pollutants [118]. Each of the Fenton processes can be classified as homogeneous or heterogeneous, both of which are advanced oxidation techniques employed to degrade or remove antibiotics from contaminated sources. The subsequent sections will provide a comprehensive examination of various laboratory methodologies employed for the removal of antibiotics utilizing different Fenton processes. Furthermore, this discussion will elucidate the respective benefits and limitations inherent to each approach.

2.5.1 Fenton and Fenton-Like Process for Antibiotic Degradation

The conventional homogeneous Fenton process has been extensively studied due to its advantageous properties for removing a wide range of antibiotics from wastewater. This process can completely degrade common antibiotics like amoxicillin, ampicillin, and cloxacillin within two minutes of treatment but requires higher concentrations of H_2O_2 (46.87 mM) and Fe^{2+} (4.687 mM). Their molar ratio was H_2O_2/ Fe^{2+} of 10 [119]. It is essential to use the optimum concentration of reagent, as higher levels can lead to a more

efficient treatment within a shorter time but can also result in excessive sludge production, increased chemical costs, and the scavenging of hydroxyl radicals, which decreases the overall efficiency of pollutant degradation, as observed in the cases of flumequine [120], ciprofloxacin [121, 122], tetracycline [123] and sulfathiazole [112]. An excessive amount of H_2O_2 and its by-products may pose adverse environmental impacts, such as oxygen depletion in aquatic ecosystems, potentially endangering marine life if not managed properly. Additionally, high Fe^{2+} levels can cause an increase in iron concentration in the effluent, surpassing acceptable wastewater discharge limits and necessitating further treatment [57, 122]. A detailed summary of research on the homogeneous Fenton process for antibiotic removal is shown in Table 2.1.

One important element in the breakdown of antibiotics is the pH of the solution. Most conventional Fenton research has focused on acidic conditions, typically elevation antibiotic breakdown efficiency at a pH range of 2.5 to 4 [112, 121, 123-125]. In 2023, Baran and Adamedk used optimized doses to degrade three antibiotics, such as ampicillin, doxycycline and tylosin at pH 3.5 and reported complete degradation during 30 minutes of treatment [94]. In contrast, the heterogeneous process is less effective at acidic pH. It has shown higher efficiency across a wider pH range, making it a more versatile option for various water treatment scenarios. Diverse solid iron and its derivative materials such as nZVI [126, 127], $Fe^0@CeO_2$ [128], rGO-Fe_3O_4 [129], Fe-BC [130], $CuCoFe_2O_4$@AC [131] can provide many advantages for heterogeneous processes and act as a catalyst in the Fenton process, including easy retrieval, prolonged use, and broader pH range. However, the recovery and reuse of catalysts are still challenging. The use of magnetic iron materials as carriers or substrates for material retrieval is a viable approach. However, magnetic iron alone is insufficient for the complete breakdown of antibiotics, necessitating further modifications. In their study, Pourshaban-Mazandarani et al. (2023) synthesized a $CuCoFe_2O_4$@AC magnetic composite, which showcased enhanced photocatalytic activity, achieving 95.77 % removal efficiency for CIP after 2 hours.

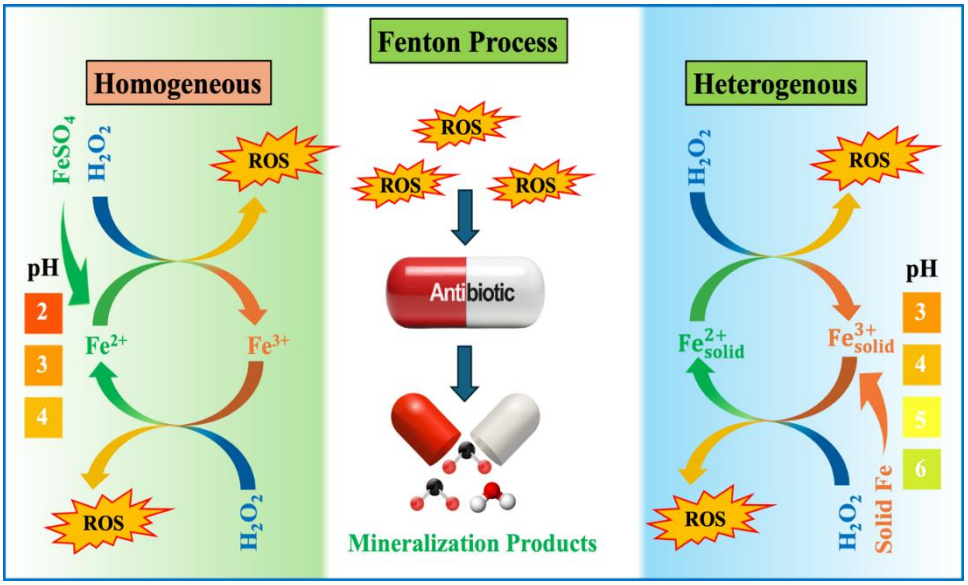

Fig. 2.4 Graphical mechanism of the conventional Fenton Process in homogeneous and heterogeneous process.

The Fenton-like reaction extends beyond the conventional Fenton oxidation process by substituting ferrous ions (Fe^{2+}) with ferric ions (Fe^{3+}) or other transition metal ions [132]. Various catalysts, including Fe(II), Fe(III), Cu(II), nZV, and carbon-based materials such as graphene oxide (GO), CNTs, g-C_3N_4, fly ash, and biochar, as well as iron confined on titania nanofibers (Fe-TNFs) and metal-organic frameworks (MOFs) like MIL-101-NH_2 and PPyC@Py-MIL (Fe), are frequently reported for antibiotic degradation [36, 98, 133-139]. A comprehensive summary of the research on the Heterogeneous Fenton and Fenton-like processes for antibiotic removal is presented in Table 2.2 and its graphical mechanism is shown in Fig. 2.4.

Ligand compounds that are suitable for Fenton-like processes can operate effectively at higher pH levels. For example, the elimination rates of norfloxacin (NOR) and ciprofloxacin (CIP) in the Fe(III)-tetra amido macrocyclic ligand (TAML)/ H_2O_2 system were minimal at pH 6.0 but significantly increased to over 95% at pH 10.0 [140]. Much of the research on removing antibiotics using the Fenton-like process has focused on heterogeneous systems. Recent studies have shown that iron-based MOF heterogeneous catalysts are highly effective in removing antibiotics. In 2023, Chen et al. synthesized MIL-101-X(Fe) with various substituents X = -H, -NH_2, -OH, -OCH_3) on the organic ligands. They achieved 100% sulfamethoxazole (SMX) removal within 70

minutes using MIL-101-NH_2, with a reaction rate 30.06 times faster than MIL-101-H [132]. The efficiency of Fenton-like processes in degrading substances is affected by the presence of complex matrices containing inorganic anions and organic components. Zhou et al. (2019) synthesized iron nanoparticles enclosed in carbon nano shells doped with boron and nitrogen (B/N-C@Fe) and found that certain inorganic anions had a detrimental impact on levofloxacin removal [141]. This highlights the importance of considering matrix effects in the application of Fenton-like processes for antibiotic degradation. In the Fenton process, the size of nanoparticles plays a significant role in determining their catalytic performance, as reactions predominantly occur on the metal surface. Nanoparticles larger than 5 nm involve fewer metal atoms in the catalytic reaction, limiting their efficiency [142]. In contrast, single-atom catalysts (SACs), which consist of individual atoms (~0.1 nm), exhibit nearly 100% atomic efficiency, making them highly effective in Fenton-like processes. According to their distinctive geometric and electrical characteristics, SACs often demonstrate superior catalytic activity compared to conventional nanoparticle catalysts (NPCs) [143]. This highlights the prominence of SACs in achieving enhanced performance in Fenton-like reactions.

2.5.2 Photo-Fenton Process for Antibiotic Degradation

The primary functions of photo-Fenton processes are to enhance catalytic efficacy and generate energy through various light sources, including solar-simulated light, sunlight, visible light, and ultraviolet light. This approach reduces the required catalyst quantity in both homogeneous and heterogeneous Fenton reactions by enhancing the conversion of Fe^{3+} to Fe^{2+} in the presence of light, thereby improving efficiency and promoting the production of higher concentrations of $HO^{\bullet}$ radicals. Additionally, this method facilitates further reactions, producing other ROS such as superoxide ($O_2^{\bullet-}$), singlet oxygen ($^1O_2$), and H_2O_2 [57, 144]. The primary $HO^{\bullet}$ radicals are generated not only by the direct breakdown of H_2O_2 but also by the fragmentation and ionization of water molecules, a phenomenon attributable to photon energies exceeding the bond dissociation energy of water [17].

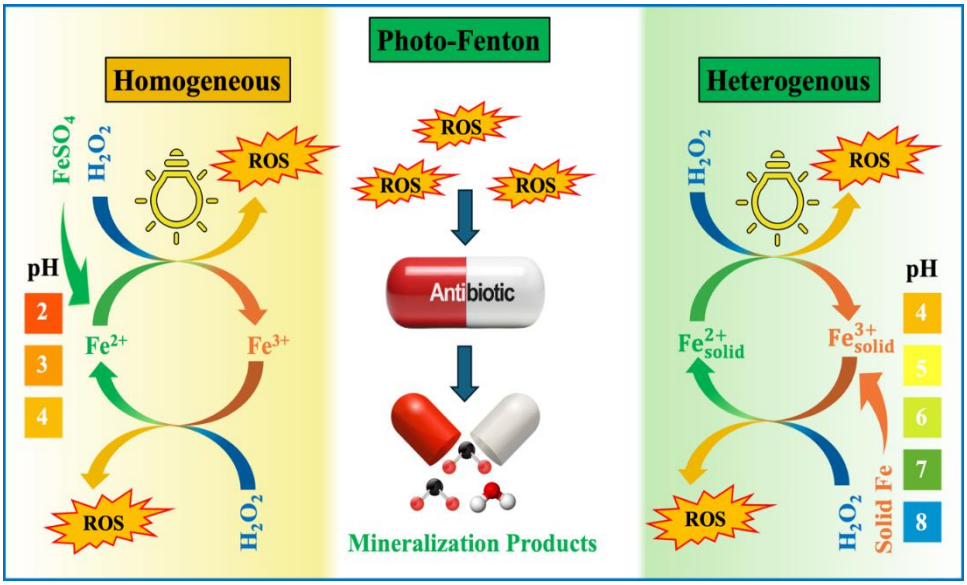

Fig. 2.5 Graphical mechanism of the photo-Fenton Process in homogeneous and heterogeneous process.

The homogeneous photo-Fenton process effectively enhances antibiotic elimination and reduces catalyst quantities and operational expenses. However, practical applications are limited due to challenges in catalyst recovery, the generation of Fe-containing sludges causing secondary pollution, and stringent pH requirements [36, 98, 145]. The heterogeneous photo-Fenton process, utilizing iron-based semiconductors, serves as an alternative technique to degrade antibiotics. Combining photocatalysis with the Fenton process enhances the generation of active species and mineralization efficiency [98, 146, 147]. Selecting appropriate photocatalytic materials can further enhance electron transport and reduce electron-hole recombination, improving overall Fenton process performance [36, 148, 149]. Addressing the rapid recombination of photogenerated carriers is crucial for improving photocatalysis efficiency, which can be achieved through incorporating co-catalysts, creating heterojunctions, introducing dopant atoms, constructing nanoscale photocatalysts, and adding sensitizers or light-absorbing dopants [52, 150-152]. Fig. 2.5 Graphical mechanism of the PF Process in homogeneous and heterogeneous systems. A comprehensive summary of the research on the homogeneous and heterogeneous PF processes for antibiotic removal is presented in Table 2.3 and Table 2.4.

Lanthanum (La) compounds are not commonly utilized as photocatalysts, yet they are known to enhance light sensitivity and catalytic reaction efficiency. A heterojunction with lanthanum-doped bismuth ferrite effectively absorbs solar-simulated light, leading to the degradation of 84.94% of norfloxacin within two hours, a rate approximately 6.9 times faster than that of undoped $BiFeO_3$ [150]. Similar enhancements have been reported for α-Fe_2O_3/BiOI [153], FePOM/CNNS-Nvac [52], g-C_3N_4/ Fe_2O_3 [151], FeS_2/g-C_3N_4[154] for tetracycline; Iron (II) phthalocyanine (FePc) with g-C_3N_4 [152] for oxytetracycline; Fe-impregnated $BiVO_4$ [155] and TiO_2/γ-Fe_2O_3/GO [156] for ciprofloxacin; α-FeOOH [157] and cephalexin by MoS_2@Fe [158] for sulfadiazine. These combinations show notable effectiveness in enhancing the degradation of various antibiotics.

Despite advancements in using iron or other semiconductor materials as catalysts in the PF process, performance issues persist due to significant iron species agglomeration and the discharge of Fe ions into solution [159]. Integrating photocatalysts with appropriate support materials can improve stability, enlarge the surface area, and promote charge separation. Carbon nanotubes (CNT), sepiolite, silica, charcoal, biochar and natural clay have been utilized to enhance photo-Fenton activity [146, 160-164]. MWCNTs have a substantial fixed surface area and excellent conductivity, which helps in separating photogenerated carriers, leading to exceptional photo-Fenton performance. When combined with $NiFe_2O_4$, MWCNTs successfully decomposed sulfamethoxazole and achieved a 68% mineralization efficiency, surpassing the performance of $NiFe_2O_4$ alone [146]. Similarly, other supported material, such as biochar integrated with Ag^0/Fe^0 bimetallic nano-catalyst showed higher mineralization efficiency of 68.0% for sulfamethoxazole (SMX) and 70.4% for amoxicillin (AMX) [165]. Additionally, FeSA/WO_3/BiOBr showed superior efficacy in degrading ciprofloxacin, achieving 100% degradation and 45% mineralization efficiency [34].

2.5.3 Sono-Fenton or Sono Photo-Fenton Process for Antibiotic Degradation

The integration of ultrasound (US) irradiation into Fenton processes, known as the sono-Fenton process, shows promise for breaking down antibiotics in wastewater. Various additives are used in ultrasound treatment to speed up antibiotic degradation

and minimize treatment expenses [110]. H_2O_2 acts as not only a potent oxidizing agent but also a promoter in sonolysis processes, decomposing into hydroxyl ($HO^{\bullet}$) radicals within cavitation bubbles due to its lower dissociation energy (213 kJ/mol) compared to the O-H bond in H_2O [166]. Antibiotics are effectively eliminated using H_2O_2/US with heterogeneous catalysts, enhancing the efficiency of sono-Fenton process (Fig. 2.6). For instance, Ma et al. (2018) demonstrated that nanosized zero-valent copper (nZVC) activated H_2O_2 in combination with ultrasound for the oxidative degradation of norfloxacin (NOR), achieving a 91.5% elimination efficiency due to the synergistic effect between sonolysis and the Fenton reaction [167]. Similarly, Damiri et al. (2020) reported that a combination of sediment catalyst, H_2O_2 and US degraded amoxicillin (AMX) by 97.66% under optimal conditions: pH 5, 50 mg/L AMX, 4.5 g/L sediment catalyst, 37 kHz US frequency, and 50 mM H_2O_2 concentration [168].

Magnetic Fe_3O_4 nanoparticles have shown potent activity in the Fenton process, with enhanced levofloxacin degradation observed in the presence of US/ H_2O_2 due to increased generation of active radicals and nucleation sites for cavity formation [169]. The inherent peroxidase-like activity of Fe_3O_4 magnetic NPs (MNPs) also contributes to the enhanced efficiency of the US/ H_2O_2/ Fe_3O_4 system, as ultrasonication inhibits catalyst aggregation and modifies surface physiochemical properties [170]. Similar US methods based on H_2O_2 have been created to remove different antibiotic pollutants and achieving high removal rates with the Fenton-based US process [37, 38]. Moreover, ultrasonic irradiation promotes the regeneration of ferrous ions and the generation of additional $HO^{\bullet}$ radicals from water, where H_2O_2 is used or not. This process facilitates the efficient degradation of antibiotics even at lower concentrations of Fenton reagents [171]. For example, treating synthetic wastewater containing metronidazole (MTZ) with 400 mg/L of Fe_3O_4@HZSM-5 at a 40 kHz ultrasound frequency resulted in nearly 98% removal of MTZ and 81% reduction of TOC after just 40-minute treatment. In contrast, the removal efficiency in real wastewater was slightly lower, at 83% [170]. Another study showed that employing lower US frequency (20 kHz) resulted in 83.1% degradation and 42% mineralization efficiency for 50 mg/L of chloramphenicol. This approach utilized sodium percarbonate, which acts as a solid carrier for H_2O_2) with n-Fe_2O_3. Here, hydroxylamine (HA) in its protonated form effectively reduced Fe^{3+} to Fe^{2+} [172].

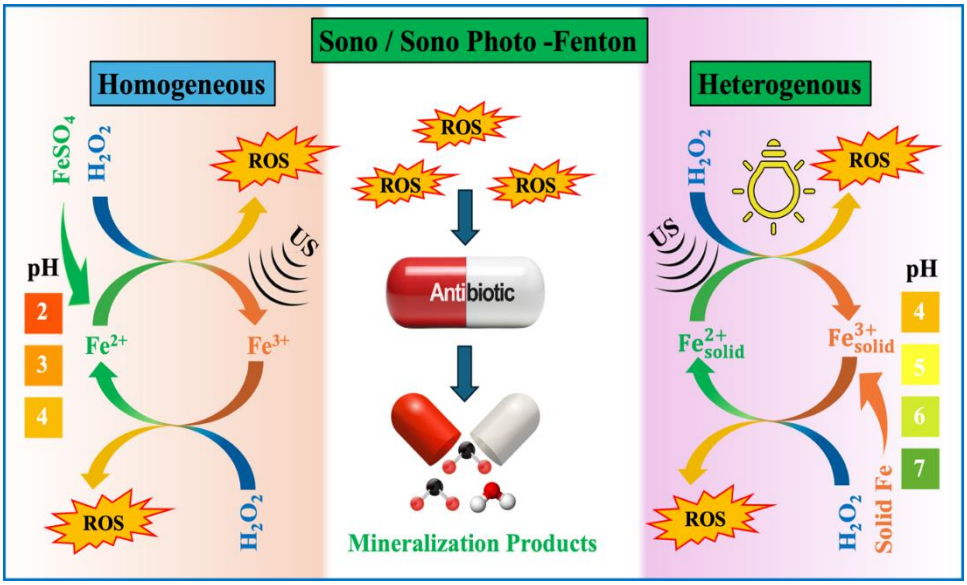

Fig. 2.6 Graphical mechanism of the sono or sono-photo-Fenton process in homogeneous and heterogeneous process.

The sono-photo-Fenton process combines ultrasonic (US) and light irradiation to create reactive species (RSs) such as $HO^{\bullet}$, $HOO^{\bullet}$, and $H^{\bullet}$, which prevents the recombination of these species and increases the efficiency of degrading contaminants at lower US frequency. For example, when using a spinel ferrite cobalt on an activated carbon nanocatalyst at a 20 kHz US frequency, nearly 95.7% degradation of MTZ was achieved within 90 minutes. This is compared to only 42.1% removal efficiency with photo-Fenton systems alone [38]. Another study showed that a bit higher US frequency (40 kHz) resulted in 95.65% of CIP degradation efficiency using red mud/rice husk biochar composite (RMR) with in situ generation of H_2O_2, compared to 75.97 for the sono-Fenton process [173]. The advantages of the sono-photo-Fenton process include reduced chemical and catalyst requirements, ease of operation, wide pH tolerance, and compatibility with other methods. However, there are also some disadvantages, such as high energy consumption and the need for special reactors using light, increasing initial and operating costs. Despite these factors, the SPF technique offers a reliable way to improve the breakdown of newly discovered pollutants in wastewater treatment. A comprehensive summary of the research on the homogeneous and heterogeneous sono Fenton processes for antibiotic removal is presented in Table 2.5.

2.5.4 Electro-Fenton Process for Antibiotic Degradation

The Electro-Fenton (EF) process employs the Fenton reaction, in which H_2O_2 is electrochemically produced at the cathode by reducing oxygen (Fig. 2.7). An iron-containing catalyst facilitates this reaction, generating highly reactive $HO^{\bullet}$ radicals that can oxidize pollutants. EF processes are classified into four types based on the addition or generation mechanism of the Fenton reagents (H_2O_2 and Fe^{2+}) [174]. Type I (actual electro-Fenton) involves the *in-situ* production of H_2O_2 and the external addition of Fe^{2+}. Type II (peroxi-coagulation) generates both H_2O_2 and Fe^{2+} electrochemically using a sacrificial iron anode. Type III (Fered-Fenton) externally adds both reagents and regenerates Fe^{2+} at the cathode. Type IV (electrochemical peroxidation) adds H_2O_2 externally while generating Fe^{2+} *in-situ.* Each type optimizes pollutant degradation differently, offering advantages such as cost-efficiency, reduced sludge production, and enhanced safety by preventing H_2 production, making EF processes effective and environmentally friendly for wastewater treatment [175]. The simultaneous on-site production of H_2O_2 and the cathodic regeneration of Fe^{2+} from Fe^{3+} enhance the reaction rate and mineralization efficiency in lab-scale operations. Initially, the EF system requires a low pH of around 3, which can be expensive due to the need for pH adjustment chemicals. However, alternative methods have been developed to maintain the optimal pH using reaction-released H^+ and OH^- without additional chemicals. Nevertheless, there are still issues with non-recoverable catalysts post-reaction [176]. To address these limitations, heterogeneous EF has been proposed as a viable alternative [177]. This process typically employs Fe-based solid catalysts, such as α-FeOOH [178], FeS [179], Pd/Fe_3O_4 [180], MWCNTs-CB/GF [181], Fe^0 [39] and $FeNi_3$@C [182] to decompose H_2O_2 into $HO^{\bullet}$ radicals. For example, Du et al. (2020) utilized Fe/Fe_3C@PC as a heterogeneous EF catalyst, achieving 99% and 97% degradation of sulfamethazine and levofloxacin, respectively, within 60 minutes. The catalyst was easily recovered and recycled using a simple H_2 thermal treatment [183]. Moreover, novel heterogeneous catalysts like Cu-Fe-NLDH have demonstrated impressive performance, with a 93% reduction of gentamicin in 100 minutes at pH 3 and 400 mA current flow [184]. Droguett et al. (2020) employed a cell with a titanium-iridium dioxide anode and a gas diffusion electrode cathode to treat cefalexin, achieving complete removal at pH 3 and 50 mA/cm^2

current density within 30 minutes and a 43% mineralization after 300 minutes. Despite some loss of surface material, these catalysts showed excellent reusability. The minimal current efficiency (MCE) was 2%, and the electrical energy consumption for TOC removal (ECTOC) was 8.67 kWh [185].

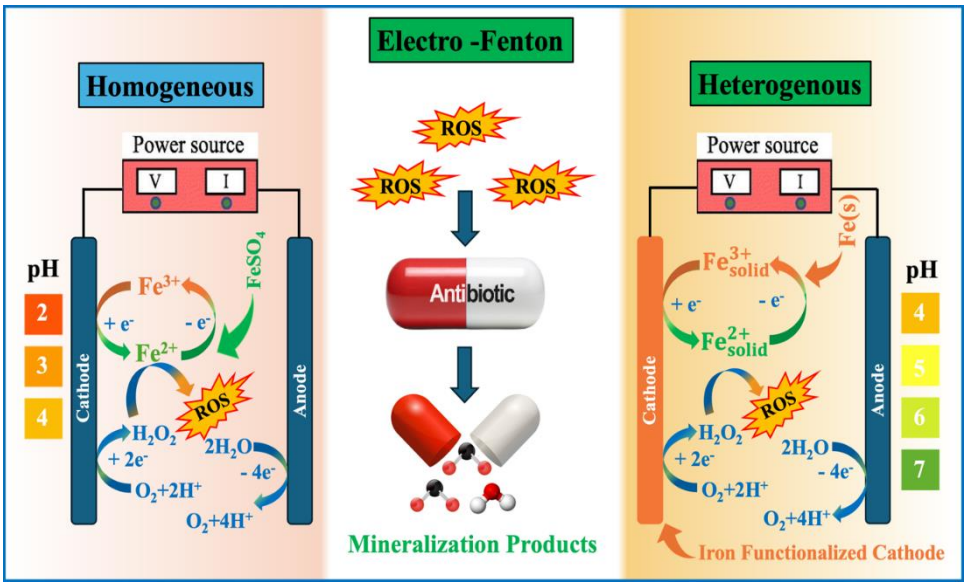

Fig. 2.7 Graphical mechanism of the electro-Fenton process in homogeneous and heterogeneous process.

The oxidation capacity of the EF process can be significantly increased when the solution is exposed to light, leading to the photo-electro-Fenton (PEF) process [186, 187]. The primary disadvantage of utilizing artificial light sources is their substantial energy expenditure in practical implementation. To address this issue, researchers have suggested using sunlight directly as a sustainable and cost-effective energy resource. The significant impact of UV irradiation in these photo-assisted electrochemical advanced oxidation processes (EAOPs) can be attributed to two main factors [188]: (i) the breakdown of $Fe(OH)^{2+}$ by photolysis and (ii) the conversion of certain Fe(III)-carboxylate complexes through photodecarboxylation. Utilizing an undivided cell in EF and solar PEF, along with a high O_2-overpotential anode (M), facilitates the simultaneous degradation of antibiotics by heterogeneous $M(HO^{\bullet})$ radicals generated as intermediates during water oxidation [188]. Boron-doped diamond (BDD) thin-film electrodes are the most desirable anodes for EAOPs due to their superior capacity to generate larger quantities of reactive BDD compared to other commonly used anodes such as Pt, PbO_2,

Ti_4O_7, carbon-felt, carbon-fiber, graphite, and dimensionally stable anodes (DSA) [111, 176, 182]. This enables more extensive mineralization of antibiotics. For instance, the BDD anode could improve the decay kinetics of ofloxacin by 1.4–2.6 times and reduce disposal costs by 28%–41%. A TOC removal efficiency of 72% was observed at a lower current of 4.2 mA/cm^2, which is better than the anodic oxidation process under 8.3 mA/cm^2 [111]. A comprehensive summary of the research on the homogeneous and heterogeneous Electro Fenton processes for antibiotic removal is presented in Table 2.6.

2.6 Practical Applications of Fenton Processes

The majority of research on Fenton processes for breaking down antibiotics focuses on individual compounds in ultrapure water, drinking water, or synthetic water matrices [18]. Only a few studies have examined the application of these processes to real-world wastewater effluents [72, 189, 190]. Additionally, there is a lack of information on using traditional Fenton and modified Fenton processes for treating real wastewater containing antibiotics at very low concentrations, such as those in the ppb range (μg/L to ng/L). Real wastewater differs significantly from synthetic samples used in laboratory studies due to its complex mix of various contaminants, variables pH levels, and unknown matrix effects. These factors can greatly impact the effectiveness of Fenton processes, as real wastewater often contains alkalinity, low conductivity, and substantial amounts of radical scavengers, such as chloride, carbonate, and bicarbonate, which can reduce the efficiency of conventional Fenton treatments. Although laboratory studies have extensively documented the effectiveness of various Fenton processes, their practical implementation shows promise for real-world application. For instance, a 1.5 L solar-Fenton reactor, using 3.0 mg/L of Fe(III)-EDDS (in a 1:2 ratio) and 2.75 mg/L of H_2O_2, achieved 90% degradation of amoxicillin and 70% degradation of acetaminophen in municipal wastewater treatment plant (MWTP) effluent after 210 minutes of operation at neutral pH [72]. Complete elimination of acetaminophen required five additional increments of 2.75 mg/L of H_2O_2, as the consumption of H_2O_2 exceeded optimal levels due to the presence of other compounds that consume hydroxyl radicals, including organic matter, humic acids, carbonates, and bicarbonates. This experiment was conducted using a solar simulator light. Multiple factors influence the cost of the PF

process, including radiation energy levels and the availability of Fenton reagents [191]. Additionally, integrating solar reactors with pre-treatment or polishing processes can lead to further costs reductions. This integration offers advantages such as lowered installation and maintenance costs, as well as reduced electricity consumption. A notable practical application was demonstrated in a study at the El Bobar wastewater treatment plant (WWTP) in Almería, Spain. This study involved the construction of a 100 m^2 raceway pond reactor (RPR) with a liquid depth of 18 cm. The operational plant served a population equivalent to 230,000 and has treatment capacity of 30,000 m^3 per day. It not only reduced construction costs but also allowed for adjustment in liquid depth based on the availability of UV radiation from sunlight. The study showed that over 85% of 115 emerging contaminants were successfully removed from the real WWTPs [190].

To operate the Fenton treatment process at a neutral pH, chelating agents were used to prevent iron precipitation by binding to iron in laboratory experiments. Lab-scale experiments demonstrated that a very low iron dose of 0.054 mM was sufficient to remove 97% of the model compounds (MCs). However, when treating real MWTP effluent with the same MCs, a higher iron dose of 0.1 mM was required, resulting in an 87% removal of the MCs. The pilot-scale reactor efficiently eliminated all the studied MCs, using optimal conditions determined at the lab scale with a solar simulator [189]. These removal percentages align with findings from previous RPR pilot-scale studies on solar photo-Fenton treatment of municipal effluents. Molina et al. [192] found that over 80% of contaminants of emerging concern (CEC) were removed within 15 minutes of treatment in a 5 cm deep RPR plant using the Fe-EDDS reagent [192]. Similarly, Arzate et al. (2017) reported 84% and 89% CEC removal rates in a 5 cm deep RPR operating in continuous flow mode with hydraulic retention times (HRT) of 40 and 80 minutes, respectively [193].

Recent advancements in wastewater treatment technologies have shown promising potential for the sono-Fenton process due to its simple operation and efficient production of reactive species. Although acoustic cavitation (AC) has shown significant promise in laboratory settings, real- world applications remain underexplored. Studies have demonstrated that high ultrasonic frequencies, typically ranging from 350 to 500

kHz, effectively eliminating antibiotics at the laboratory scale. Furthermore, pilot-scale applications suggest that even higher frequencies (>500 kHz) could enhance wastewater treatment in practical scenarios [194]. However, the considerable expenses associated with ultrasonic treatments prompt a reconsideration of the method by incorporating light irradiation to achieve synergistic effects and lower treatment costs. For example, a half liter sample of real wastewater containing a reactor was effectively utilized to degrad fifteen pharmaceuticals by using ultrasound and photocatalytic system in Colombian hospital wastewater. This approach achieved approximately 91% removal efficiency within 1.5 hours using a sonochemical process (375 kHz and 88 W L^{-1}, 1.5 h) with Fe^{2+} (5 ppm) and UVC light (4 W). These results surpassed the efficiency of the SPF process, which achieved an 82.86% removal rate [195].

The electro-Fenton (EF) process is gaining attention due to its potential application at pilot or full-scale levels for real wastewater treatment, which handles complex and diverse contaminants. Despite most EF studies being laboratory-based, scaling up poses challenges such as optimizing degradation efficiency, hold-up time, area requirements, and economic feasibility. The investment and operating costs are significant considerations, particularly for electrode development and energy consumption. For example, Basturk et al. [196] conducted an economic feasibility study of the EF process for degrading cephalexin, ciprofloxacin, and clarithromycin antibiotics from medical laboratory wastewater. However, translating these findings to industrial scales presents challenges due to the idealized conditions of laboratory experiments. Effective scale-up of EF process requires innovative approaches, such as developing cost-effective, high-performance electrode materials, optimizing operational conditions, and integrating hybrid systems. Bugueño-Carrasco et al. [187] evaluated a solar photo-electro-Fenton pilot facility for degrading pharmaceuticals, including ampicillin, sulfamethazine, tetracycline, and non-steroidal anti-inflammatories. This pilot plant features an electrochemical filter press cell with a dimensionally stable anode (DSA) and an air-diffusion cathode connected to a solar photoreactor exposed to sunlight. Complete degradation of all pharmaceutical drugs was achieved within 10 minutes, and TOC removal efficiency reached 99.2% after 100 minutes, with an energy consumption of 534.23 kWh and 7.15 kWh/m^3. The treatment costs ranged from 0.064 to 1.01 USD per

cubic meter of pharmaceutical wastewater. Over the past decades, the Brillas working group has published numerous articles on EF processes using a pre-pilot plant for treating various wastewater [197, 198]. In photo-electro-Fenton (PEF) setups, the plant is connected to an annular photoreactor with a 160W UVA lamp, enhancing oxidation power in the order EO-H_2O_2 ≪ EF < PEF. The superiority of PEF over EF is attributed to additional Fe^{2+} regeneration and $HO^{\bullet}$ production induced by light. Moreover, continuous electrochemical reactors are gaining attraction for their improved treatment efficiency, chemical reduction, high reproducibility, and ease of scale-up. A novel system termed the solar electrochemical raceway pond reactor (SEC-RPR) combines a raceway pond reactor with an electrochemical system. It has shown promising results in degrading contaminants of emerging concern (CECs) in MWWT effluents [186]. This involves the reaction of Fe^{2+} with H_2O_2, generated through the reduction of O_2 at an air diffusion cathode. The SEC-RPR process further boosts the mineralization efficiency up to 55% with extended treatment time. A comprehensive summary of the research on the degradation of antibiotics on a pilot scale study is presented in Table 2.7.

Table 2.1. Degradation of Antibiotics by Homogenous Fenton Process

Antibiotics Name & dose (mg/L)	**Fe^{2+} dose (mg/L or mM)**	**Dose of H_2O_2 (mM)**	**Solution pH**	**Removal efficiency (%)**	**Reaction time (min)**	**Reference**
Amoxicillin (104)	4.687	46.87	3.0	100	2	[119]
Ampicillin (105)				100		
Cloxacillin (103)				100		
Amoxicillin (105)	25	0.007	3.5	100	2.5	[199]
Ampicillin (20)	0.87	0.373	3.7	100	10	[200]
Doxycycline (100)	25	17.99	5	100	10	[201]
Chlortetracycline (34.22)	0.3	0.3	3	76	106	[87]
Sulfamethoxazole (200)	1	4	3	100	10	[124]
Trimethoprim (14.5)	4 mM	1	3	100	20	[125]
Ciprofloxacin (53.21)	17.46	74.55	4.57	74	25	[202]
Ciprofloxacin (10)	5	25.6	3	76	45	[121]
Ciprofloxacin (100)	1.42	14.2	7	70	15	[122]
Ciprofloxacin (8)	20	2.35	5.8	64	80	[203]
Amoxicillin (100)	112	0.03	3	82.67	20	[204]

Tetracycline (50)	0.05	0.1	3	71	10	[123]
Sulfathiazole (0.1)	0.15	2	3.45	<90	10	[112]
Ampicillin (0.27)	1	2.5	3.5	100	30	[94]
Doxycycline (0.1)	1	1	3.5			
Tylosin (0.19)	5	20	3.5			

Table 2.2. Degradation of Antibiotics by Heterogeneous Fenton and Fenton-Like Process

Antibiotics Name & dose (mg/L)	Catalyst Name and dose (mg/L or mM)	Dose of H_2O_2 (mM)	Solution pH	Removal efficiency (%)	Reaction time (min)	Reference
Ofloxacin (10)	50 mg/L of alginate beads/CDTA	10.0	3	94	120	[205]
Ciprofloxacin (10)	280 mg/L of nZVI	100.0	7	100	30	[127]
Ciprofloxacin (10)	500 mg/L of $FeCuO_2$	10.0	6	10	30	[73]
Ciprofloxacin (10)	200 mg/L of sludge Biochar	60.0	4	90	240	[206]
Metronidazole (20)	0.5g/L of 3D-GN@Cu^0	2.0	3.2	92	120	[207]
Tetracycline (100)	100 mg/L of Fe^0@CeO_2	100	5.8	94	60	[128]
Tetracycline (30)	500 mg/L of Pig manure Biochar	5.0	7.4	100	240	[135]
Ofloxacin (30)	1000 mg/L of $MnFe_2O_4$@C-NH_2	29.4	3	97.4	180	[102]
Amoxicillin (30)				99.1	180	
Tetracycline (30)				95.5	180	
Ofloxacin (20)	230 mg/L of rGO-Fe_3O_4	50.0	7	99.9	60	[129]
Tetracycline (30)	1000 mg/L of $MnFe_2O_4$-HSO_3	29.4	3	87.6	180	[136]
Ciprofloxacin (20)	500 mg/L of Fe $(Fe_{0.69}Al_{0.31})_2O_4$@C	1.2	3	51	180	[208]
Ofloxacin (20)	20 mg/L of (Fe-$PW_{12}O_{40}$)/ Bi_4TaO_8Cl	1.5	3	52.77	60	[209]
Tetracycline (20)	20 mg/L of Fe-polyoxometalate decorated Bi_2MoO_6	1.5	3.5	37.16	18	[98]
Sulfamethoxazole (10)	10 mg/L of MIL-101-NH_2 -Fe	1.0	5.4	100	70	[132]
Ciprofloxacin (20)	1g/L of $CuCoFe_2O_4$@AC	73.5	7.0	95.77	120	[131]
Sulfamethoxazole (130)	1.2 g/L of iron-loaded biochar	20	3.0	98.37	480	[130]

Table 2.3. Degradation of Antibiotics by Homogenous Photo-Fenton and Fenton-Like Process

Antibiotics Name & dose (mg/L)	**Catalyst Name & dose (mg/L or mM)**	**H_2O_2 dose (mM)**	**Light Sources and Solution pH**	**Removal efficiency (%)**	**Reaction time (min)**	**Reference**
Ciprofloxacin (15)	0.05 mM of Fe^{2+}	5.0	6 W of UV lamp pH = 4, UPW/SWW	100	45	[210]
Sulfamethazine (50)	50 mg/L of Fe^{2+}	17.6	300 W Sunlight lamp pH = 3, UPW	100	2	[211]
Chloramphenicol (209)	10 mg/L of Fe^{2+}	11.75	400 W High-pressure mercury vapor lamps pH = 2.8, UPW	98	16	[212]
Thiazole (0.047)	0.157 mM of Fe^{2+}	1.2	20 W UV light pH = 3, DW	90	8	[213]
Sulfamethazine (50)	0.2mM of Fe^{2+}	1.0	White LED light pH = 3, UPW	90	30	[214]
Tylosin (15)	6 mg/L of Fe^{2+}	0.01	11W UV light pH = 2.6, UPW	97.1	210	[215]
Sulfamethoxazole (40)	0.179mM of Fe^{2+}	0.1	1500 W Xenon lamp pH = 3, DW	99.7	50	[33]
Cephalexin (50)	0.2 mg/L of Fe^{2+}	9.0	UV lamp pH = 3.5, UPW	51.7	180	[158]
Chloramphenicol (6.5)	0.04 mM Fe^{3+}	0.5	Xenon arc lamp pH = 3, UPW	100	60	[216]

Table 2.4. Degradation of Antibiotics by Heterogeneous Photo-Fenton and Fenton-Like Process

Antibiotics Name & dose (mg/L)	**Catalyst Name & dose (mg/L or mM)**	**H_2O_2 dose (mM)**	**Light Sources and Solution pH**	**Removal efficiency (%)**	**Reaction time (min)**	**Reference**
Cefuroxime (20)	1000 mg/L of α-Fe_2O_3-TiO_2	5.3	30W Solar simulator light pH = 3, DW	100	150	[217]
Tetracycline (20)	500 mg/L of CuCN	80	300W Xenon lamp pH = 7, UPW	93.6	60	[218]
Cephalexin (50)	0.63 mg/L of FS/FA/TiO_2 beads	4.4	36 W UV Tubes pH = 3.5, UPW	89	240	[219]
Norfloxacin (0.5)	1200 mg/L of Fe_3O_4/ multi walled carbon nanotubes	0.098	300 W Xenon lamp pH = 3, UPW	90	180	[220]
Ofloxacin (10)	500 mg/L of ferrocene@ sepiolite (FeCp@Sep)	2.0	300 W Xenon lamp pH = 3, UPW	100	150	[160]
Tetracycline (40)	50 mg/L of $MnFe_2O_4$/biochar	100	300W Xenon lamp pH = 5.5, UPW	93	120	[163]
Amoxicillin (50)	1000 mg/L of flyash	10	150 W UV lamp pH = 7.1, UPW	36.1	240	[139]
Tetracycline (20)	1000 mg/L of α-Fe_2O_3/BiOI	10	35 W Xenon lamp pH = 6.5, UPW	80.3	30	[153]
Ciprofloxacin (10)	200 mg/L of Fe-$BiVO_4$	0.04	35 W Xe lamp pH = -	99	30	[155]

Ciprofloxacin (10)	20 mg/L of TiO_2/γ-Fe_2O_3/GO	9.7 mM	300 W of Xenon lamp pH = 6.6, UPW	99	140	[156]
Sulfamethoxazole (5)	25 mg/L of $NiFe_2O_4$-MWCNT	8.82	150 W of Xenon arc lamp (UV light), pH = 5, UPW	99	120	[146]
Tetracycline (20)	1.0 g/L of FePOM/CNNS-Nvac	10	300 W of Xenon lamp pH = 4.5, UPW	96.5	18	[52]
Tetracycline (60)	300 mg/L of $ZnFe_2O_4$	20	LED lamp (420 nm) pH = 2, UPW	94.2	40	[221]
Tetracycline (20)	200 mg/L of g-C_3N_4/ND Fe_2O_3	50	300W of Xenon lamp (UV) pH = 7, UPW	87	60	[151]
Tetracycline (50)	50 mg/L of FeS_2/g-C_3N_4	50	50 W of Xenon lamp (UV) pH = 10, UPW	93	60	[154]
Tetracycline (20)	200 mg/L of $CuFeO_2$/ biochar	20	300 W of Xenon lamp (UV) pH = 5.5, UPW	92.5	120	[162]
Cephalexin (50)	150 mg/L of MoS_2@Fe	26.4	UV lamp pH = 3.5, UPW	73	180	[158]
Sulfamethoxazole (20)	100 mg/L of PPyC@Py-MIL (Fe)	0.1	300 W Xenon lamp pH = 6.5, UPW	93	60	[138]
Sulfamethoxazole (5)	300 mg/L of Fe_3S_4	9.79	10 W of LED (UV) pH = 5, UPW	100	25	[147]

Tetracycline (20)	500 mg/L of Fe-doped porous carbon nitride	80	300 W of Xenon lamp pH = 7, UPW	94.6	80	[222]
Ciprofloxacin (20)	500 mg/L of FeSA/WO_3/ BiOBr	1.6	500 W of Xenon lamp pH = 5.6 - 5.8, UPW	100	60	[34]
Ofloxacin (10)	20 mg/L of (Fe-$PW_{12}O_{40}$)/ Bi_4TaO_8Cl (FPWBT)	3.0	5W LED light pH = 3, UPW	98.87	60	[209]
Norfloxacin (10)				98.18	90	
Ciprofloxacin (10)				97.26	90	
Tetracycline (50)	40 mg/L of Cd/CdS-CuO/Fe_2O_3/ $CuFe_2O_4$	20	300W of Xenon lamp pH = 7, UPW	82.43	90	[149]
Norfloxacin (20)	500 mg/L Fe-TNFs	17.6	100 W White LED pH = 6.8, UPW	95	300	[36]
Tylosin (20)				60	300	
Tetracycline (20)				95	300	
Tetracycline (20)	20 mg/L of Fe-polyoxometalate decorated Bi_2MoO_6	1.5	5W White LED pH = 3.5, UPW	99.79	18	[98]
Ofloxacin (20)				98.68		
Norfloxacin (20)				93.69		
Ciprofloxacin (20)				89.78		
Sulfamethoxazole (20)				81.82		
Tetracycline (20)	400 mg/L of $NaFeSi_2O_6$/ Fe_3O_4 – Fe_2O_3	20	300 W Xenon arc lamp pH = 6.5, UPW	91.8	50	[148]

Oxytetracycline (10)	125 mg/L of FePc/g-C_3N_4	1000	300 W Xenon lamp pH = 5, UPW	88.48	60	[152]
Norfloxacin (10)	1500 mg/L La-doped $BiFeO_3$	15	300 W Xenon lamp pH = 5, UPW	84.94	120	[150]
Oxytetracycline (10)	1000 mg/L iron-doped resorcinol formaldehyde (FRF) resin	-	5 W Simulated solar light pH = 5, UPW	99.9	60	[159]
Sulfamethoxazole (2.0)	250 mg/L Ag^0/Fe^0/biochar	0.10mL/L	9 W UV-A lamps pH = 3, UPW	82.6	120	[165]
	150 mg/L Ag^0/Fe^0/biochar	0.25 mL/L		92.8		

Table 2.5. Degradation of Antibiotics by Sono-Fenton Process

Antibiotics Name & dose (mg/L)	**Catalyst Name & dose (mg/L or mM)**	**H_2O_2 dose (mM)**	**Ultrasound irradiation and other parameters**	**Removal efficiency (%)**	**Reaction time (min)**	**Reference**
Tinidazole (45)	200 mg/L of Fe^0	1000	US = 130 kHz, 800W, pH = 3, UPW	93	150	[223]
Levofloxacin (20)	1000 mg/L of Fe_3O_4	5.0	US = 20 kHz, 195 W, pH = 7.14, UPW	99	150	[224]
Tetracycline (100)	1000 mg/L of Fe_3O_4	150	US = 20 kHz, 100 W, pH = 3.7, UPW	93.6	60	[104]
Clindamycin (45)	200 mg/L of Fe^0	1000	US = 130 kHz, 500 W, pH = 3, UPW	95	150	[225]
Metronidazole (500)	3 mM/L of Fe^{2+}	60	US = 20 kHz, -W, pH = 3, UPW	90	120	[171]
Norfloxacin (5)	0.25 g/L of nZVC	20	US = 20 kHz, 240 W, pH = -, UPW	91.5	30	[167]
Azithromycin (20)	1000 mg/L of ZnO	50	US = 35 kHz, -W, pH = 3, UPW	98.4	15	[226]
Amoxicillin (100)	800 mg/L of ZnO/Fe_3O_4	2.0	US = 20 kHz, 60W, pH = 3, UPW	90	120	[227]
Cephalexin (50)	8 mg/L of Fe^{2+}	60 mg/L	US = 130 kHz, -W, pH = 3, UPW	90	60	[228]
Amoxicillin (5)	4.5 g/L of sea sediment	50	US = 37 kHz, 320 W, pH = 5, UPW	97.7	60	[168]
Tetracycline (10)	300 mg/L of Fe-MOF (MIL-88B)	44	US = 40 kHz, 60W, pH = 5, UPW	>80	7	[229]

Tetracycline (8)	1000 mg/L of nano-pyrite	4.0	US = 26 kHz, 200W, pH = 3, UPW	93.1	20	[230]
Tetracycline (10)	300 mg/L of $MnFe_2O_4$/rGO	12	US = 40 kHz, 450W, pH = 3, UPW	92.85	120	[37]
Metronidazole (25)	400 mg/L of Fe_3O_4@HZSM-5	1.0	US = 40 kHz, 50W, pH = 7, SWW	98	40	[170]
Metronidazole (30)	300 mg/L of spinel ferrite cobalt on activated carbon	4.0	US = 20 kHz, 50W, pH = 3, UPW	89	90	[38]
Chloramphenicol (50)	2500 mg/L of n-Fe_2O_3	-	US = 20 kHz, 200W, pH = 3, UPW	83.1	120	[172]
Ciprofloxacin (20)	1000 mg/L of red mud/rice husk biochar	-	US = 40 kHz, 600W, pH = 3, Distilled water	75.97	180	[173]
		-	US = 40 kHz, 600W, pH = 3, 8W UVA lamp, Distilled water	95.65		

Table 2.6. Degradation of Antibiotics by EF Process

Antibiotics Name & dose (mg/L)	Catalyst Name & dose (mg/L or mM)	H_2O_2 dose (mg/L or mM)	Electrode, pH and Other Parameters	Removal efficiency (%)	Reaction time (min)	Reference
Sulfadiazine (10)	0.4 mM of Fe^{2+}	73.5	DSA/graphene, pH = 7.1, I = 50 mA	99	120	[231]
Amoxicillin (100)	0.5 mM of Fe^{2+}	309	MWCNTs-CB/GF electrode Ti|RuO_2-IrO_2/MWCNTs-CB/GF pH = 5.5, J = 12mA cm^{-2}	98.7	30	[181]
Amoxicillin (10)	26.17 mg/L of $FeSO_4.7H_2O$	17.68	Cubic cell (BDD, DSA/SS pH = 2.29, I = 366.08 mA	97	30	[232]
Amoxicillin (20)	1000 mg/L of Fe_2O_3	38.0	Pt sheet/GF, pH = 3, I = 300 mA	98.2	60	[233]
Metronidazole (80)	500 mg/L of Fe_3O_4–GO	-	Pt gauze/CF, pH = 3, I = 300 mA	100	15	[234]
Gentamicin (20)	1.25 g/L of Cu-Fe-NLDH	20 μM	Pt sheet/graphite, pH = 6, I = 400 mA	91.3	100	[184]
Cephalexin (50)	1 g/L of chalcopyrite	4.5 mM	IrO_2/air diffusion cathode pH = 3, I = 125 mA	94	15	[185]
Sulfamethazine (10)	50 mg/L of Fe/Fe_3C@CP	68.0	Ti–RuO_2/CB–CF, pH = 4, I = 25 mA	99	30	[183]
Levofloxacin (80)			Ti–RuO_2/CB–CF, pH = 3, I = 25 mA	97	60	

Cefazolin (20)	1.25 g/L of CuFeNLDH-CNTs	-	Pt sheet/CUFeNLDH–CNTs-graphite, pH = 6, I = 300 mA	89.9	100	[235]
Sulfamethazine (10)	224 mg/L of Fe^0 20 mg/L of MoS_2	-	Ti|RuO_2-IrO_2/GF, pH = 4, I = 50 mA	100	10	[39]
Levofloxacin (20)	1 mM of Fe^{2+}	-	CF/FeNC, pH = 3, I = 100 mA	96.1	40	[40]
Ofloxacin (0.1 mM)	0.2 mM of Fe^{2+}	6.7 mg/h	EEGr and BDD, pH = 3, I = 8.33 mA	100	30	[111]
Levofloxacin (30)	0.1 mM of Fe^{2+}	-	Fe@Co/GF, pH = 3, I = 5 mA/cm^2	90.38	160	[236]
Sulfamethoxazole (20)	-	-	CeO_2@MoS_2@GF, pH = 3, I = 5 mA/cm^2	97.1	60	[237]
Sulfamethoxazole (10)	-	-	Cu-Al LDO/HGF, pH = 5.6, I = 5 mA/cm^2	100	60	[238]
Metronidazole (20)	metal-free	-	AGF/BN-GF, pH = 5.8, I = 5 mA/cm^2	99.9	30	[176]
Oxytetracycline (10)	30 mg/L of $FeNi_3$@C	-	$FeNi_3$@C/CP, pH = 3, I = 60 mA	95.4	90	[182]
Tetracycline (20)	-	-	CuFe@NCNT/CMM, pH = 6.5, I = -	82.2	120	[177]

Table 2.7. Degradation of Antibiotics in a Pilot Scale Study

Antibiotics Name & dose (mg/L)	Catalyst Name & dose (mg/L or mM)	H_2O_2 dose (mM)	Operating parameters	Removal efficiency (%)	Reaction time (min)	Reference
Ofloxacin (0.1)	5 mg/L Fe^{2+}	75 (mg/L)	Sunlight, CPC pilot plant pH = 2.8-2.9, SWTP (250 L)	100	180	[239]
Trimethoprim (0.1)				100		
58 Micropollutants (MPs)	5.5 mg/L of Fe^{2+}	30 mg/L	Sunlight, RPR pilot plant, pH = 2.8, WWTP secondary effluent	84	40	[193]
				89	80	
18 Chemical emerging contaminants (CECs)	5.6 mg/L (0.1 mM of) of Fe^{3+}:EDDS (1:1)	0.88 mM	Sunlight, RPR pilot plant (19 L, 5 cm depth), pH = 7.4 ± 0.2, WWTP secondary effluent	> 80	15	[192]
15 Pharmaceutical drugs	5.0 mg/L of Fe^{2+}	-	UVC light (4W), pH = 7.9, hospital wastewater (350 mL)	82.86	90	[195]
17 Micropollutants (MPs)	5.0 mg/L of Fe^{2+}	-	UVA light (4W), pH = 7.48, municipal effluents (300 mL)	47.36	90	[51]
15 Pharmaceutical drugs	5.0 mg/L of Fe^{2+}	-	US frequency 375 kHz, US power 88 W L^{-1}, UVC (4W), pH = 7.9, hospital WW (350 mL)	91	90	[195]
17 Micropollutants (MPs)	5.0 mg/L of Fe^{2+}	-	US frequency 375 kHz, US power 88 W L^{-1}, pH = 7.48, municipal effluents (300 mL)	45.99	90	[51]
46 Microcontaminants	5.6 mg/L (0.1 mM of) of Fe^{3+}:EDDS (1:1)	1.47 mM	Sunlight, RPR pilot plant (90 L, 15 cm depth), pH = 7.4 ± 0.2, MWWTP effluent	> 80	20	[189]
115 Chemical emerging contaminants (CECs)	0.1 mM $FeSO_4$	1.47 mM	Sun light, RPR pilot plant, pH = 2.8, WWTP's effluents	> 85% CEC	60	[190]

2.7 Key Knowledge Gaps and Future Directions

Complex contamination and assessment in natural water bodies

Current research on Fenton processes frequently focuses on simplified, controlled environments that fail to capture the complexity of real-world water contamination. The presence of multiple contaminants in natural water bodies, including surface and groundwater, significantly complicates the assessment and effectiveness of these treatment processes. Future research should aim to elucidate the interactions between multiple pollutants in natural water environments, with an emphasis on simulating real-world conditions to evaluate the efficacy of Fenton processes in removing a diverse array of contaminants, not limited to antibiotics. This necessitates a comprehensive exploration of Fenton reactions in complex matrices, including investigating the impact of various environmental factors such as pH, ionic strength, and the presence of natural organic matter on treatment efficiency. By adopting a more holistic approach that reflects the intricate nature of environmental water systems, future studies can provide a more accurate assessment of Fenton processes and their potential for real-world applications.

Scale-up from laboratory to pilot-scale applications

The majority of research on antibiotic degradation employing Fenton processes are conducted at the laboratory scale, resulting in a limited understanding of their performance at larger pilot or full scales, particularly concerning operational stability, cost-effectiveness, and scalability. For Fenton processes to transition from laboratory to industrial applications, research should prioritize developing and testing pilot-scale reactors. These reactors could include commercial photoreactors or membrane bioreactor (MBR) systems integrated with Fenton processes. Key focus areas should involve optimizing reactor design to enhance efficiency, rigorously evaluating long-term operational stability under real-world conditions, and performing comprehensive cost-benefit analyses. Such efforts are crucial for demonstrating these processes' feasibility and economic viability on an industrial scale, thereby facilitating their broader adoption for wastewater treatment.

Development of cost-effective and high-performance plants

To transition from lab to practical applications, it is essential to address challenges such as optimizing energy efficiency, reducing chemical consumption, and ensuring cost-effectiveness. Economic assessments highlight the need for further improvements to make Fenton processes competitive with other treatment technologies. Despite these successes, pilot-scale applications of Fenton and modified Fenton processes face challenges that must be addressed for full-scale implementation. These improvements encompass minimizing iron-laden sludge formation, enhancing efficiency under environmentally relevant pH conditions, designing affordable electrodes, and reducing chemical requirements. These advancements aim to facilitate the scaling and commercialization of Fenton-based technologies, rendering them effective for treating real wastewater contaminated with antibiotics.

Comprehensive by-product analysis and toxicity assessment

The degradation of antibiotics via Fenton processes can result in the formation of various by-products, some of which may exhibit unknown or increased toxicity. Comprehensive studies on identifying, quantifying, and toxicity assessment of these by-products are currently lacking. Future research should employ advanced analytical methods, such as differential electrochemistry mass spectroscopy (DEMS), to identify and quantify the by-products generated during antibiotic degradation. Furthermore, it is imperative to prioritize the evaluation of the toxicity of these by-products to prevent the inadvertent production of more harmful compounds during treatment processes. Investigating the degradation pathways of specific antibiotics, including how reactions affect the stability and toxicity of resulting breakdown products, is crucial for enhancing the safety and efficacy of Fenton processes.

Optimization of reaction conditions and process parameters

A comprehensive understanding of the optimal reaction conditions and process parameters essential for maximizing the efficiency of Fenton processes in antibiotic removal remains limited. Parameters including pH, temperature, catalyst concentration, and reaction time warrant further investigation. Future research endeavors should prioritize systematic optimization studies aimed at elucidating the most favorable

operational parameters across different Fenton processes. This necessitates that the exploration should prioritize systematic optimization studies aimed at elucidating the most favourable impacts of various catalysts, oxidizing agents, and reactor configurations. By meticulously fine-tuning these parameters, it is possible to significantly enhance degradation efficiency and cost-effectiveness, thereby rendering the processes more suitable for large-scale applications.

Environmental impact and sustainability assessment

Although Fenton processes demonstrate efficacy in antibiotic degradation, a thorough understanding of their broader environmental implications and sustainability remains lacking. This encompasses considerations such as energy consumption, potential secondary pollution, and long-term ecological impacts. To address these knowledge gaps, comprehensive life cycle assessments (LCAs) and environmental impact studies are warranted to evaluate the sustainability profile of Fenton processes. Future research endeavours should be directed towards minimizing energy consumption, mitigating the generation of secondary pollutants, and fostering the development of eco-friendly treatment methodologies. Integrating renewable energy sources, particularly solar power, into solar photo-Fenton processes presents a promising avenue for enhancing these treatments' sustainability and environmental benefits.

Chapter 3: MATERIALS AND METHODOLOGY

3.1 Chemicals and Reagents

Ammonium iron Sulfate Hexahydrate (99.5 %, JHD), Sodium Tungstate Dihydrate (98 %, Sisco research lab), Cetyltrimethyl ammonium bromide (99%, SRL), NaOH (Research lab), Absolute Ethanol (SigmaAldrich), Ciprofloxacin Hydrochloride hydrate (98-102%, SRL), Hydrogen peroxide (30% w/w, Scharlau), Potassium Ferrocyanide (99%, Giant Chem solutions), Potassium Chloride (99%, Qualikems), Sulfuric acid (98%), Ampicillin sodium salt, Tetracycline hydrochloride (H_2SO_4, ACS reagent, 95-98%, Sigma-Aldrich), LB Broth with agar (Miller), Sodium Chloride (NaCl), Sodium Azide (99.5%, SigmaAldrich), Triethanolamine (98%, SigmaAldrich), Iso Propyl alcohol (99.8%, Research lab), Superoxide Dismutase bovine (30KU, SigmaAldrich), Potassium Dichromate (BDH Chemical Ltd., England), 18.2 MΩ UPW.

3.2 Instruments

The instruments and apparatus used for the synthesis and the photocatalytic activity of $FeWO_4$ are as follows: Digital balance (BEL M254Ai), Hotplate magnetic stirrer (MS-H380-Pro, USA), Direct-Q®3 UV Water purification System, Centrifuge machine (CTF-TH16, China), Sonicator (Hwashin Powersonic 405, Korea), Hot air Oven (Memmert UN55), Vortex, UV-Vis spectrophotometer (T80+, UK), Xenon Light Source (Perfect light PLS-SXE300UV, China), Potentiostat (μStat-i 400s Potentiostat / Galvanostat / Impedance Analyzer), Laminar Air Flow, Refrigerate, Centrifuge machine, Rotator Incubator.

3.3 Synthesis of $FeWO_4$ Nanomaterials

The $FeWO_4$ nanomaterials were synthesized using a facile hydrothermal method, resulting in the development of three different morphologies: particles, rod-like, and fiber-like shapes. The precursors, Mohr's salt ($(NH_4)_2Fe(SO_4)_2{\cdot}6H_2O$) and sodium tungstate ($Na_2WO_4{\cdot}2H_2O$) were separately dissolved in deionized water and then mixed

under constant stirring for 10 minutes to obtain a homogenous solution. After that, 2.5 g of cetyl trimethyl ammonium bromide (CTAB) was added into the homogeneous solution dropwise and stirred for 1 h. Then, three unlike concentrations of NaOH solution (0.66 g, 1.32 g, and 2.64 g) were prepared and poured into the mixture dropwise to synthesize particles, rod-like, and fiber-like shapes nanomaterials, respectively. After that, the mixture was vigorously stirred for an additional 2 hours, and the resulting solution was moved into a 250 mL Teflon-lined stainless-steel autoclave and heated to 160°C for 24 hours. Upon reaching room temperature, the obtained precipitates were washed several times with deionized water and ethanol, followed by drying at 70 °C for 6 hours. Subsequently, the dried samples were subjected to calcination at 500 °C for 2 hours to obtain the different crystalline $FeWO_4$ nanomaterials.

3.4 Characterization of $FeWO_4$ Nanomaterials

Synthesized $FeWO_4$ nanomaterials were characterized through different physiochemical characterization processes. The optical properties of the synthesized $FeWO_4$ nanomaterials were analyzed using UV-Vis diffuse reflectance spectrophotometry (UV-Vis DRS) with a Lambda 365 UV/Vis spectrophotometer from PerkinElmer, USA. The analysis provided information on absorbance and bandgap energy in order to understand the material's photocatalytic potential in Fenton processes. The FESE Microscope (FESEM, JSM 7600F, JEOL Ltd., Tokyo, Japan) was used to investigate the surface morphology, lattice structure, particle size, and distribution in order to present a full view of structural integrity and homogeneity within the $FeWO_4$ nanomaterials. XRD (XRD, EMPREAL, Netherlands) was used to investigate the crystalline structure and phase composition of synthesized nanomaterials to confirm their phase purity. The EIS and CV measurements were performed on a Potentiostat/Impedance Analyzer (Metrohm, μStat-i 400s, Switzerland). The EIS was conducted to determine the CTR and the conductivity of nanomaterials, indicating their electrochemical performance and efficiency for ROS generation. CV was performed to investigate the redox behavior and electrochemical stability of nanomaterials with the objective of probing deeply into the catalytic activity in Fenton reactions.

3.4.1 The Debye-Scherrer Formula for Crystalline Size

The crystalline size and average crystallite size have been estimated by the Debye-Scherrer formula from the diffractogram of the $FeWO_4$ NP, NR and NF. By using the Scherrer equation calculate the crystallite size and average crystallite size from XRD data -

$$D = \frac{K\lambda}{\beta \cos\theta}$$

Where, D = crystallite size (nm), K = 0.9 (Scherrer constant), λ = 0.15406 nm (wavelength of X-ray sources), β = FWHM (radians) and θ = Peak position (radians)

3.4.2 Determination of Band Gap

The band gap energy (E_g) of $FeWO_4$ can be calculated from the diffuse reflectance spectroscopy (DRS) data using Tauc plots. To determine the values of the direct/indirect bands gap energy (E_g), the reflectance was recalculated into the dependence of Kubelka–Munk function [240]

$$(F(R) \cdot h\nu)^{\left\{\frac{1}{2}\right\}} = A\left(h\nu - E_g\right)$$

Where F(R) is the Kubelka-Munk function, related to the reflectance, h\nu is the photon energy, A is a constant, E_g is the band gap energy.

By using Tauc's relation, band gap energies were calculated. This relationship is between the absorbance and the photon energy (hν). By plotting ($\alpha h\nu)^n$ against $h\nu$, and extrapolating the linear portion of the curve to the x-axis, the band gap energy can be determined [241]. In the case of an indirect band gap material, the Tauc equation is utilized for this purpose as follows-

$$(\alpha h\nu)^n = A\left(h\nu - E_g\right)$$

In this relation, α is the absorption coefficient, $h\nu$ is the photon energy, A is a constant, E_g is the band gap energy and n = 2 for direct band gap energy for these nanomaterials. The absorption coefficient (α) is estimated by the following relation:

$$\alpha = \frac{-1}{t} lnT$$

Where, T is the transmittance value and t is the thickness of the substance that is placed under UV-Vis irradiation.

3.4.3 Electrochemical Characterizations

3.4.3.1 Preparation of Modified Working Electrode:

Before modifying the electrodes, the glassy carbon electrode (GCE) was polished with an alumina slurry. Subsequently, the GCE was sonicated in ethanol, rinsed with DI water, and dried at room temperature. Following this, 1 mg of $FeWO_4$ NP, NR, NF was dispersed in 2 mL of 0.5% chitosan and sonicated in a bath sonicator for 20 minutes to achieve a homogeneous dispersion. Approximately 10 µL of the homogeneously dispersed composite suspension was carefully applied to the pre-cleaned GCE surface and then dried in a hot air oven at 50 ºC. For the ensuing electrochemical detection tests, the working electrodes were kept at ambient temperature.

3.4.3.2 Measurement of EIS and CV

The electrochemical characteristics of three different nanomaterials were assessed using EIS and CV. EIS is a valuable methodology in electrochemistry that provides insight into the conductivity of electrode surfaces during either oxidation or reduction reactions. This technique also yields information about an electrode's alteration in conductance or impedance after its modification. In this regard, EIS was conducted using three different modified electrodes: $FeWO_4$-NP/CHI-modified GCE (GCE/CHI/$FeWO_4$-NP), $FeWO_4$-NR/CHI-modified GCE(GCE/CHI/$FeWO_4$-NR), $FeWO_4$-NF/CHI-modified GCE (GCE/CHI/ $FeWO_4$-NF). The GCE was first polished using an alumina slurry before any electrode modifications. Following this, the GCE was sonicated in ethanol, rinsed with DI water, and dry at RT. Next, 1 mg of $FeWO_4$-NP, NR, and NF was dispersed in 2 mL of 0.5% chitosan and sonicated in a bath sonicator for 20 minutes to ensure uniform dispersion. Approximately 10 µL of the resulting composite suspension was then carefully applied to the pre-cleaned GCE surface and dried in a hot air oven at 50 ºC. The measurements were made in the frequency range from 2.5×10^3 Hz to 5×10^5 Hz, using a modulation amplitude of 40 mV in applied electrode potential. The Nyquist plots of bare and modified electrodes were recorded in the solution of 5.0 mM $[Fe(CN)_6]^{3-/4-}$ and 0.1 M KCl. In this plot, two-time constants may be well distinguished: a semicircular portion at high frequency due to electron transport processes and a linear portion at low frequency due to mass transport processes.

CV is a very powerful technique in the analysis of electro-active species and especially in the studies of the redox reactions of the analytes. In this study, the preliminary electroactive properties of the bare and modified GCE electrodes were characterized in the potential range from -0.2 to - 0.7 V with a scan rate of 50 mV/s. This was conducted in a solution comprising 5.0 mM [$K_4Fe(CN)_6$] with 0.1M KCl.

3.5 Degradation of Ciprofloxacin by Various Heterogeneous Fenton Process

For evaluating the catalytic activity of Iron Tungstate degradation of Ciprofloxacin antibiotic was examined under different conditions.

3.5.1 Preparation of Ciprofloxacin Solution

An aqueous solution of ciprofloxacin was prepared in a Duran bottle by adding 10mg of ciprofloxacin in 1000 mL DI water and used as a stock solution, the concentration of the stock solution was 10mg/L, and it was further diluted to various concentrations by adding de-ionized water.

3.5.2 Batch Experiment of Degradation of Ciprofloxacin

In this research, ciprofloxacin (CIP) antibiotic was used as a model contaminant. The model antibiotic was prepared according to the standard operating procedure, and the concentration of CIP was 10 mg/L. The antibiotic degradation experiments were conducted in a 150-mL beaker containing 50 mL of CIP. The pH value of the solution was 7.0 ± 0.2, adjusted with 0.1 M NaOH and 0.1 M H_2SO_4. A fixed amount (100 mg/L) of $FeWO_4$ nanomaterials was mixed with the 10 mg/L of CIP solution. The reaction mixture was continuously stirred at 600 rpm using a magnetic stirrer for 10 minutes under dark conditions to achieve adsorption and desorption equilibrium. After that, the required volume of hydrogen peroxide (H_2O_2) stock solution was added to the CIP and catalyst-containing solution to obtain the desired 2 mM of H_2O_2 and initiate the Fenton process. In the PF process, the visible light source was turned on after the dark condition. The PLS-SXE300E/UV (Beijing Perfect Light Technology Co. Ltd. China) was used as a visible light source over the reactor and used a 300W xenon (Xe) lamp with a range of 320–780 nm VISREF filter. The average light intensity was 126.75 mW/$cm^{2,}$ and the

surface of the reaction media was kept at 16 cm from the bulb. The sono-Fenton process utilized an ultrasonicator (Hwashin Powersonic 405, Korea). The sonication volume was high, and the sonicator's average frequency, voltage, and temperature were 40 KHz, 220V, and 30 ºC ± 2.0, respectively. Aliquots of 3 mL sample were collected from the reaction mixture at chosen time intervals: -10, 0, 10, 20, 30, and 40 minutes, and were immediately quenched with a small quantity of sodium thiosulfate to stop the reaction. The samples were filtered using 0.22 μm syringe filter to eliminate the $FeWO_4$ catalyst. The concentration of ciprofloxacin was determined using a UV-Vis spectrophotometer (T80+, UK) at its 275nm wavelength. The degradation efficiency was calculated according to the following Eq (3.1) [49, 50].

$$\text{Degradation efficiency} = \frac{C_0 - C}{C_0} \times 100\% \qquad \text{Eq. 3.1}$$

Where, C_0= initial concentration of CIP, C = final concentration of CIP.

3.6 Response Surface Methodology

Optimization of the catalytic Process was conducted using the design expert software 13 through the central composite design framework. A series of experiments was conducted to determine the degradation efficiency of ciprofloxacin at five levels (-alpha, low, central, high, + alpha) of the three independent variables - pH, catalyst concentration, and time, as shown in Table 3.1.

Table 3.1. Variables and Experimental Design Using CCD

Variables	Units	-alpha	Low	Central	High	+alpha
pH		1.95	4	7	10	12.05
Catalyst	mg/L	15.91	50	100	150	184.09
Time	min	4.7	15	30	45	55.2

A mathematical model is developed to describe the relationship between the independent variables and the degradation efficiency. The model is usually represented by a second-order polynomial equation. The efficacy of the constructed polynomial

model in forecasting the experimental removal efficiency outcomes was assessed by statistical analysis (ANOVA). Catalytic Activity Experiment for Optimization

To evaluate the catalytic efficiency of $FeWO_4$ nanoparticles, firstly 50 mL of ciprofloxacin (10 mg/L) for the degradation efficiency test, with different pH (1.95, 4,7,10, 12.05). Then, different amounts of catalyst (15.91 mg/L, 50 mg/L, 100 mg/L, 150 mg/L, 184.09 mg/L) were added into the CIP solution and magnetically stirred the solution for 10 minutes under dark conditions to disrupt the equilibrium of absorption. After that 2 mM of H_2O_2 to the solution after 10 minutes of dark conditions, allowing the photo-Fenton reaction to continue under visible light irradiation. At different intervals, 3 mL of the solution was taken out and filtered with a 0.22 μM syringe filter. The absorbance of ciprofloxacin was measured from the beginning of the reaction until it reached equilibrium after 45 minutes. A UV-visible spectrophotometer observed the degradation of ciprofloxacin at various time intervals by measuring the absorbance at 275 nm while DI water as a blank sample.

3.7 Reactive Species Analysis

Five scavengers, including sodium azide (SA), isopropanol (IPA), triethanolamine (TEA), superoxide dismutase (SOD), and potassium dichromate ($K_2Cr_2O_7$) were further used to identify ROSs such as $^1O_2$, $HO^\bullet$, h^+ $O_2^{\bullet-}$, and e^- during photo-Fenton process, respectively. 1mM of TEA, IPA, and SA were used to reduce the catalytic effect and elavate the scavenging effect. Low concentrations such as 0.025 mM of $K_2Cr_2O_7$ and 6 U/mL of SOD were used in this study [24]. The influence of scavengers was determined by measuring the absorbance of ciprofloxacin after different time intervals.

3.8 Reusability Test

For reusability test, optimum amount (100 mg/L) of $FeWO_4$ nanoparticles was mixed with the 10 mg/L of CIP solution. The reaction mixture was continuously stirred at 600 rpm using a magnetic stirrer for 10 minutes under dark conditions to achieve adsorption and desorption equilibrium. After that, the required volume of hydrogen peroxide (H_2O_2) stock solution was added to the CIP and catalyst-containing solution to obtain the desired 2 mM of H_2O_2 and turn on light to initiate the photo-Fenton process. Aliquots of 3 mL sample were collected from the reaction mixture at 40 minutes, and

were immediately quenched with a small quantity of sodium thiosulfate to stop the reaction. The samples were filtered using 0.22 μm syringe filter to eliminate the $FeWO_4$ catalyst. The concentration of ciprofloxacin was determined using a UV-Vis spectrophotometer (T80+, UK) at 275nm wavelength. Then the catalyst recovers by centrifuge the remaining solution. The remaining catalyst dried at 70 ºC. Then reuse this catalyst to run another catalytic experiment as previously described procedure.

3.9 Inactivation of ARB by Photo-Fenton Process

To evaluate the photocatalytic activity of $FeWO_4$ to degrade antibiotic-resistant bacteria.

3.9.1 Preparation of *E. coli* and Enumeration of ARB

A single colony of *E. coli* RP4 containing plasmid LE392 was transferred from an overnight LB agar plate into 10 mL of LB broth containing 10 mg/L of tetracycline and 100 mg/L of ampicillin and grown at 37°C for 6 h to stationary phase. The bacterial cell broth (200 μL) was sub cultured into 10 mL of LB broth containing 10 mg/L of tetracycline and 100 mg/L of ampicillin and incubated for 16 h. The bacterial biomass was washed by centrifuging at 6000 rpm for 5 minutes, discarding the broth and rinsing thrice with normal saline solution. The *E. coli* cell concentration in these primary stocks was ~10^9 CFU/ml. The cells were re-suspended into normal saline at 10^6 colony-forming units per mL (CFU/mL), as determined by monitoring the solution absorbance at λ of 600 nm, which concentration was used as an initial treatment concentration. For bacterial colony enumeration, 0.1 mL samples were serially diluted in normal saline and inoculated onto LB agar plates supplemented with 10 mg/L tetracycline and 100 mg/L ampicillin, the MIC for the plasmid-mediated ARGs [242].

3.9.2 Catalytic Activity Experiment to Inactivate ARB

To evaluate the catalytic efficiency of $FeWO_4$ nanoparticles, firstly, 50 mL of bacteria-containing solution (10^6 CFU/ml). For the inactivation efficiency test, the optimum dose of $FeWO_4$ nanoparticles (100 mg/L) was added into the solution and magnetically stirred the solution for 10 minutes under dark conditions to disrupt the equilibrium of absorption. After that 2 mM of H_2O_2 to the solution after 10 minutes of

dark conditions, allowing the photo-Fenton reaction to continue under visible light irradiation. At different intervals, 1 mL of the solution was taken out and put into Eppendorf. Then the samples were serially diluted with normal saline solution and 0.1 mL of the solution spread on LB agar plates containing 10 mg/L tetracycline and 100 mg/L ampicillin. Then the plates were incubated for 16 h at 37°C and count the colony grew on the plates.

3.9.3 Bacterial Regrowth and Recovery Analysis

The regrowth and recovery analyses were conducted to explore the ability of bacteria to undergo repair after PF treatment. During the treatment, 20 μL bacterial cell suspension was collected at each time interval, followed by incubation in 20 mL liquid LB broth at 37 °C in the dark, with constant shaking (180 rpm) for 24 h, 48 h and 72 h. For each day during the regrowth period, 1mL of sample was collected and measure the absorbance of the media at 600nm. In addition, LB broth was used as the blank control.

Chapter 4: RESULTS AND DISCUSSION

4.1 Characterization of $FeWO_4$ Nanomaterials

4.1.1 Ultraviolet-Visible Diffuse Reflectance Spectroscopy Analysis (UV-Vis DRS)

The UV-Vis DRS is the most crucial measurement technique for the optical properties of semiconductor materials like $FeWO_4$. The application of the DRS technique is particularly helpful in measuring the band gap energy of materials. The potential of a material to absorb visible light and generate electron-hole pairs is vital for its photocatalytic efficiency. A reduced band gap broadens the range of absorption into the visible spectrum, which may lead to an improvement in photocatalytic efficiency [243]. The bandgap energy (Eg) of $FeWO_4$ nanomaterial was determined from the DRS data employing Tauc plots, with further details provided in the Methods and Materials chapter section 3.4.2. The bandgap energies for $FeWO_4$ NPs, NRs, and NFs are measured at 1.45 (Fig. 4.1a), 1.97(Fig. 4.1c), and 1.95 eV (Fig. 4.1e) respectively. These observations indicate that the band gap of $FeWO_4$ NPs is the smallest among the three morphologies, which implies a potential performance increase under visible light irradiation due to a broader absorption spectrum. Consequently, the bandgap energies of NRs and NFs were slightly higher compared to the NPs shape but effective in utilizing the full spectrum of visible light.

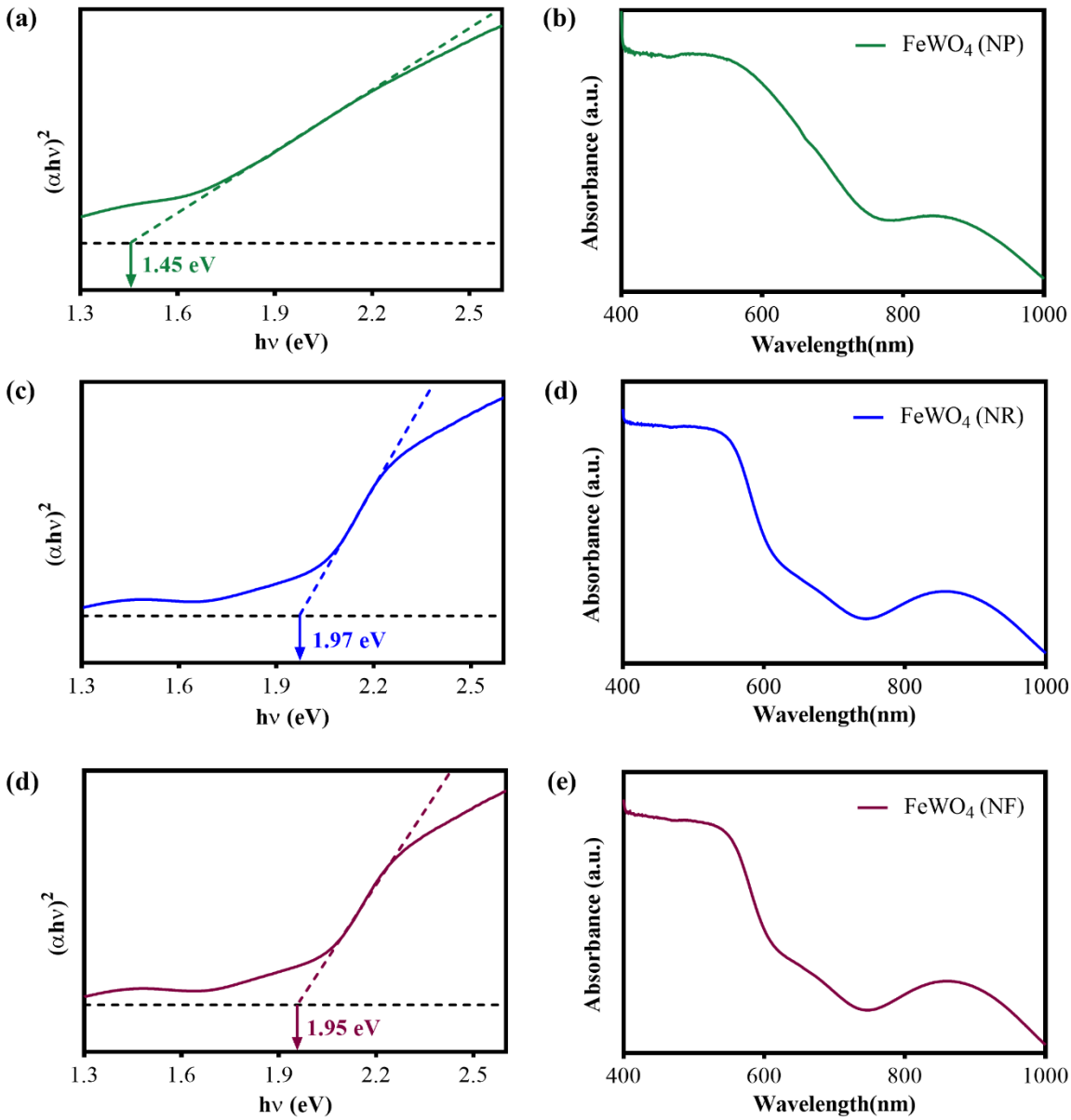

Fig. 4.1 Tauc plot and UV-Vis absorbance of synthesized $FeWO_4$ nanomaterials (a, b) $FeWO_4$ NPs, (c, d) $FeWO_4$ NRs, and (e, f) $FeWO_4$ NFs.

4.1.2 Field Emission Scanning Electron Microscopy (FESEM)

Field emission scanning electron microscopy (FESEM) is an advanced, high-resolution imaging technique used to understand the morphology, particle size, and other structural features of nanomaterials. High-resolution imaging using FESEM enables detailed observation of the shape and size distribution of $FeWO_4$ nanomaterials. This is crucial for understanding their catalytic activity in the Fenton processes. The FESEM images of $FeWO_4$ nanomaterials were synthesized by adding different

concentrations of NaOH in the reaction medium, and their morphologically changed images are represented in Fig. 4.2.

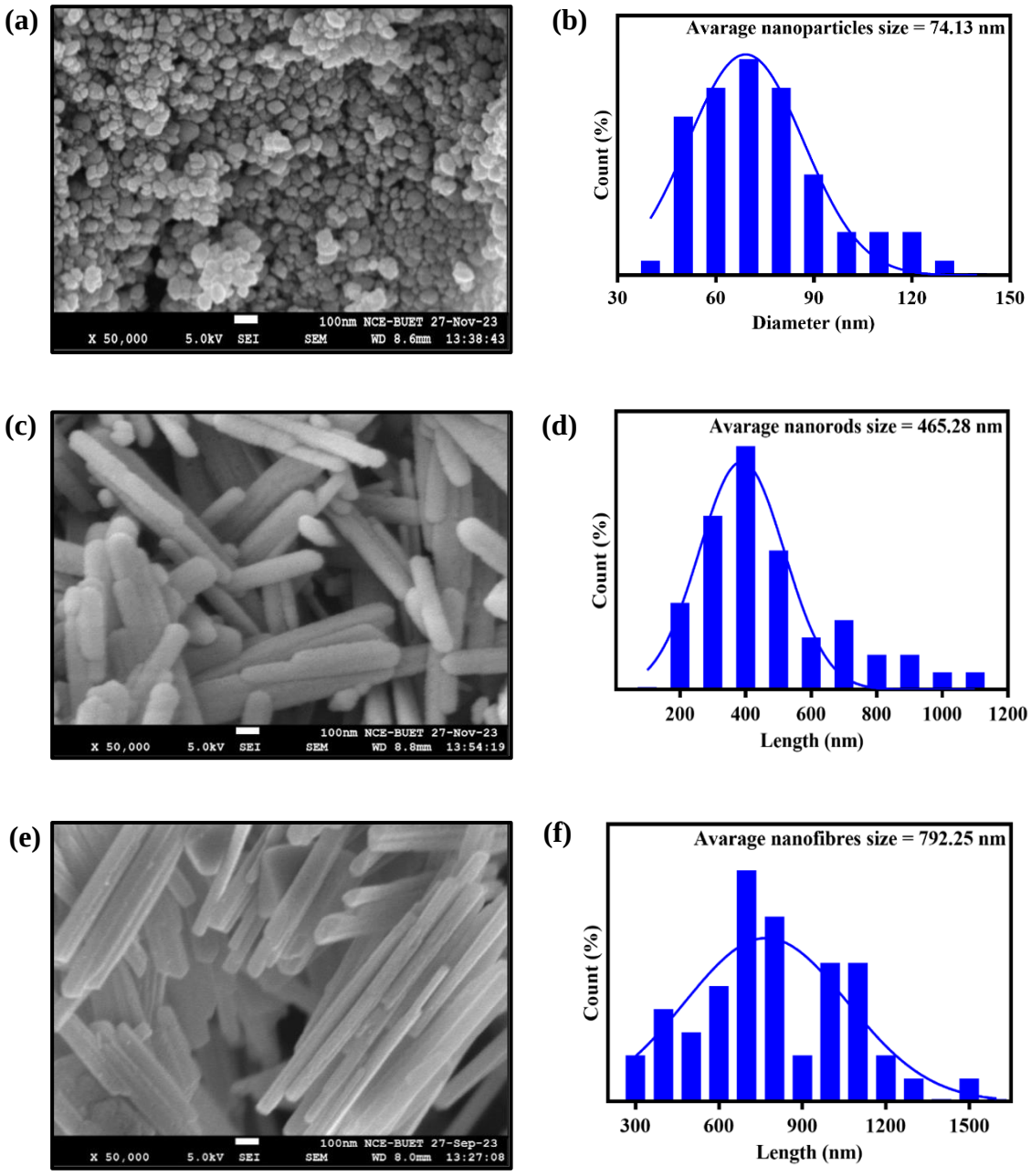

Fig. 4.2 FESEM images and corresponding histogram of $FeWO_4$ NPs (a-b), NRs (c-d) and NFs (e-f).

It is evident from the reaction that increasing the NaOH concentration leads to a morphological transformation in $FeWO_4$, resulting in the formation of $FeWO_4$ nanomaterials with diverse structures such as particles, rod-like, and fiber-like

configurations. In the first image (Fig. 4.2a), the nanoparticles (NPs) appear spherical with an average radius of approximately 74 nm (Fig. 4.2b). These NPs have a relatively high surface area-to-volume (SA: V) ratio of about 0.040 nm^{-1}, which allows for a greater surface area exposed [244]. In contrast, the second image (Fig. 4.2c) shows nanorods (NRs) with a length of approximately 465 nm and a radius of 102 nm (Fig. 4.2d). The elongated shape of the nanorods results in a higher radius than that of the nanoparticles and a lower SA:V ratio of approximately 0.021 nm^{-1}, providing less surface area for reactions than spherical nanoparticles. The third FESEM image (Fig. 4.2e) depicts nanofibers (NFs). These materials have a notably large aspect ratio, resulting in a surface area to volume ratio of 0.035 nm^{-1}, which is higher than that of NRs but lower than NPs. The NFs have an estimated length of 792 nm and a radius of 57 nm (Fig. 4.2f). It is evident that these NFs exhibit a more significant increase in surface area compared to their volume. Therefore, FESEM images show distinct morphological differences in shape and size that are very important to optimize catalytic efficiency for $FeWO_4$ nanomaterials toward environmental remediation applications.

4.1.3 X-ray Diffraction analysis (XRD)

The X-ray diffraction (XRD) analysis of $FeWO_4$ nanomaterials with diverse shapes, including nanoparticles, nanorods, and nanofibers, indicate variations in their crystallinity, phase purity, and structural arrangement. The XRD pattern of $FeWO_4$ nanoparticles displays broad peaks with small crystallite sizes, indicating lattice strain, which is typical of nanoscale materials. The XRD pattern of $FeWO_4$ nanomaterials with three morphological changes synthesized is depicted in Fig. 4.3. The diffraction peaks correspond to a highly crystalline monoclinic phase of $FeWO_4$, with lattice parameters of a = 4.75Å, b = 5.72 Å, c = 4.97 Å and $\alpha = \gamma = 90°$, $\beta = 90.17°$. The space group is $P_{2/c}$, in line with the reference values (JCPDS powder diffraction file no. 71-2391) [243]. There are nine peaks in the XRD diffraction patterns at 15.158°, 24.168°, 31.893°, 40.496°, 45.099°, 48.604°, 53.490°, 55.064°, 63.027° which are closely matched with the diffraction peaks of reference card file at 2θ = 15.479°, 24.338°, 31.249°, 41.012°, 45.098°, 48.491°, 53.339°, 55.067°, 63.029° that are corresponded to (010), (110), (020), (-121), (-211), (022), (-221), (-131), (-222) crystal planes with interplanar spaces (d -value) 5.72 Å, 3.65 Å, 2.86 Å, 2.19 Å, 2.008 Å, 1.87 Å, 1.716 Å, 1.66 Å, 1.47 Å [243]. The broad nature of these peaks

in nanoparticles indicates some lattice defects, but the absence of extra peaks confirms the phase purity without impurities. On the other hand, the XRD pattern for the nanorods and nanofibers show sharper and better-defined peaks at the same characteristic 2θ positions, providing evidence of enhanced crystallinity and improved structural order. The nanorods showed the sharpest and strongest peaks, demonstrating high crystallinity and phase purity among the three morphologies. The higher intensities of these peaks may indicate larger crystallites with less lattice strain in the nanorods favoring better electron-hole separation and improved charge transfer, which are critical factors for high photocatalytic performance [245]. These findings confirm that the morphological differences in nanoparticles, nanorods, and nanofibers directly affect the crystal quality and phase purity of $FeWO_4$. These characteristics are paramount in enhancing their effectiveness in catalytic activity in the heterogeneous Fenton reaction for pollutant degradation.

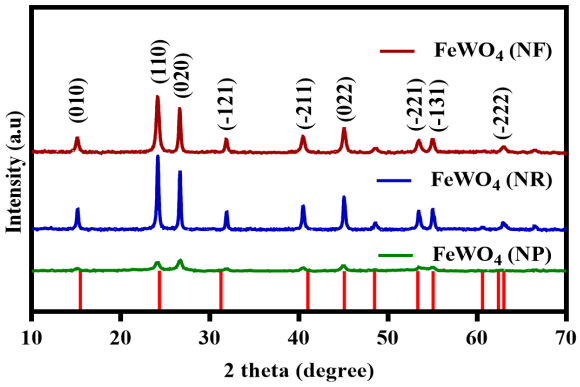

Fig. 4.3 XRD analysis of $FeWO_4$ NPs, NRs, and NFs.

The size of the crystal of $FeWO_4$ nanoparticles (NPs), nanorods (NRs), and nanofibers (NFs) was estimated using the Debye-Scherrer formula [246, 247] based on their diffractogram (refer to 3.4.1). Gaussian function fitting was conducted on the peaks observed to obtain the FWHM that is needed to be used in estimating the crystallite size. FWHM was obtained using OriginPro 8.5. The average crystalline size of the synthesized $FeWO_4$ NPs, NRs, and NFs were 14.89 nm, 26.47 nm, and 19.72 nm, respectively. The $FeWO_4$ NPs, with a reduced crystalline dimension of 14.89 nm, faced the common problems linked to elevated electron-hole recombination rates in little crystallites but

showed higher photocatalytic performance compared with nanofibers and nanorods. The pronounced effectiveness can be attributed to the much-increased surface area of the nanoparticles. The presence of such a feature provides a considerably large number of active sites that are favourable for photocatalytic reactions, thus promoting efficient adsorption of reactant molecules and increasing their interaction with photogenerated charge carriers accordingly [248]. Additionally, the presence of surface defects or defect states in nanoparticles can significantly affect the performance by acting as trapping sites, leading to an increase in the lifetime of the charge carriers by mitigating the recombination process, hence enhancing photocatalytic activities [249]. Furthermore, the unique morphology possessed by nanoparticles tends to improve their adsorption and scattering of light radiation significantly; hence, better exploitation of light energy increases the rate of generation of reactive species involved in degrading pollutants. On the other hand, $FeWO_4$ nanorods with a relatively larger crystallite dimension of 26.47 nm presumably decreased the surface area, restricting the availability of catalytic active sites. In this regard, although $FeWO_4$ nanofibers with crystalline dimensions of 19.72 nm can have an optimum compromise between the available surface area and charge separation, they do not exhibit the defect-laden structure along with the higher surface-to-volume ratio in the case of nanoparticles. Consequently, the enhanced photocatalytic efficacy of the $FeWO_4$ nanoparticles might be effectively ascribed to its extensive surface area, plenty of defect-related features, and enhancements in light adsorption capability, which in turn mitigate certain shortcomings typically associated with reduced crystallite dimensions.

4.1.4 X-ray Photoelectron Spectroscopy (XPS)

The chemical composition and ionic states of the synthesized materials have been investigated by XPS measurements. The Fig. 4.4 shows the XPS spectra of the synthesized $FeWO_4$ nanoparticles. Fig. 4.4a represents the entire X-ray photoelectron spectroscopy (XPS) spectrum of $FeWO_4$. One can see the peaks assignable to the binding energies of W 4f, C 1s, O 1s, and Fe 2p [243]. Fig. 4.4(b-e) enlarged XPS spectra for carbon, iron, tungsten and oxygen. Fig. 4.4c clearly assigns the two BE peaks at 710.9 eV and 723.6 eV to Fe $2p_{3/2}$ and Fe $2p_{1/2}$, respectively. These two characteristic peaks of Fe^{2+} in the

$FeWO_4$ nanoparticles indicate the purity of this composite photocatalyst [243, 250]. In the $FeWO_4$ tungstates studied here, the XPS results indicated iron atoms have a formal valence of +2. The binding energy peaks at 35.4 eV and 37.7 is as shown in Fig. 4.4d originating from the binding energies of W $4f_{7/2}$ and W $4f_{5/2}$ indicated the presence of W^{6+} in the prepared samples [250, 251]. O 1s corresponds to the binding energy peak at 530 as shown in the Fig. 4.4e.

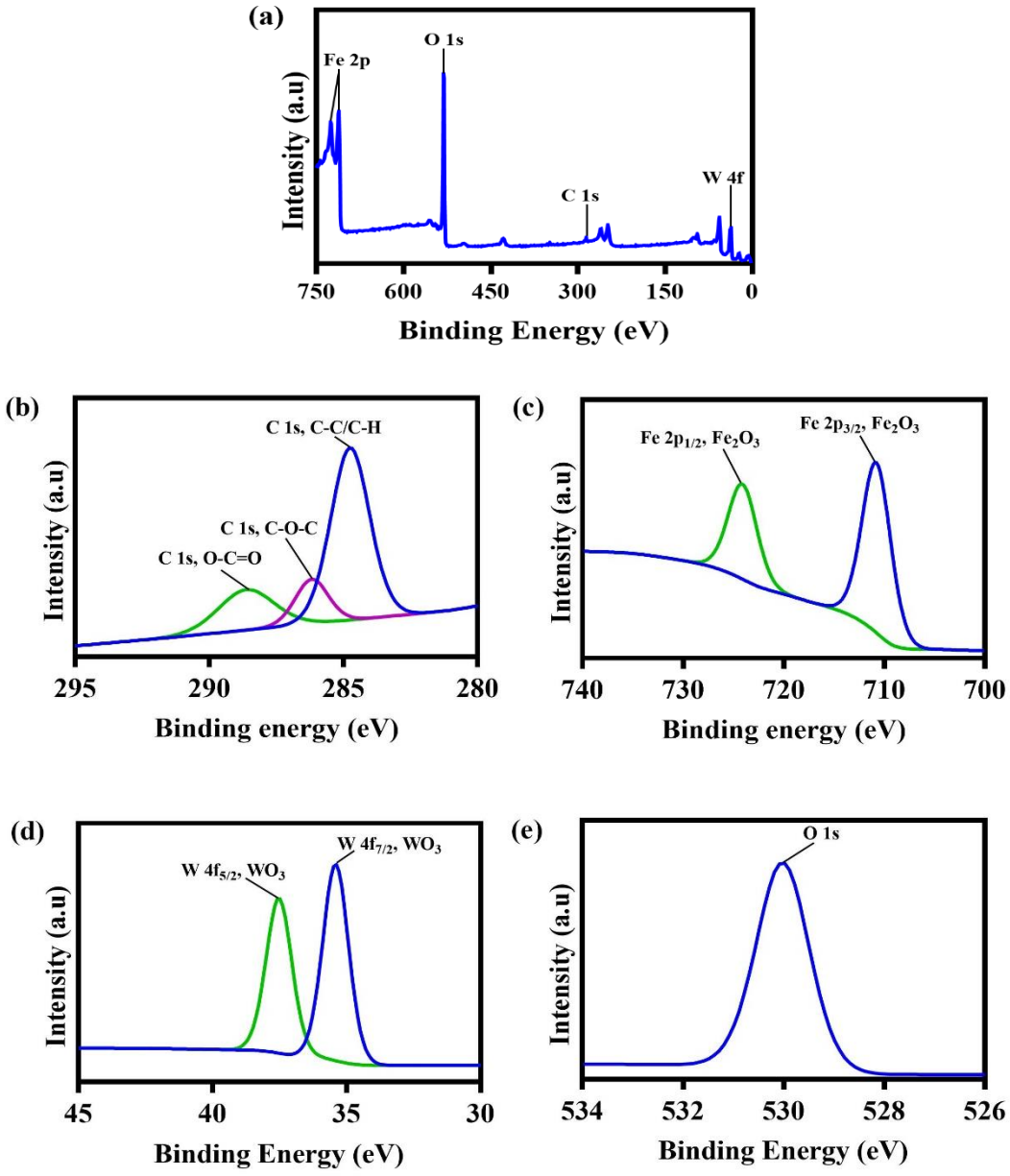

Fig. 4.4 Full survey XPS spectra (a), XPS Spectra of (b) C 1s, (c) Fe 2p, (d) W 4f and (e) O 1s for $FeWO_4$ nanoparticles

The C1s peak (Fig. 4.4b) in the survey XPS spectra appears to arise from hydrocarbons adhering to the surfaces of the $FeWO_4$ nanostructures. However, the survey XPS spectra suggested relatively small C 1s core-level line intensities for the material. Generally, XPS examines the alterations in surface composition and structure of a material before and after etching. After etching, this reduced surface can be masked by adsorbed contaminants such as oxides, carbonaceous species from hydrocarbons due to atmospheric exposure, or other surface defects. Among other processes, ion sputtering removes such surface layers after etching. Consequently, the XPS peaks that are characteristic of surface impurities, such as C 1s and O 1s diminish while the peaks of the substrate-underlying material become more intensive. This transition will evidence that the outside layer is decaying and real mass substance is unveiled underneath. From these XPS data, one can clearly realize that the nanoparticles really represent pure-phase $FeWO_4$.

4.1.5 Electrochemical Impedance Spectroscopy (EIS)

The electrochemical impedance spectroscopy is considered a significant methodology to investigate the interfacial charge transfer processes occurring in semiconductor materials [252]. It provides detailed insight into the conductive properties of semiconductor material surfaces during both the oxidation and the reduction reaction. This technique also offers information on any modification done with the electrode regarding its conductance or impedance [253]. In EIS spectra, normally, the real component (Z') should be plotted on the x-axis, and the imaginary component (Z'') in a Nyquist plot is plotted on the y-axis [254]. Fig. 4.5a depicts the Nyquist plots of various modified electrodes of $FeWO_4$. This can be explained by the use of an equivalent circuit from Inset-Randles containing Warburg impedance (W or Z_w), charge transfer resistance (R_{ct}), solution resistance (R_s), and double-layer capacitance (C_{dl}) in Fig. 4.6. The values corresponding to the mentioned components are given in Table 4.1Usually, a smaller EIS semicircle implies a higher electron transfer rate, while a larger diameter suggests a slower rate of electron transfer (Magar et al., 2021). As shown in Fig. 4.5a, the R_{ct} values of $FeWO_4$ were 88.5 Ω, 93.4 Ω, and 92.5 Ω, respectively. From the Nyquist plots, it is very much clear that the nanoparticles have minimum $R_{ct,}$ and nanorods have shown maximum R_{ct}. Thus, the nanoparticle shape has better electron transfer ability.

Their well-aligned structure offers higher surface area which provides easy mobility to the charge carriers [255]. It is to be noticed that R_s maintains quite constant for all morphologies, indicating the properties are the same in an electrolyte. Due to a slow diffusion of ions inside the electrolyte, Z_w is more dominant in nanoparticles compared to nanorods and nanofibers. The nanorods had a bigger semicircle diameter, indicating higher double-layer capacitance and the ability to store more charge at the electrode-electrolyte interface. Compared to other morphologies, nanofibers of $FeWO_4$ exhibit better electron transfer and ion diffusion characteristics due to their lower R_{ct} and Z_w, respectively. Therefore, the three morphologies of synthesized $FeWO_4$ can contribute substantially to the breakdown of antibiotics via photocatalytic processes.

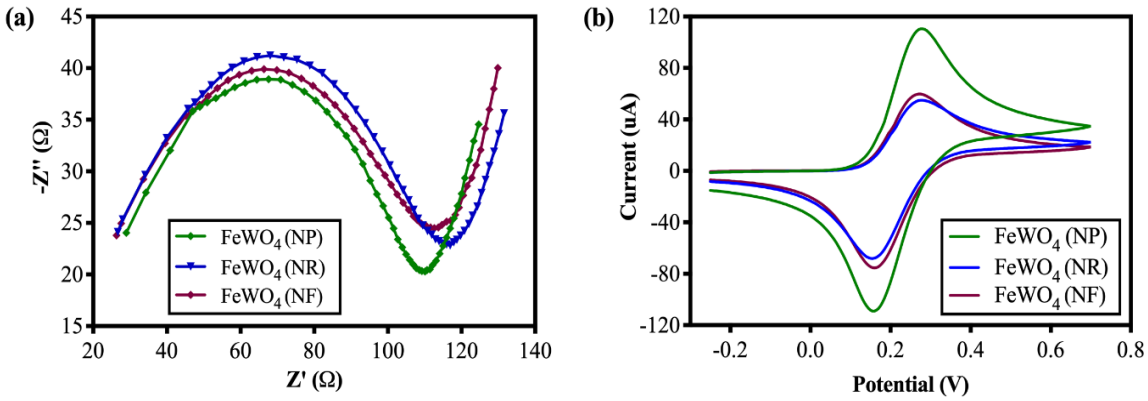

Fig. 4.5 Electrochemical analysis of $FeWO_4$ nanomaterials using (a) EIS spectra and (b) CV of $FeWO_4$ nanoparticles, nanorods, and nanofibers.

Table 4.1. Components of the Randles equivalent circuit for different morphological $FeWO_4$ nanomaterials.

Electrode	**R_s (Ω)**	**R_{ct} (Ω)**	**C_{dl}(F)**	**W($\Omega s^{-1/2}$)**
CHI/GCE/NP	11.6	88.5	1.11×10^{-8}	0.000192
CHI/GCE/NR	16.7	93.4	6.42×10^{-7}	0.000231
CHI/GCE/NF	14.5	92.5	3.12×10^{-8}	0.000210

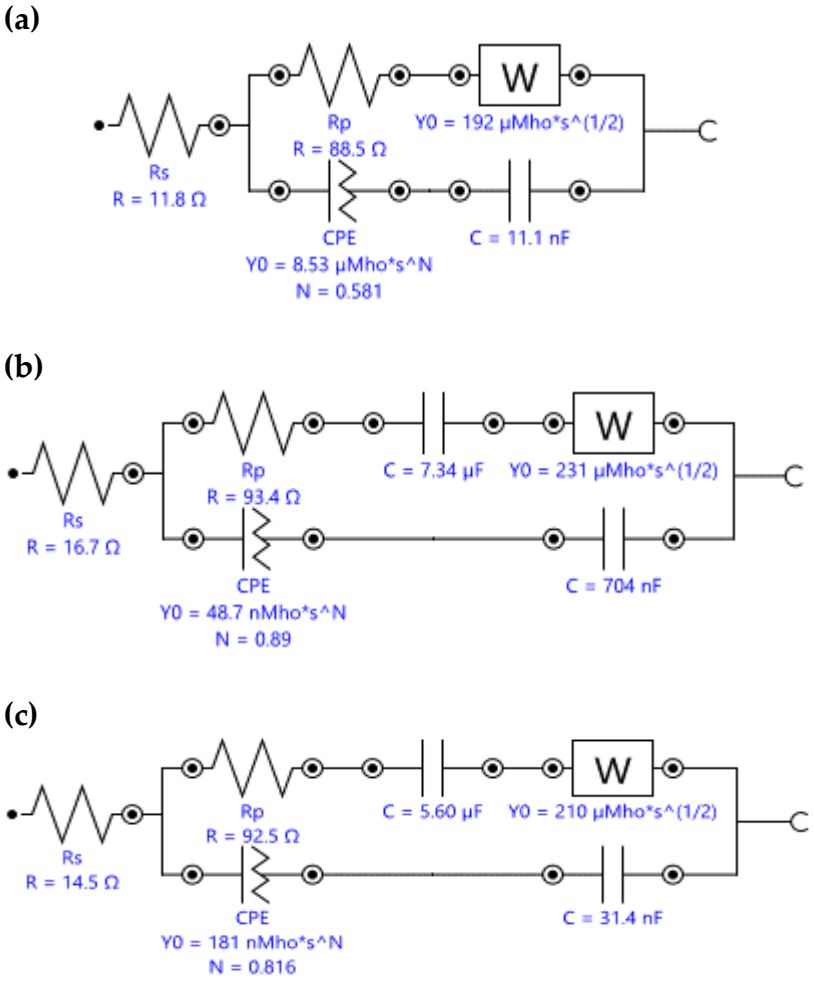

Fig. 4.6 Randles equivalent circuit model for $FeWO_4$ nanomaterials (a) NP, (b) NRs, and (c) NFs.

4.1.6 Cyclic voltammetry (CV)

The cyclic voltammetry (CV) analysis revealed a distinct redox peak associated with the oxidation and reduction processes of the $FeWO_4$ nanomaterials (Fig. 4.5b). The shape and position of these peaks provide insights into the electrochemical activity and reversibility of the redox processes. The comparison was made based on the CV of $FeWO_4$ NPs, NRs, and NFs under the same scan rate of 50 mV/s, identifying that the peak anodic current of the NPs reached to about 110 µA with a potential of 0.3 V; this can be clarified by their strong oxidation activity. However, it showed that the peak currents of NRs and NFs were comparatively low, about 54 µA and 56 µA respectively, due to their poor oxidation activity. Similarly, in the cathodic region, the $FeWO_4$ NPs

showed the highest peak current of 108 μA, representing high reduction activities, while the NRs and NFs again gave lower peak currents (67 μA and 68 μA, respectively) for reduction. This higher redox performance of NPs indicates a higher electrochemical surface area and a higher amount of electrochemically active sites. $FeWO_4$ nanoparticle's structural features help to increase the area related to ion exchange particular surface; hence, $Fe(CN)_6^{3-/4-}$ on the electrode surface may act effectively in rapid interaction between ions and electrons. These results confirm the study of EIS that showed a lower R_{ct} for NPs compared to NRs and NFs. These results emphasized the crucial role of electron transfer properties in determining the overall electrochemical performance of nanomaterials.

4.2 Degradation of Ciprofloxacin by $FeWO_4$ Nanomaterials Using Heterogeneous Fenton Processes

The extensive utilization of heterogeneous catalysis processes for the degradation of antibiotics has garnered significant interest due to their exceptional efficiency. The $FeWO_4$ nanomaterials serve as a solid-phase catalyst in the heterogeneous Fenton processes, thereby producing various ROS through a reaction with H_2O_2, that degrades the antibiotics present in aqueous solution. The influence of different structural and morphological shapes of $FeWO_4$ nanomaterials on the degradation of CIP antibiotics was investigated for the reaction conditions (10 mg/L of CIP, 2 mM of H_2O_2, 100 mg/L of $FeWO_4$ nanomaterials, pH = 7) by changing the four Fenton processes.

4.2.1 Degradation of Ciprofloxacin by Conventional Fenton Process

The efficiency of $FeWO_4$ nanomaterials was assessed in the degradation of CIP antibiotics through the conventional Fenton (CF) process, where only the $FeWO_4$ nanomaterials were added to the reaction media with 2 mM of H_2O_2. Fig. 4.7 presents the efficiency of three different morphological varieties of $FeWO_4$ during the conventional heterogeneous Fenton process. In the absence of H_2O_2, the adsorption efficiencies of NPs, NRs, and NFs on CIP were found to be 15 %, 4 %, and 6 %, respectively. As an oxidizing agent, H_2O_2 could also be inefficient in CIP degradation without catalysts. Only 1-2% of the CIP degradation was obtained after 40 min treatment

(Fig. 4.11). When H_2O_2 was added with the catalyst in the Fenton processes, the removal efficiencies were found to be 33 %, 18 %, and 15 % for $FeWO_4$ NPs, NRs, and NFs, respectively (Fig. 4.7). The catalytic activity is augmented by the synergistic action of H_2O_2 and catalysts [256, 257]. The morphology of NPs, NRs, and NFs plays a crucial role in improving catalytic activity in the studied heterogeneous Fenton process. Among the samples exhibited in the study, it is evident that the NPs exhibit the highest level of catalytic efficiency. This can be attributed to improved catalytic activity of the NPs as the relative concentration of Fe^{2+}/Fe^{3+} species on the surface increases. Similar findings were also observed for $MnFe_2O_4$ nanorods, which exhibited higher efficiency in the decomposing of ofloxacin antibiotic compared with its nanospheres and nanocubes in the Fenton process [257].

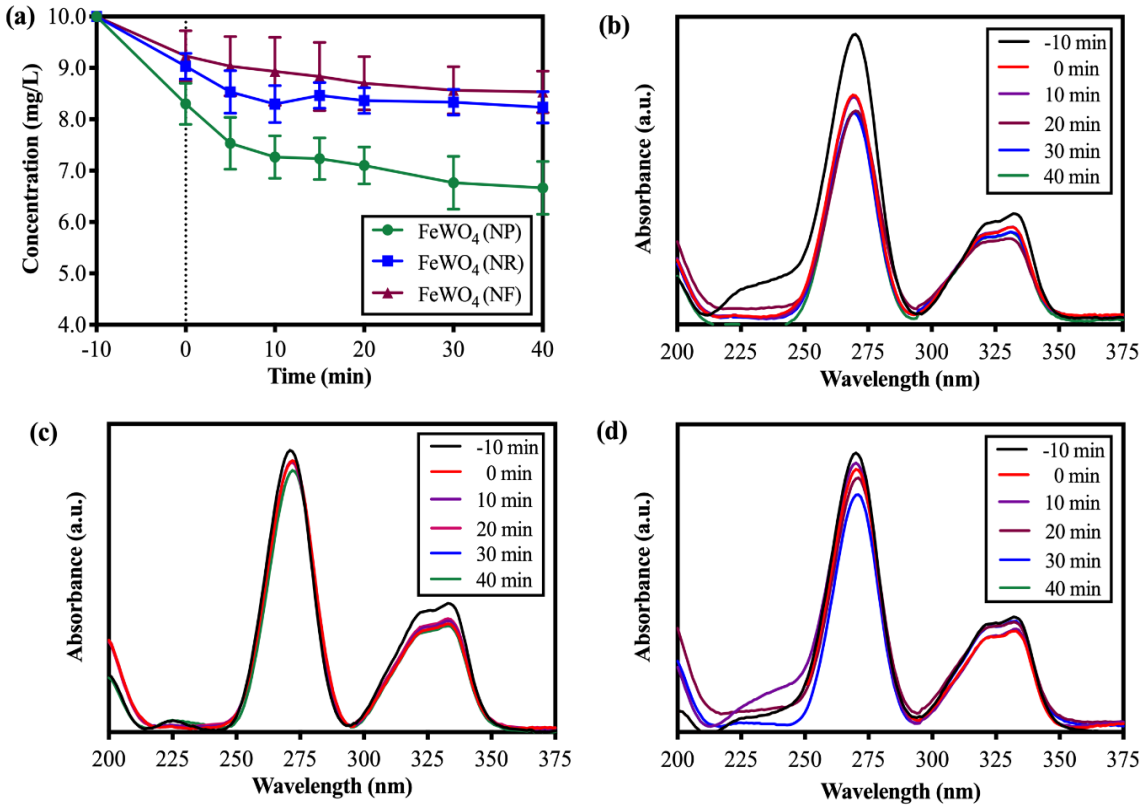

Fig. 4.7 Degradation of ciprofloxacin antibiotic by $FeWO_4$ nanomaterials (a), and the UV-Vis absorption spectrum for NPs (b), NRs (c), and NFs (d) using the conventional Fenton process at the following reaction conditions: 10 mg/L of CIP, 2 mM of H_2O_2, 100 mg/L of $FeWO_4$ nanomaterials, pH = 7.

4.2.2 Degradation of Ciprofloxacin by Photo-Fenton Process

In the heterogeneous photo-Fenton process, the main differences from the homogeneous or conventional Fenton are related to the use of a solid-phase catalyst instead of dissolved iron (Fe^{2+}/Fe^{3+}) in solution under light irradiation. The solid catalyst is usually prepared by using iron or other transition metals impregnated onto materials such as iron oxides, iron-doped material, or metal-organic frameworks (MOFs), which can offer catalytic reactions on their surface. The utilization of light in this process yields a higher generation of ROS, which are responsible for the degradation of antibiotics [57]. In the blank test, the elimination efficiency of CIP was 36 % after 40 minutes of treatment under visible light irradiation (Fig. 4.11). This suggests that CIP molecules are sensitive to light and break down at the exposure of light. Only nanomaterials such as NPs, NRs, and NFs exhibit degradation rates of 56 %, 40 %, and 43 %, under visible light irradiation, as shown in (Fig. 4.11). This demonstrates that the catalyst enhances degradation efficiency through photocatalysis. In the absence of a catalyst, the addition of H_2O_2 to CIP solution, along with light irradiation, enhances its degradation rate, increasing from 36 % to 58 %. This indicates that the combination of H_2O_2 and light has a synergistic impact on the degradation of CIP. The degradation rates in the heterogeneous photo-Fenton system were found to be 99 %, 93 %, and 96 % for NPs, NRs, and NFs, respectively, as shown in Fig. 4.8. This indicates that the photo-Fenton process achieved almost complete degradation of CIP within 40 minutes. There are several explanations for the constructive relationship between photocatalysis and Fenton reactions: (i) light illumination plays a crucial role in breaking down H_2O_2 molecules to generate ROS, and (ii) leads to the Fe^{2+} ion regeneration caused by the irradiation, which in turn improves the system's H_2O_2 catalytic reactions [57, 258]. This discovery indicates that the generation of ROS is significantly enhanced in the presence of light and thereby accelerates the degradation of CIP. As a result of the synergy between photolysis and Fenton catalysis, CIP can almost be fully degraded by $FeWO_4$ NPs and NFs [45]. These findings thus suggest that morphology should have an influence on determining the catalytic properties of $FeWO_4$ nanomaterials. All NPs demonstrated higher photocatalytic activities than their counterparts, NRs and NFs. Smaller-sized particles provide a larger number of active sites that could explain the higher CIP degradation

rates. In the same way, the degradation of tetracycline antibiotic, nanosheets-like Fe_2O_3/BC (97%), cube-like and ring-like shape was found to degrade TC about 66% and 17%, respectively [258].

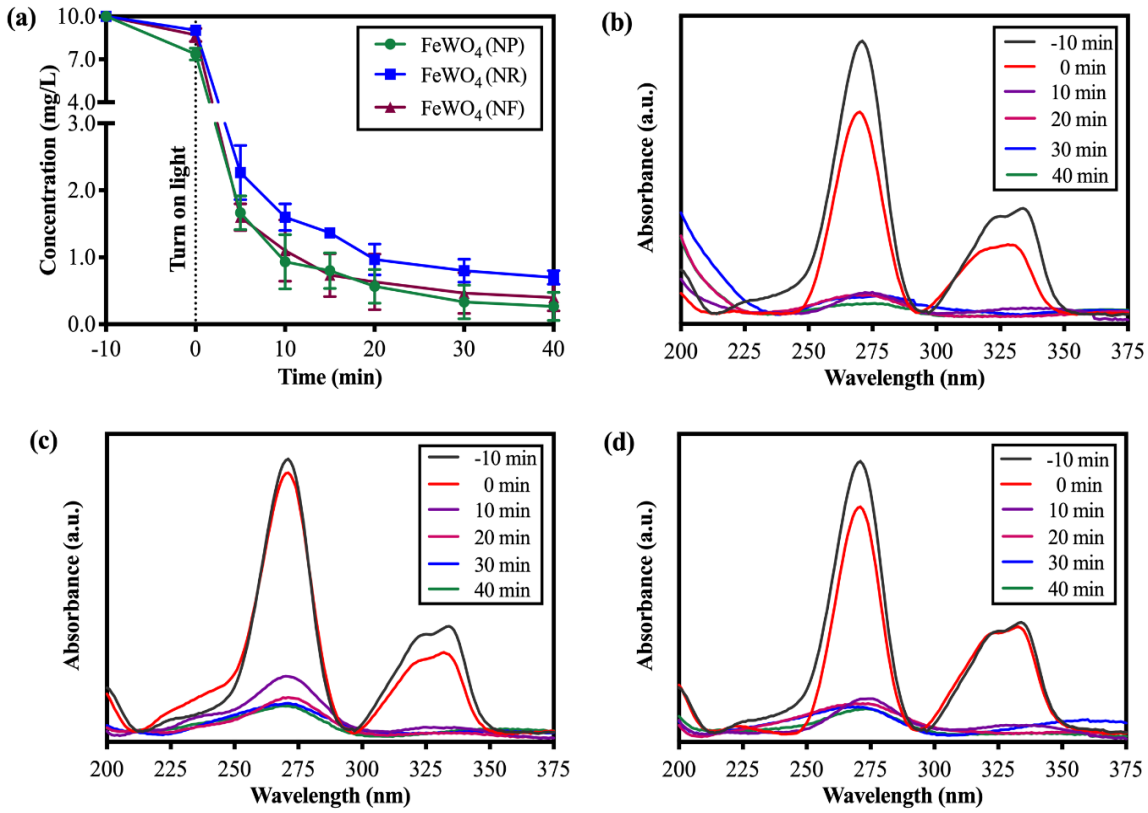

Fig. 4.8 Degradation of ciprofloxacin antibiotic by $FeWO_4$ nanomaterials (a), and the UV-Vis absorption spectrum for NPs (b), NRs (c), and NFs (d) using the photo-Fenton process at the following reaction conditions: 10 mg/L of CIP, 2 mM of H_2O_2, 100 mg/L of $FeWO_4$ nanomaterials, pH = 7.

4.2.3 Degradation of Ciprofloxacin by Sono-Fenton Process

The sono-Fenton process is an AOP, based on the coupling of the classical Fenton reaction with ultrasound irradiation-usually in the high-frequency range greater than 20 kHz. Ultrasonic irradiation enhances the Fenton reaction by the bubbles of cavitation generated across the solution, which collapse to promote local high temperatures and pressures. This improves the yield of ROS, a species responsible for antibiotic degradation [259, 260]. In the blank test (Fig. 4.11), it was observed that the sonication alone had a minimal effect on the degradation of CIP, achieving degradation of only 6 %. When H_2O_2 was added with sonication, there was also negligible or no degradation.

A similar lower degradation efficiency also observed for only catalysts under ultrasound irradiation (data not shown). The limited activity of the catalysts is due to the ineffective enhancement of antibiotic degradation in the presence of cavitation phenomenon [260]. However, when $FeWO_4$ nanomaterials were used as a catalyst in combination with ultrasound and H_2O_2, CIP elimination rates of 36 %, 9 %, and 17 % were achieved, as displayed in Fig. 4.9. The elevated catalytic performance of antibiotic degradation was observed during the initial 10 minutes of treatment; subsequent degradation occurred at a markedly slower rate. The Fe^{3+} ions were generated initially in the Fenton reaction under solar irradiation, while it became sluggish with the preceding time interval as non-degraded CIP molecules may restrict iron availability [260]. It is essential to acknowledge that the formation of ROS at low-frequency ultrasonics is minimal, and the accumulation of H_2O_2 is insignificant, particularly when operating at low power levels below 100 W [261].

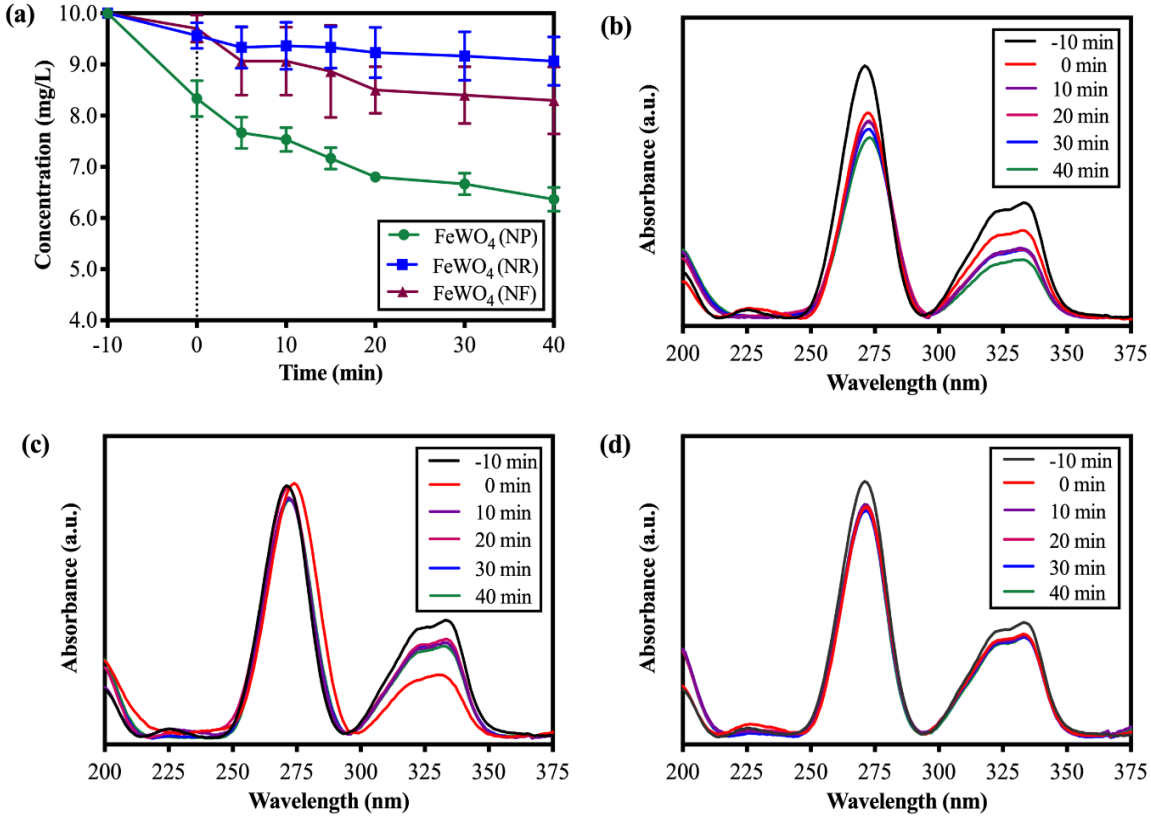

Fig. 4.9 Degradation of ciprofloxacin antibiotic by $FeWO_4$ nanomaterials (a), and the UV-Vis absorption spectrum for NPs (b), NRs (c), and NFs (d) using the sono- Fenton process at the following reaction conditions: 10 mg/L of CIP, 2 mM of H_2O_2, 100 mg/L of $FeWO_4$ nanomaterials, pH = 7.

4.2.4 Degradation of Ciprofloxacin by Sono Photo-Fenton Process

The sono photo-Fenton process is widely utilized as a hybrid AOP, in which Fenton reaction is assisted by both ultrasound and light irradiation. The integration of the Fenton process with light along with ultrasound improves removal efficiency via the synergistic interplay of light and ultrasound irradiation. Furthermore, ultrasound can produce active radicals and perpetually refresh the catalyst surface to inhibit the buildup of pollutants and their byproducts formed during the treatment operation. Therefore, it promotes pollutant degradation efficiency [38]. In the control test, H_2O_2 and ultrasound did not show a noticeable degradation of CIP (Fig. 4.11). The combination of light and H_2O_2 with ultrasound produced the degradation of CIP to up to 58% without a catalyst. The integration of ultrasound in a Fenton process or visible light in a sono-Fenton system greatly enhanced the efficacy of the Fenton process on the degradation of ciprofloxacin. Indeed, CIP rates reached 36%, 9%, and 17% in the sono-Fenton process under three sets of experimental conditions (Fig. 4.9) but these rates increased significantly with the addition of visible light in the SPF system to 99%, 89%, and 94%, respectively (Fig. 4.10). The results presented herein have shown that the SPF process is much more effective than the SPF alone for achieving higher levels of pollutant degradation. This remarkable improvement in the efficiency of CIP degradation underlines the synergistic effect of the combination of ultrasound with visible light, which favors the formation of reactive species, accelerating the decomposition of CIP. On the other hand, the efficiency of the photo-Fenton system was considerably found to be lowered (97%) compared to the sono-photo-Fenton reaction, which had a degradation efficiency of 99 %. This phenomenon can be attributed to the photolysis of H_2O_2 and the photo reduction of ferric ions (Fe^{3+}) to ferrous ions (Fe^{2+}), leading to the generation of ROS in the PF reaction [38, 57]. This finding is consistent with the previous studies. The degradation rate of metronidazole by sono-Fenton increased from 89.0% to 95.7% for spinel $CoFe_2O_4$/AC catalyst after inducing light in the reaction system [38].

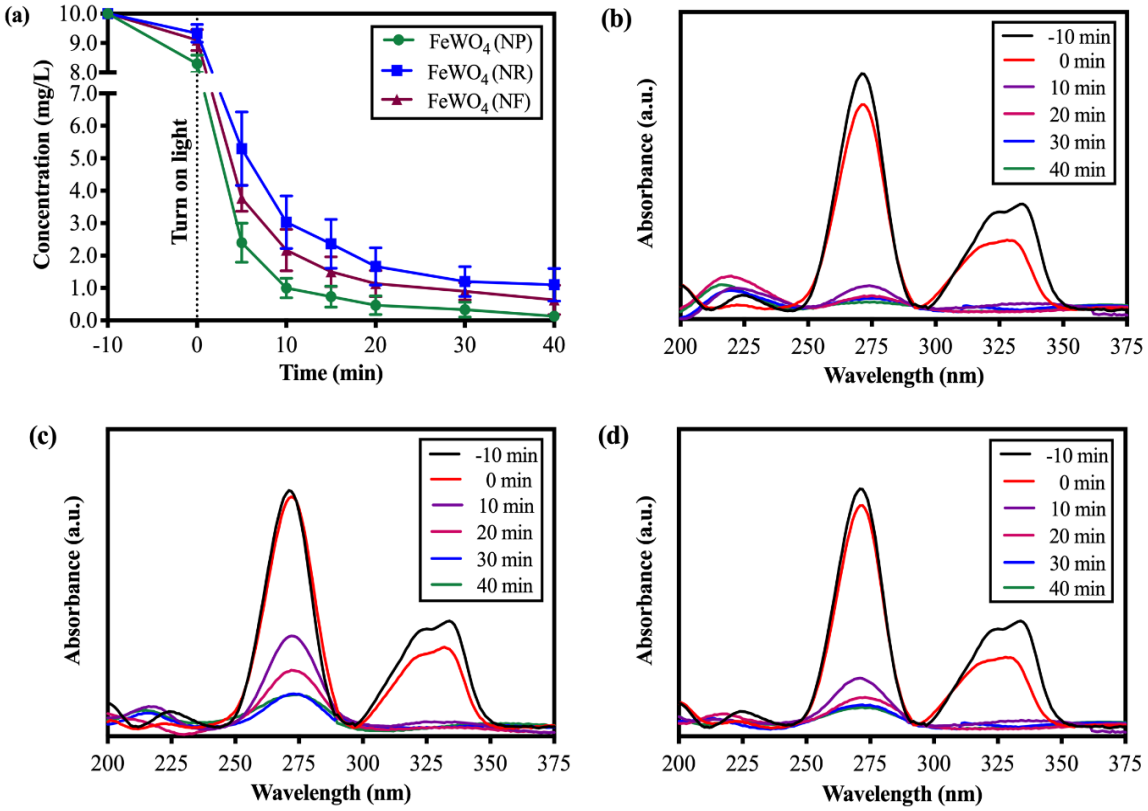

Fig. 4.10 Degradation of ciprofloxacin antibiotic by $FeWO_4$ nanomaterials (a), and the UV-Vis absorption spectrum for NPs (b), NRs (c), and NFs (d) using the sono-photo-Fenton process at the following reaction conditions: 10 mg/L of CIP, 2 mM of H_2O_2, 100 mg/L of $FeWO_4$ nanomaterials, pH = 7.

4.2.5 Control Test for Validation

Various control test was carried out to validate the process and find out the effect of individual elements in the catalytic degradation reaction. The descriptions of this tests are briefly described previously.

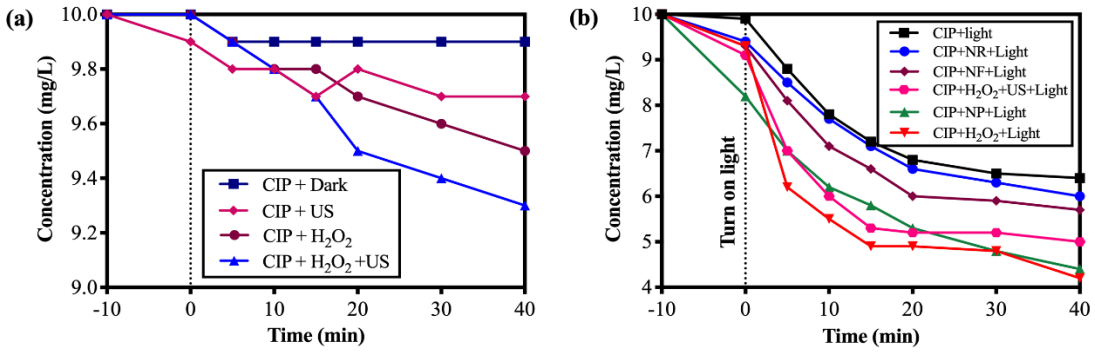

Fig. 4.11 Control test in dark and light conditions

4.3 Parameters Optimization for $FeWO_4$ Nanoparticles by RSM

4.3.1 Model Fitting and Statistical Analysis:

The degradation percentage of ciprofloxacin (CIP) was determined over 20 experimental runs, with the independent variables and their corresponding values provided in Table 4.2.

Table 4.2. Degradation Efficiency of Ciprofloxacin by $FeWO_4$ nanoparticles

Run	Factor 1	Factor 2	Factor 3	Response Value	Predicted value
	pH	Catalyst (mg/L)	Time (min)	CIP Degradation (%)	CIP Degradation (%)
1	7	100	30	99	98.53
2	4	150	45	81	82.38
3	7	100	30	100	98.53
4	4	50	15	52	51.57
5	7	100	30	98	98.53
6	10	150	15	55	53.76
7	7	15.91	30	70	69.96
8	4	150	15	54	54.97
9	12.04	100	30	45	45.92
10	1.95	100	30	60	58.04
11	7	100	30	100	98.53
12	7	100	30	98	98.53
13	7	184.09	30	75	74.00
14	7	100	30	96	98.53
15	4	50	45	76	77.98
16	10	50	45	65	64.77
17	10	150	45	65	66.17
18	7	100	4.7	54	55.16
19	10	50	15	54	53.36
20	7	100	55.22	90	87.80

Table 4.2 presents the degradation efficiency of ciprofloxacin by $FeWO_4$ nanoparticles. The degradation efficiency, Ef (%) was calculated using the equation:

$$Ef\ (\%) = (1 - C_f/C_0) \times 100\% \qquad \text{Eq. 4.1}$$

Where C_f represents the final concentration and C_0 the initial concentration.

The experimental results underwent statistical analysis using analysis of variance (ANOVA) and p-values. Initially, a linear regression model was considered. Still, a second-order model was ultimately found to be the most suitable for predicting the degradation percentage of CIP based on the experimental data obtained from the central composite design and the specified input variables. The degradation efficiency of CIP was evaluated by considering three factors: the initial pH of the solution (A), the dosage of the catalyst (B), and the reaction time (C). The efficiency was modelled as the sum of a constant, three first-order effects (A, B, and C), three interaction effects (AB, AC, and BC), and three second-order effects (A^2, B^2, and C^2). Model selection was based on several criteria: the R^2 value, the adjusted R^2 value, the predicted R^2 value, and the p-value for lack of fit. These values were 0.9953, 0.9911, 0.9738, and 0.2441, respectively.

The predicted values were calculated using Design-Expert software. The variation in response values across different experimental designs indicates that pH, catalyst dosage, and reaction time changes lead to different degradation efficiencies. The comparison between actual and predicted values shows that the model accurately represents real conditions, as these values have a high correlation.

Table 4.3 further supports this by indicating a lack of fit for the actual degradation efficiency responses and projections. To validate the model, we conducted a lack-of-fit test for the coefficients and assessed the significance of the regression model. The significance of the factors was ranked based on p values and F values. The lack of fit test assesses the model's precision in explaining the data. The chosen model, labelled as "suggested," has a p-value (Prob > F) of 0.2441, which is above the 0.05 significance level, indicating that the model does not suffer from a significant lack of fit. This suggests that the model is statistically significant and accurately describes the data. Significant model

terms include A, B, C, AC, A^2, B^2, and C^2, while terms greater than 0.1000 are considered non-significant. The analysis indicates that the chosen model is quadratic

Table 4.3. Lack of Fit tests

Source	Sum of Squares	df	Mean Square	F-value	p-value	
Linear	5685.5	11	516.86	224.72	< 0.0001	
2FI	5568	8	696	302.61	< 0.0001	
Quadratic	**22.18**	**5**	**4.44**	**1.93**	**0.2441**	**Suggested**
Cubic	2.73	1	2.73	1.19	0.3254	Aliased
Pure Error	11.5	5	2.3			

In Table 4.4, the ANOVA results show a sum of squares of 7146.87, mean squares of 794.1, an F-value of 235.74, and a p-value of less than 0.0001, signifying the model's significance. The Model F-value suggests a mere 0.01% probability of such a high F-value occurring due to noise. P-values less than 0.0500 indicate significant model terms, emphasizing the importance of A, B, C, AC, A^2, B^2, and C^2. The Lack of Fit F-value of 1.93 indicates a non-significant lack of fit relative to pure error, with a 24.41% chance that such a large F-value could occur due to noise, further confirming the model's suitability.

In summary, the quadratic model, with a p-value of less than 0.05, accurately represents the data and significantly influences the degradation efficiency response. The statistical significance and lack of significant lack of fit demonstrate that the chosen model is appropriate and that any inaccuracies have a negligible impact on the model's reliability.

Table 4.4.ANOVA for Ciprofloxacin degradation

Source	Sum of Squares	df	Mean Square	F-value	p-value	
Model	**7146.87**	**9**	**794.1**	**235.74**	**< 0.0001**	**Significant**
A-pH	177.44	1	177.44	52.68	< 0.0001	
B-Catalyst Dosage	19.72	1	19.72	5.85	0.0361	
C-Time	1286.39	1	1286.39	381.89	< 0.0001	
AB	4.5	1	4.5	1.34	0.2746	
AC	112.5	1	112.5	33.4	0.0002	
BC	0.5	1	0.5	0.1484	0.7081	
A^2	3903.83	1	3903.83	1158.93	< 0.0001	
B^2	1270.02	1	1270.02	377.03	< 0.0001	
C^2	1318.3	1	1318.3	391.36	< 0.0001	
Residual	33.68	10	3.37			
Lack of Fit	**22.18**	**5**	**4.44**	**1.93**	**0.2441**	**Not significant**
Pure Error	11.5	5	2.3			
Cor Total	7180.55	19				

The equation representing the degradation response efficiency in the quadratic model is as follows:

Coded Equation:

CIP degradation efficiency = 98.5299 + -3.60456A + 1.20152B + 9.70535C + -0.75AB + -3.75AC + 0.25BC + -16.4587A^2 + -9.38758B^2 + -9.56436C^2

Actual Equation:

CIP degradation efficiency = -100.289 + 27.4008A + 0.800037B + 3.74752C + -0.005AB + -0.0833333AC + 0.000333333BC + -1.82874A^2 + -0.00375503B^2 + -0.0425083C^2

CIP degradation efficiency response value (%), A is the Initial pH of the Solution, B is the Catalyst Dosage (mg/L) and the C is reaction time (minutes).

4.3.2 Optimization Result

Through our numerical analysis, we have identified the optimal conditions for achieving maximum degradation efficiency of ciprofloxacin (CIP). Our results show that the highest degradation efficiency occurs at a pH of 7, with a catalyst dose of 100 mg/L and a reaction time of 32.78 minutes. To validate our optimization, we have established a correlation between the predicted efficiency and the experimental data. Our findings indicate that a catalyst concentration of 100 mg/L at pH 7 can achieve complete degradation of ciprofloxacin within 40 minutes. These results confirm the robustness and effectiveness of our developed model in optimizing the degradation process of ciprofloxacin. This demonstrates its practical applicability and reliability in predicting the optimal operational conditions.

4.3.2.1 Effect of Catalyst Dose

The concentration of the catalyst in the Fenton process significantly impacts the removal efficiency of antibiotics and other contaminants by playing a crucial role in activating oxidants such as H_2O_2. The amount of catalyst used directly affects the rate at which antibiotics decompose [86]. At low dosages of catalysts, the degradation efficiency decrease. With the increase of catalyst dosage, the degradation efficiency is also increased. However, each additional increase in catalyst dosage diminishes the degrading efficacy. Generally, the efficiency of degrading antibiotics tends to increase with higher catalyst dosages up to a certain point [86, 88]. With a fixed pH (pH = 7), the highest degradation efficiency was achieved 99% at 100mg/L of $FeWO_4$. This improvement is due to the increased surface area and availability of functional groups resulting from the greater mass of the catalyst. However, further increasing the catalyst dose 185mg/L of $FeWO_4$, the degradation efficiency decreased from 99% to 75% after 30 min reaction time. The quantity of reactive species served as a limiting factor at elevated catalyst levels when the quantity of H_2O_2 was constant in the reaction solution [262, 263]. It has been shown that the self-quenching processes of active species may occur at elevated catalyst dosages [264]. Another reason of decreasing the The removal effectiveness of CIP at an elevated catalyst dosage is attributable to the light reflection by the catalyst [265].

4.3.2.2 Effect of pH

The pH variable is a very crucial operational variable in wastewater treatment [266]. The pH of the reaction medium significantly influences the degradation of antibiotics in Fenton processes, with changes in pH impacting reaction rate and efficiency [267]. Research indicates that Fenton reactions typically occur under acidic conditions, with pH levels between 2.0 and 3.0 being the most favourable [119]. If the pH value is less than 2, H_2O_2 would be decomposed under strong acid conditions to produce H^+, which acts as a scavenger of $HO^\bullet$ to inhibit the degradation of pollutants. At a fixed Catalyst dosage (100 mg/L), The highest degradation rate achieved at pH 7. The CIP removal elevated from 60% to 99% when the pH was elevated from 2 to 7, with a consistent initial CIP concentration of 10 mg/L and 100 mg/L of $FeWO_4$ catalyst. The optimum pH for the decomposition of CIP is 7 [268]. A notable reduction in CIP removal was recorded, decreasing from 99% at pH 7.0 to 45% at pH 12. The noted decrease may be associated with zeta potentials (ZPs) and the existing species of CIP in the reaction solution. The literature indicates that ciprofloxacin has two pKa values: 5.90 ± 0.15, corresponding to the carboxylic acid group, and 8.89 ± 0.11, related with the basic nitrogen moiety. CIP can manifest as a cation, zwitterion, or anion, contingent upon pH conditions [269]. When the pH surpasses the zero-point charge, the surface charge density of the synthesized nanocatalyst becomes negative. This affects the adsorption of the CIP, which are anionic at pH levels above 7. Similarly, when the pH is below the zero-point charge, the surface charge density of the synthesized nanocatalyst exhibits a positive value. The adsorption of the cationic CIP is affected at pH levels below 7. The degradation rate of CIP is limited at pH 2 and 12 [270].

4.3.2.3 Effect of Reaction Time

The duration of treatment or reaction time is a critical factor influencing the efficiency of antibiotic removal in the Fenton process. Longer reaction times typically allow for more extensive contact between the ROS and the antibiotics, resulting in a higher degradation rate. If complete mineralization is the objective, an extended reaction time becomes essential to ensure thorough removal [101]. The analysis of effect of reaction time reveals that the increase in reaction time increase the degradation

efficiency. The analysis indicates that optimal degradation efficiency, approaching nearly 100%, is achieved at the 40 minutes reaction time. Further increase in reaction time does not change the degradation efficiency greatly, the degradation rate almost same as 40 minutes. Nevertheless, depending on the wastewater and treatment method, the deterioration rate stabilized at specific intervals, with only marginal improvements noted subsequently [271, 272].

4.3.2.4 Effect of Catalyst Dosage and pH

The analysis of the effect of catalyst dosage and pH on the degradation efficiency reveals several critical insights. The Fig. 4.12 indicate that there is an optimal pH of approximately 7 and a catalyst dosage of around 100 mg/L, which together achieve maximum degradation of ciprofloxacin.

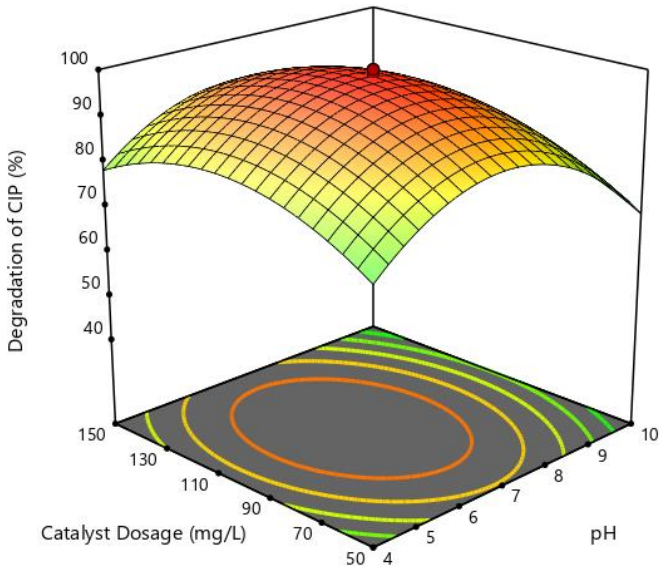

Fig. 4.12 Effect of catalyst dosage and pH in degradation of ciprofloxacin by photo-Fenton process

The interaction between pH and catalyst dosage is evident in the response surface plot, demonstrating that both parameters significantly influence degradation efficiency. The combined effect of pH and catalyst dosage is non-linear, highlighting the complexity of their interaction. Furthermore, the color gradient and contour lines on the plot illustrate that even small deviations from these optimal conditions can result in significant reductions in degradation efficiency. This finding underscores the

importance of precise control over pH and catalyst dosage in practical applications to maintain high degradation efficiency.

4.3.2.5 Effect of Reaction Time and pH

The analysis of the effect of reaction time and pH on degradation efficiency reveals that the highest degradation efficiency is achieved at higher pH values and longer reaction times (Fig. 4.13). This observation suggests that the degradation process is more effective under basic conditions and requires sufficient reaction time to achieve optimal degradation percentages. The optimal conditions for maximum degradation efficiency are identified at a pH range of 9 to 10 and a reaction time of approximately 39 minutes. This region corresponds to the peak of the response surface plot, where the highest degradation efficiency is observed. The influence of pH is particularly significant, with degradation efficiency increasing substantially as pH becomes more basic. This trend is crucial for designing effective treatment processes, as it indicates that adjusting the pH to a more basic level can enhance degradation performance. Additionally, the dependency on reaction time is notable, with longer reaction times generally resulting in higher degradation percentages. This suggests that the reaction kinetics are relatively slow, necessitating extended periods to reach completion. Therefore, optimizing both pH and reaction time is essential for maximizing degradation efficiency in practical applications.

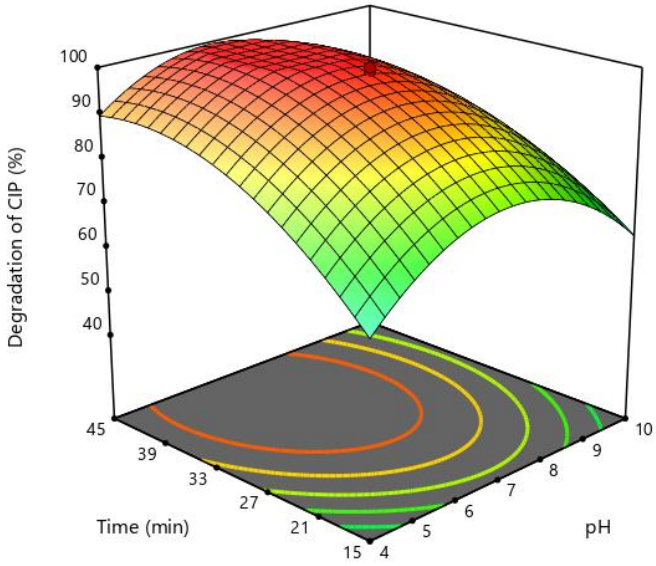

Fig. 4.13 Effect of reaction time and pH in degradation of ciprofloxacin by photo-Fenton process

4.3.2.6 Effect of Reaction Time and Catalyst Dosage

The analysis of catalyst dosage and reaction time on degradation efficiency reveals a clear positive correlation between these variables and the degradation percentage (Fig. 4.14).

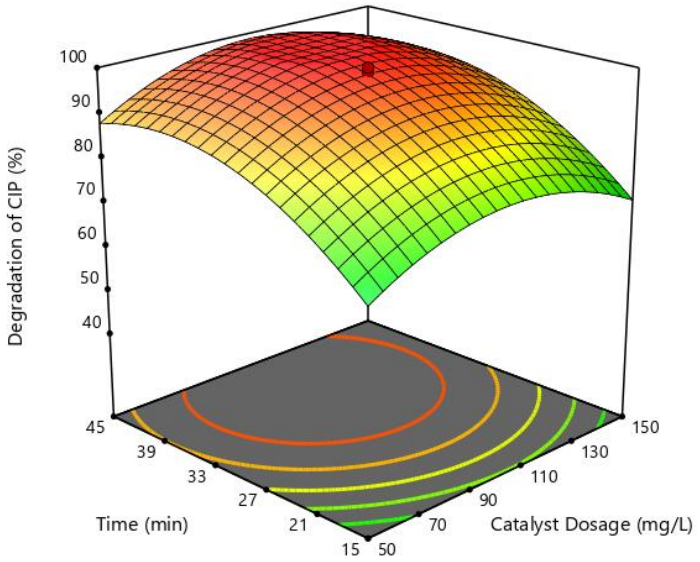

Fig. 4.14 Effect of catalyst dosage and reaction time in degradation of ciprofloxacin by photo-Fenton process

As both the reaction time and catalyst dosage increase, the degradation efficiency correspondingly improves. The analysis indicates that optimal degradation efficiency, approaching nearly 100%, is achieved at the highest values of both catalyst dosage and reaction time. This consistent improvement across the gradient underscores the importance of sufficient catalyst quantity and adequate reaction time in maximizing degradation efficiency. These findings are critical for optimizing operational parameters in practical applications to achieve the highest possible degradation rates.

4.4 Reactive Species Analysis of $FeWO_4$ Nanoparticles

Radical trapping experiments with $FeWO_4$ nanoparticles were carried out to degraded ciprofloxacin (50 mg/L) in order to determine the mechanism of the heterogeneous photo-Fenton catalytic process. Five scavengers, including isopropanol (IPA), sodium azide (SA), superoxide dismutase (SOD), triethanolamine (TEA) and potassium dichromate ($K_2Cr_2O_7$) were utilized for identification of $HO^{\bullet}$, $^1O_2$, $O_2^{\bullet-}$, h^+ and e^- during heterogeneous PF processes, respectively [24]. Fig. 4.15 represents the scavenger test of $FeWO_4$ nanoparticles and in the absence of a scavenger, it was shown that 99% of CIP was degraded after 40 minutes, however the corresponding figure substantially dropped upon the addition of 1 mM triethanolamine (TEA) and isopropanol (IPA), 71.3% and 78% of CIP degradation was achieved, respectively, indicating that the inhibition of CIP degradation reaction was caused by triethanolamine (TEA) and isopropanol (IPA). Conversely, the degradation efficiency of CIP somewhat reduced after the addition of 1 mM of sodium azide (SA), 0.025 mM of potassium dichromate ($K_2Cr_2O_7$) and 6u/mL of superoxide dismutase (SOD), nearly 83.7%, 86% and 88.7% of CIP degradation was still observed, respectively. This result indicating that sodium azide (SA), potassium dichromate ($K_2Cr_2O_7$) and superoxide dismutase (SOD) was less participate in the degradation of CIP. These findings demonstrated that the primary radicals causing CIP degradation were h^+ and $HO^{\bullet}$ radicals. by heterogeneous photo-Fenton system using $FeWO_4$ nanoparticle. The constraining impact of superoxide dismutase (SOD) indicated that 88.7% of CIP degradation was still evident, and the presence of SOD had a minimal quenching effect on the degradation of CIP which demonstrated that $O_2^{\bullet-}$ were minor radicals and minimal responsible for CIP degradation

[134]. The following is the reaction rate of different scavengers.: SOD > $K_2Cr_2O_7$ > SA> IPA > TEA, the following radicals have the matching contribution ability: $O_2^{\bullet-}$ < e^- < $^1O_2$ < $HO^\bullet$ < h^+.+. It suggested that the h^+ and $HO^\bullet$ are the main active species in the degradation process [45].

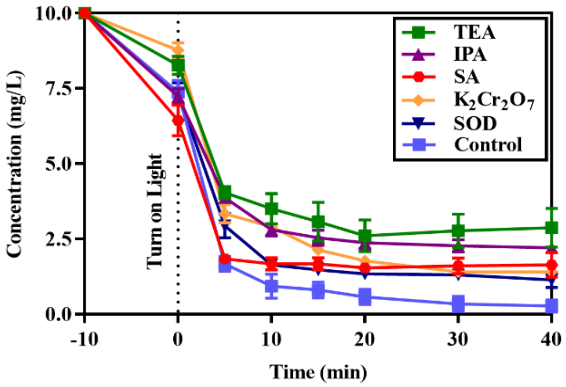

Fig. 4.15 Reactive Species Analysis of $FeWO_4$ NPs by photo-Fenton at the optimum doses (10 mg/L of CIP, 2 mM of H_2O_2, 100 mg/L of $FeWO_4$, pH = 7) and various reaction times.

A potential heterogeneous photo-Fenton catalytic mechanism for $FeWO_4$ nanoparticles has been proposed. The $FeWO_4$ nanoparticle experienced moderate distortion, resulting in the accumulation of substantial positive and negative charges (h^+/e^-) on its opposing surfaces. Photo-Fenton-induced h^+ is a pivotal element in the degradation process. It may directly participate in catalytic processes, degrading pollutants, or it can react with H_2O or OH^- adsorbed on the surface of the $FeWO_4$ nanoparticle to generate $HO^\bullet$ radicals. Consequently, the catalytic process was significantly inhibited by the introduction of an H^+ scavenger, as indicated by the outcomes of radical trapping experiments. Photo-Fenton-induced electrons can substantially augment the catalytic process as well. The electron can react with the adsorbed O_2 on the FeWO4 nanoparticle to produce $O_2^{\bullet-}$. Conversely, the e^- atoms would have promoted the Fe^{3+}/Fe^{2+} cycle, so catalytically promoting the Fenton reaction [273, 274]. The following illustrations demonstrate the key mechanisms involved in the breakdown of antibiotics by heterogeneous PF process using $FeWO_4$ [45, 275-277].

$$Fe^{2+} + H_2O_2 \rightarrow Fe^{3+} + HO^\bullet + OH^- \quad \text{Eq. 4.2}$$

$$Fe^{3+} + H_2O_2 \rightarrow Fe^{2+} + HO_2^\bullet + H^+ \quad \text{Eq. 4.3}$$

$$H_2O_2 + HO_2^\bullet \rightarrow HO^\bullet + O_2 \quad \text{Eq. 4.4}$$

$Fe^{3+} + HO_2^{\bullet} \rightarrow Fe^{2+} + H^+ + O_2$ Eq. 4.5

$O_2^{\bullet-} + H_2O_2 \rightarrow HO^{\bullet} + HO^- + O_2$ Eq. 4.6

$4HO^{\bullet} \rightarrow 2H_2O + {}^1O_2$ Eq. 4.7

$Fe^{3+} + H_2O + h\nu \rightarrow Fe^{2+} + HO^{\bullet} + H^+$ Eq. 4.8

$HO^{\bullet} + RH \rightarrow R^{\bullet} + H_2O$ Eq. 4.9

$HO^{\bullet} + RH \rightarrow R\text{-}OH$ Eq. 4.10

$FeWO_4 + h\nu \rightarrow FeWO_4 (h^+ + e^-)$ Eq. 4.11

$e^- + Fe^{3+} \rightarrow Fe^{2+}$ Eq. 4.12

$h^+ + H_2O/OH^- \rightarrow HO^{\bullet}$ Eq. 4.13

$e^- + O_2 \rightarrow {}^{\bullet}O_2^-$ Eq. 4.14

$H_2O_2 + Fe^{2+} \rightarrow Fe^{3+} + HO^{\bullet} + OH^-$ Eq. 4.15

$CIP + HO^{\bullet} \rightarrow H_2O + \text{Degradation products} \rightarrow CO_2 + H_2O$ Eq. 4.16

4.5 Stability and Reusability Test of $FeWO_4$ Nanoparticles

Two important characteristics of the nanomaterial that can help in reducing the treatment costs are its reusability and structural integrity. Five cycles of the tests were conducted in order to investigate the reusability of $FeWO_4$. Following that, $FeWO_4$ nanoparticles' catalytic activity did not significantly decline, and their performance was nearly constant across all cycles (Fig. 4.16). This finding suggests that the synthesized $FeWO_4$ nanoparticles can be an economical photocatalyst for environmental remediation.

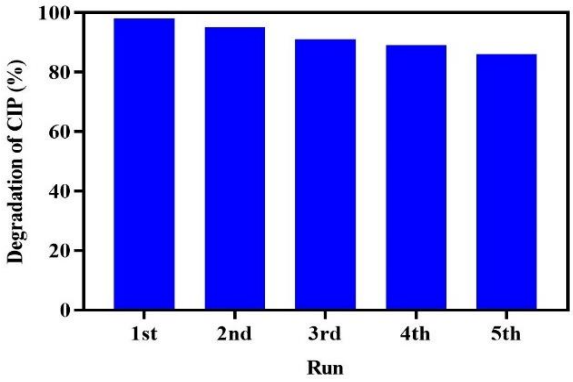

Fig. 4.16 Reusability test of $FeWO_4$ nanoparticle

4.6 Inactivation of ARB by $FeWO_4$ Nanoparticles Using Photo-Fenton Process

Fenton process is a potential advanced oxidation process (AOP) that is utilized for the degradation of antibiotics and the inactivation of microorganisms, including bacteria, fungi, viruses, and yeasts [278-280]. The process is augmented by H_2O_2 and light radiation, which produce $HO^{\bullet}$ that penetrate the bacterial outer membrane, resulting in heightened membrane permeability, triggering internal cellular processes, and ultimately inactivating the cells [281].

To assess the efficacy of $FeWO_4$ nanoparticle heterogeneous catalysts in inactivating antimicrobial-resistant bacteria (ARB), the concentration of *E. coli* was quantified in the UPW matrix. Initially, $FeWO_4$ nanoparticles and evaluated their efficacy in H_2O_2, Fenton, and photo-Fenton systems, contrasting their inactivation performance. The H_2O_2 and Fenton systems attained reductions of 2.08-log and 0.40-log, respectively. In the dark Fenton procedure, the combination of catalyst and H_2O_2 is insufficient to effectively inactivate ARB, resulting in a minimal inactivation of 0.40-log. Conversely, only H_2O_2 enhanced the ARB inactivation efficiency (2.08-log) but failed to achieve the detection limit after 40 minutes of treatment.Fig. 4.17 demonstrates that the PF system exhibited superior efficiency compared to the other two, achieving a complete (6.45-log) inactivation of ARB within 20 minutes of light irradiation. The superior disinfection efficacy achieved by $FeWO_4$ nanoparticles may be attributed to the improved interconversion between Fe^{3+} and Fe^{2+} ions. In this heterogeneous process, neither the catalyst nor H_2O_2 alone was adequate; however, the synergistic impact of $FeWO_4$ nanoparticles combined with H_2O_2 under illumination may inactivate all ARB. A comparable outcome was noted by Ahmed et al [26] , they found that 0.25 g/L of FeS_2@GO and 1 mM of H_2O_2 can efficiently inactivate 6.35 log ARB after 30 minutes of reaction time. In another study, Ahmed et al. applied photo-Fenton treatment with a lamp that simulates the visible sun spectrum with light-emitting diodes to evaluate the inactivation of *E. coli* DH5α and two ARGs (*tet*A and *bla*TEM-1) present in external and internal plasmids. The maximum bacterial inactivation (6.17-LRV) was achieved after 30 min of treatment in simulated wastewater using 2.8/340.2 mg/L (0.5/10 mM) of Fe^{2+}/H_2O_2 [71].

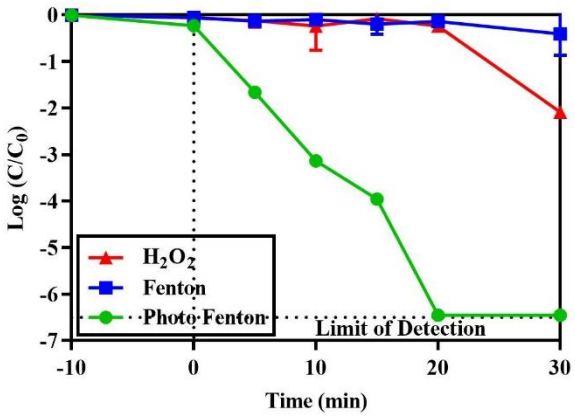

Fig. 4.17 Inactivation of ARB *E. coli* RP4 by Fenton and photo-Fenton process

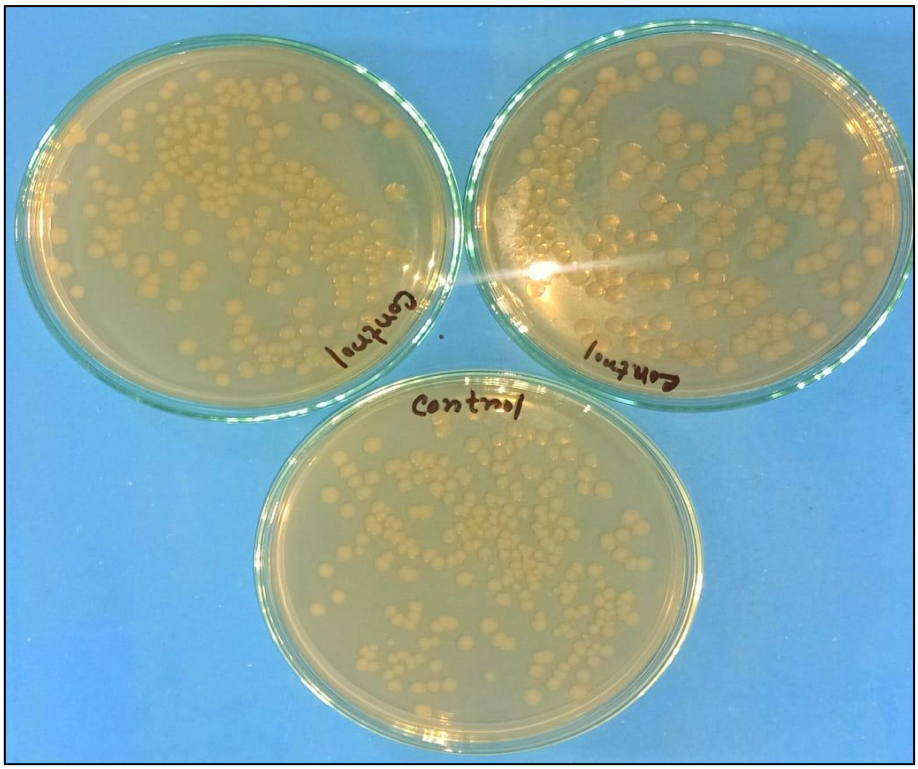

Fig. 4.18 ARB *E. coli* RP4 before starting the reaction (Control Test)

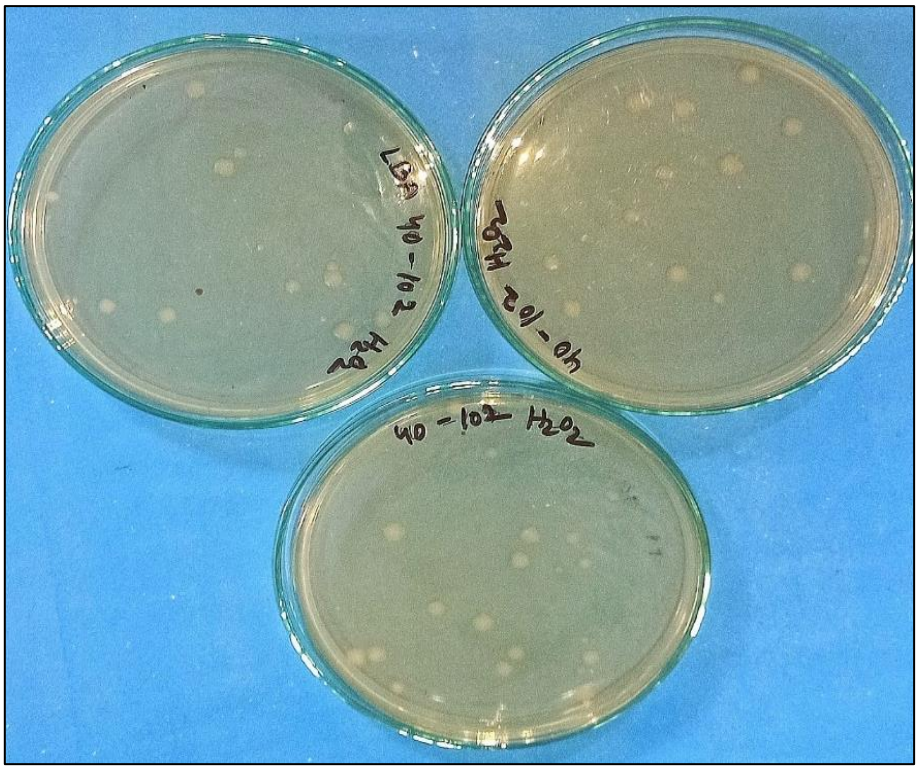

Fig. 4.19 Inactivation of ARB *E. coli* RP4 by H_2O_2

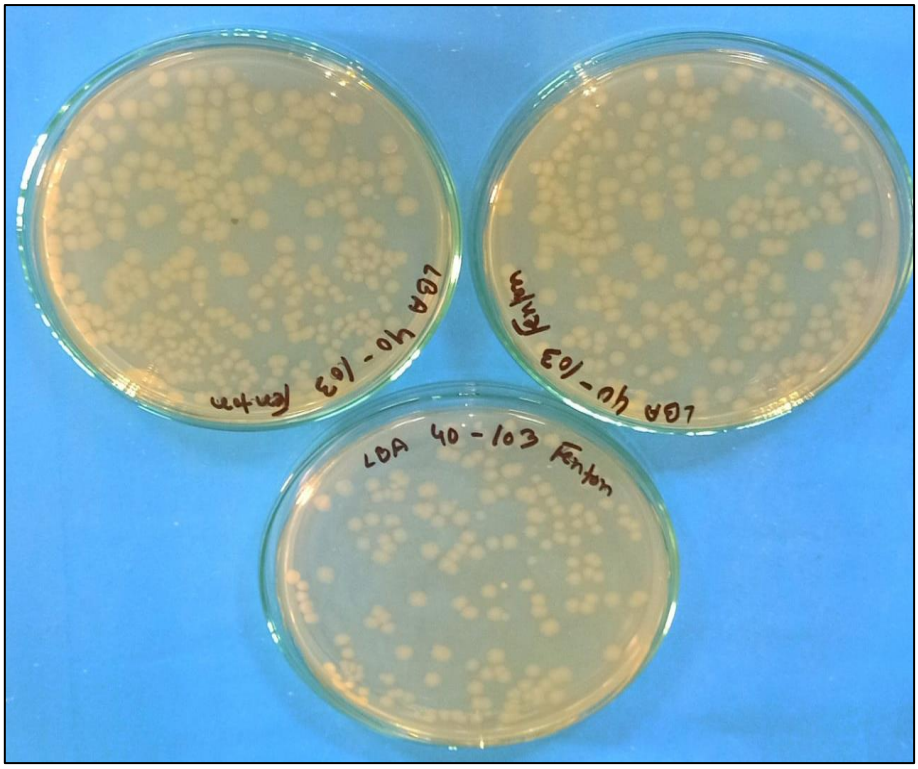

Fig. 4.20 Inactivation of ARB *E. coli* RP4 by Fenton Process

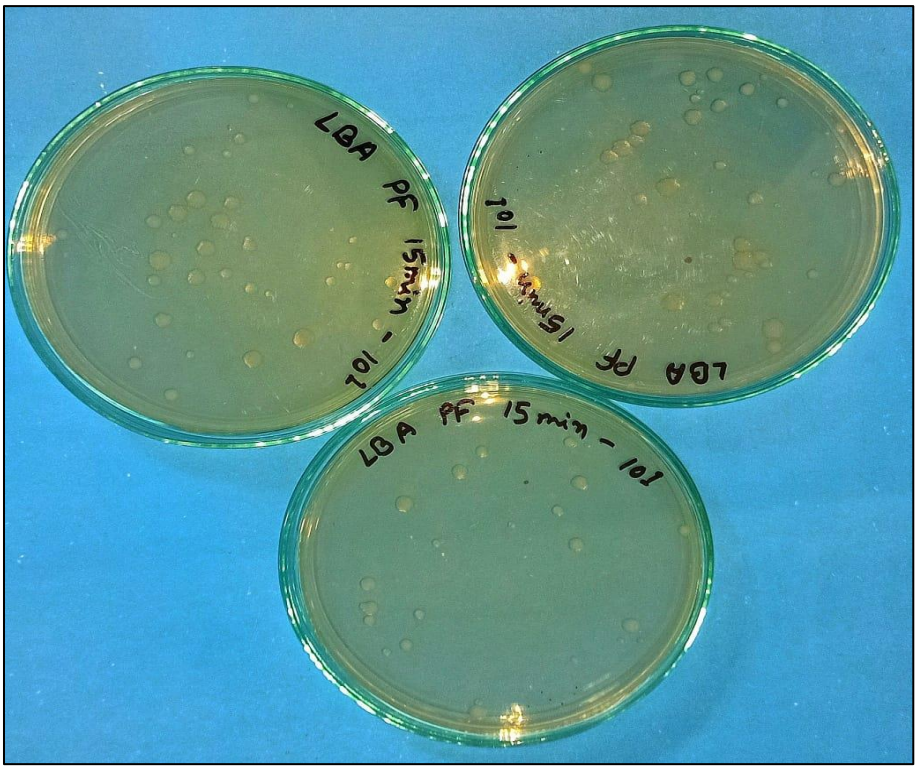

Fig. 4.21 Inactivation of ARB *E. coli* RP4 by photo-Fenton Process after 15 min treatment

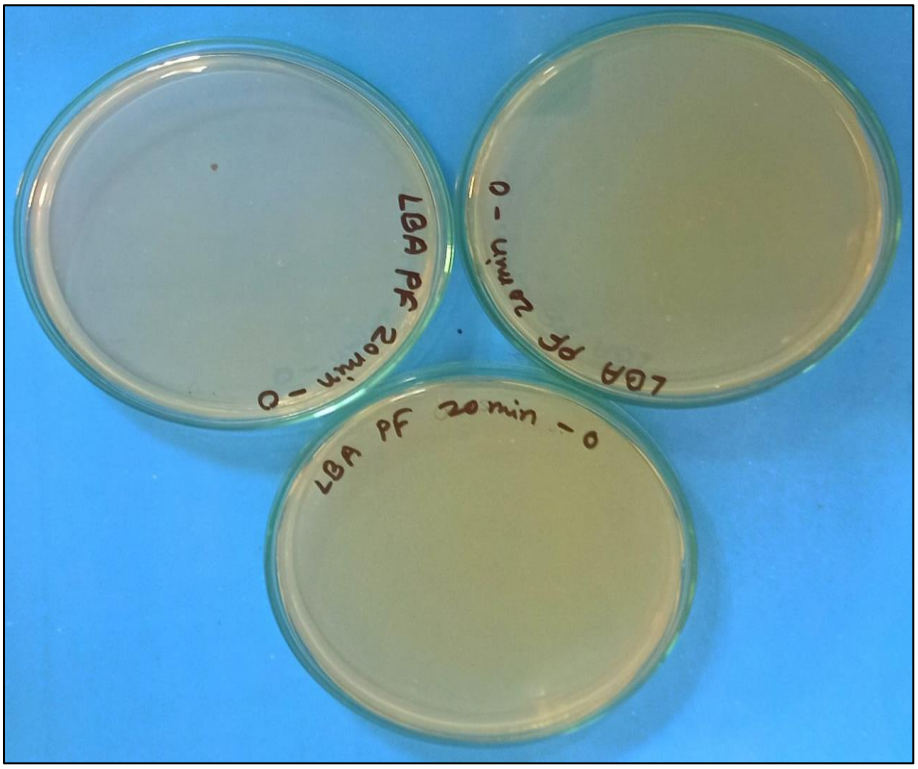

Fig. 4.22 Inactivation of ARB *E. coli* RP4 by photo-Fenton Process after 20 min treatment

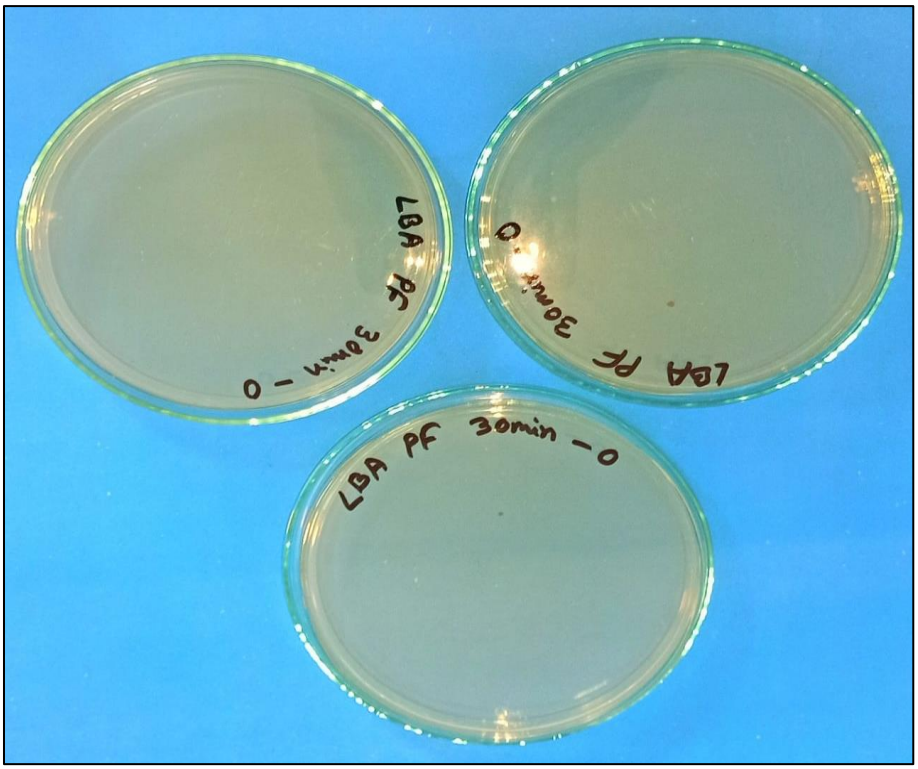

Fig. 4.23 Inactivation of ARB *E. coli* RP4 by photo-Fenton Process after 30 min treatment

Reagent concentration, solution pH, and HO• generation have been regarded as the key impacting factors affecting the effectiveness of the PF process. The inactivation efficiency distinctly improved when the molar ratio of Fe^{2+}/H_2O_2 was increased. The PF process is so sensitive to the Fe^{3+} concentration, mainly because its efficiency is dependent on ferric iron regeneration from ferrous iron-a rate-limiting phase [282]. Researchers suggest the solar-based PF procedure for the inactivation of ARB in the presence of UV visible sun light in order to improve the regeneration of Fe^{2+} [280]. Giannakis, Stefanos et al. (2018) demonstrated that a duration of 60 minutes of photo-Fenton treatment was necessary to achieve a 4-log reduction value of streptomycin-resistant *E. coli*, with no observed post-treatment regrowth, utilizing a concentration of 1/20 mg/L of Fe^{2+}/H_2O_2 [283]. Another study demonstrated that modifications improved bacterial inactivation compared to conventional SPF, achieving 6-LRV in 300 minutes for citric acid and 60 minutes for persulfate [284].

4.7 Regrowth Analysis of Antibiotic-Resistant Bacteria

The regrowth possibility of ARB was assessed to determine the relationship between treatment duration and bacterial cell damage, hence preventing bacterial regrowth post-treatment. As treatment duration increased, bacterial regeneration activity diminished, demonstrating that treatment time significantly influenced the complete removal of bacteria from the aqueous matrix. Following a 20-minute treatment, no ARB was detected (0 CFU/mL) in the sample. The regrowth became highly apparent after 48-h and 72-h incubation (Fig. 4.24).

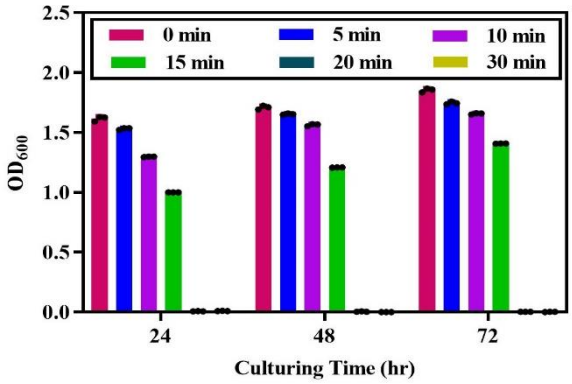

Fig. 4.24 Regrowth analysis of ARB *E. coli* RP4

Chapter 5: CONCLUSIONS

5.1 Conclusion

The $FeWO_4$ nanomaterials were successfully synthesized by hydrothermal process. By adjusting the NaOH concentration in a facile and affordable hydrothermal approach, the morphological changes were achieved and confirmed through FESEM characterization. The optical examination by UV-Vis DRS showed that the synthesized $FeWO_4$ nanoparticles have excellent photo-response ability and lowered bandgap energy compared to nanorods and nanofibers. The XRD characterization confirmed the excellent crystallinity of synthesized $FeWO_4$ nanomaterials. The binding energy peaks of Fe 2p, W 4f, and O 1s in XPS confirmed that synthesized $FeWO_4$ is in the pure phase. The electrochemical analysis (EIS and CV) results suggest that $FeWO_4$ is highly conductive and stable, making it suitable for applications in energy storage and catalysis. The catalytic activity of synthesized $FeWO_4$ nanomaterials has been explored by four types of Fenton processes and revealed that NPs possess notable catalytic efficiency than NR and NF in the degradation of ciprofloxacin (CIP) antibiotic by photo-Fenton and sono-photo-Fenton processes at neutral conditions. When exposed to visible light and H_2O_2, the $FeWO_4$ NPs can almost completely degrade CIP within 40 min. This study has proven that morphological structures of $FeWO_4$ nanomaterials substantially influence the elimination of CIP antibiotics present in contaminated water through photo-driven Fenton processes. However, the photo-Fenton process was optimized by Response Surface Methodology (RSM) and Central Composite Design (CCD) were used to improve the degradation of CIP by altering three independent variables: solution pH, catalyst dose (mg/L), and reaction time (min). The quadratic model was found to be significant through analysis of variance (ANOVA). Almost complete degradation was achieved at the optimum doses of 100 mg/L of $FeWO_4$, pH=7, and a 40-minute reaction time with initial concentrations of 10 mg/L for CIP and 2 mM for hydrogen peroxide (H_2O_2). The optimized dose is used to inactivate ARB *E. Coli* RP4 strain and found that 6.45 log ARB was removed after 20 minutes of reaction time and no bacteria regrowth

occur after 72h incubation period. The scavenger assay demonstrated the $HO^{\bullet}$ is the primary reactive species that is involved in the degradation of ciprofloxacin by $FeWO_4$ nanoparticles. The superior degradation of CIP antibiotics by $FeWO_4$ NPs can be attributed to the enhanced photo-response ability, which efficiently promotes the electron-hole separation rate to ensure fast generation of ROS during the photo-Fenton process. The photoexcited electrons could enhance the Fe^{3+}/Fe^{2+} cycle and expedite the Fenton catalytic process. The reusability test indicates that $FeWO_4$ nanoparticles can be an economical photocatalyst to use to remove environmental pollutants. The current study can be a standard for creating efficient and economical catalytic materials, which is necessary for addressing environmental problems and promoting the use of renewable energy.

5.2 Key Findings

- $FeWO_4$ nanoparticles showed a lower band gap and higher photocatalytic activity as a heterogenous catalyst at neutral pH solution as compared to other two nanomaterials.
- Removal efficiency of ciprofloxacin was up to 99% after 40 min by PF and SPF process.
- 6.45 log ARB *E. Coli* RP4 reduction occurs by photo-Fenton process after 20 min, without further regrowth risk.
- $HO^{\bullet}$ was revealed as the dominant radical in the degradation of antibiotic and antibiotic-resistant bacteria.
- Five cycles of use of $FeWO_4$ nanoparticles demonstrate it can be an economical photocatalyst for environmental remediation.

5.3 Limitation of the Study

- The study was carried out only on a lab-scale base experiment.
- UV spectrophotometer may not able to detect extremely low concentrations of antibiotic.
- Some physicochemical characterization could not do due to unfavoured situation.
- Unable to check the performance efficiency in the real-life wastewater for commercial application.

5.4 Recommendation for Further Study

Given the alarming global water scarcity, treated and reused wastewater could be a cost-effective, sustainable, and long-term solution. There are many kinds of pollutants being discharged by living beings which makes the water sources vulnerable for human health. So, this is a big matter of concern regarding future aspects. To improve the pollutant removal performance, Heterogeneous Fenton processes will be cost-effective and sustainable. As $FeWO_4$ shows a great result, further study should continue to see its effectiveness in real wastewater and also inactivate antibiotic resistant bacteria and antibiotic resistance genes from real wastewater samples to see how effective the nano catalyst is in the inactivation of those resistant bacteria and control the spread of antibiotic resistance.

REFERENCE

[1] S. Manzetti and R. Ghisi, "The environmental release and fate of antibiotics," *Marine Pollution Bulletin*, vol. 79, no.1, pp. 7-15, 2014.

[2] L. O. Omuferen, B. Maseko, and J. Olowoyo, "Occurrence of antibiotics in wastewater from hospital and convectional wastewater treatment plants and their impact on the effluent receiving rivers: Current knowledge between 2010 and 2019," *Environmental Monitoring and Assessment*, vol. 194, no.4, pp. 306, 2022.

[3] T. P. Van Boeckel, J. Pires, R. Silvester, C. Zhao, J. Song, N. G. Criscuolo, M. Gilbert, S. Bonhoeffer, and R. Laxminarayan, "Global trends in antimicrobial resistance in animals in low-and middle-income countries," *Science*, vol. 365, no.6459, pp. eaaw1944, 2019.

[4] M. J. Focazio, D. W. Kolpin, K. K. Barnes, E. T. Furlong, M. T. Meyer, S. D. Zaugg, L. B. Barber, and M. E. Thurman, "A national reconnaissance for pharmaceuticals and other organic wastewater contaminants in the United States — II) Untreated drinking water sources," *Science of The Total Environment*, vol. 402, no.2, pp. 201-216, 2008.

[5] P. Sahay, D. Mohite, S. Arya, K. Dalmia, Z. Khan, and A. Kumar, "Removal of the emergent pollutants (hormones and antibiotics) from wastewater using different kinds of biosorbent—A review," *Emergent Materials*, vol. 6, no.2, pp. 373-404, 2023.

[6] A. Pruden, Production and transport of antibiotics from CAFOs, in *Hormones and Pharmaceuticals Generated by Concentrated Animal Feeding Operations: Transport in Water and Soil*, A. Pruden and L. S. Shore, Editors. Springer US: New York, NY. pp. 63-70,2009.

[7] T. Heberer, "Occurrence, fate, and removal of pharmaceutical residues in the aquatic environment: A review of recent research data," *Toxicology Letters*, vol. 131, no.1, pp. 5-17, 2002.

[8] E. European Commission, J. R. Centre, I. Sanseverino, R. Loos, A. Navarro Cuenca, D. Marinov, and T. Lettieri, State of the art on the contribution of water to antimicrobial resistance. Publications Office2018.

[9] K. Kümmerer, "Antibiotics in the aquatic environment – A review – Part II," *Chemosphere*, vol. 75, no.4, pp. 435-441, 2009.

[10] V. Homem and L. Santos, "Degradation and removal methods of antibiotics from aqueous matrices–A review," *Journal of Environmental Management*, vol. 92, no.10, pp. 2304-2347, 2011.

[11] B. L. Phoon, C. C. Ong, M. S. M. Saheed, P.-L. Show, J.-S. Chang, T. C. Ling, S. S. Lam, and J. C. Juan, "Conventional and emerging technologies for removal of antibiotics from wastewater," *Journal of Hazardous Materials*, vol. 400, 122961, 2020.

[12] K.-J. Choi, S.-G. Kim, and S.-H. Kim, "Removal of antibiotics by coagulation and granular activated carbon filtration," *Journal of Hazardous Materials*, vol. 151, no.1, pp. 38-43, 2008.

[13] Z.-P. Xing and D.-Z. Sun, "Treatment of antibiotic fermentation wastewater by combined polyferric sulfate coagulation, Fenton and sedimentation process," *Journal of Hazardous Materials*, vol. 168, no.2, pp. 1264-1268, 2009.

[14] N. S. Mdluli, P. N. Nomngongo, and N. Mketo, The occurrence, effect and biodegradation of antibiotics using metallic biogenic nanomaterials in water, in

Biogenic Nanomaterials for Environmental Sustainability: Principles, Practices, and Opportunities. Springer. pp. 473-495,2024.

[15] J. Jeong, W. Song, W. J. Cooper, J. Jung, and J. Greaves, "Degradation of tetracycline antibiotics: Mechanisms and kinetic studies for advanced oxidation/reduction processes," *Chemosphere*, vol. 78, no.5, pp. 533-540, 2010.

[16] J. A. Garrido-Cardenas, B. Esteban-García, A. Agüera, J. A. Sánchez-Pérez, and F. Manzano-Agugliaro, "Wastewater treatment by advanced oxidation process and their worldwide research trends," *International Journal of Environmental Research and Public Health*, vol. 17, no.1, pp. 2019.

[17] Z. Li, J. Wang, J. Chang, B. Fu, and H. Wang, "Insight into advanced oxidation processes for the degradation of fluoroquinolone antibiotics: Removal, mechanism, and influencing factors," *Science of The Total Environment*, vol. 857, 159172, 2023.

[18] X. Wang, J. Jing, M. Zhou, and R. Dewil, "Recent advances in H_2O_2-based advanced oxidation processes for removal of antibiotics from wastewater," *Chinese Chemical Letters*, vol. 34, no.3, pp. 107621, 2023.

[19] J. Zhang, K.-H. Lee, L. Cui, and T.-s. Jeong, "Degradation of methylene blue in aqueous solution by ozone-based processes," *Journal of Industrial and Engineering Chemistry*, vol. 15, no.2, pp. 185-189, 2009.

[20] S. B. Verinda, M. Muniroh, E. Yulianto, N. Maharani, G. Gunawan, N. F. Amalia, J. Hobley, A. Usman, and M. Nur, "Degradation of ciprofloxacin in aqueous solution using ozone microbubbles: spectroscopic, kinetics, and antibacterial analysis," *Heliyon*, vol. 8, no.8, pp. e10137, 2022.

[21] H.-s. Ou, J.-s. Ye, S. Ma, C.-h. Wei, N.-y. Gao, and J.-z. He, "Degradation of ciprofloxacin by UV and UV/H_2O_2 via multiple-wavelength ultraviolet light-emitting diodes: Effectiveness, intermediates and antibacterial activity," *Chemical Engineering Journal*, vol. 289, 391-401, 2016.

[22] H. Masoumbeigi and A. Rezaee, "Removal of methylene blue (MB) dye from synthetic wastewater using UV/H_2O_2 advanced oxidation process," *Journal of Health Policy and Sustainable Health*, vol. 2, no.1, pp. 2015.

[23] R. Saleh and A. Taufik, "Degradation of methylene blue and congo-red dyes using Fenton, photo-Fenton, sono-Fenton, and sonophoto-Fenton methods in the presence of iron (II, III) oxide/zinc oxide/graphene (Fe_3O_4/ZnO/graphene) composites," *Separation and Purification Technology*, vol. 210, 563-573, 2019.

[24] Y. Ahmed, J. Zhong, Z. Yuan, and J. Guo, "Simultaneous removal of antibiotic resistant bacteria, antibiotic resistance genes, and micropollutants by a modified photo-Fenton process," *Water Research*, vol. 197, 117075, 2021.

[25] Y. Ahmed, Z. Yaakob, and P. Akhtar, "Degradation and mineralization of methylene blue using a heterogeneous photo-Fenton catalyst under visible and solar light irradiation," *Catalysis Science & Technology*, vol. 6, no.4, pp. 1222-1232, 2016.

[26] Y. Ahmed, J. Zhong, Z. Wang, L. Wang, Z. Yuan, and J. Guo, "Simultaneous removal of antibiotic resistant bacteria, antibiotic resistance genes, and micropollutants by FeS_2@GO-based heterogeneous photo-Fenton process," *Environmental Science and Technology* vol. 56, no.21, pp. 15156-15166, 2022.

[27] O. Baaloudj, I. Assadi, N. Nasrallah, A. El Jery, L. Khezami, and A. A. Assadi, "Simultaneous removal of antibiotics and inactivation of antibiotic-resistant bacteria by photocatalysis: A review," *Journal of Water Process Engineering*, vol. 42, 102089, 2021.

[28] S. M. Tichapondwa, J. P. Newman, and O. Kubheka, "Effect of TiO_2 phase on the photocatalytic degradation of methylene blue dye," *Physics and Chemistry of the Earth, Parts A/B/C*, vol. 118-119, 102900, 2020.

[29] G. Li, S. Zhou, Z. Shi, X. Meng, L. Li, and B. Liu, "Electrochemical degradation of ciprofloxacin on BDD anode using a differential column batch reactor: mechanisms, kinetics and pathways," *Environmental Science and Pollution Research*, vol. 26, no.17, pp. 17740-17750, 2019.

[30] M. R. Samarghandi, A. Dargahi, A. Shabanloo, H. Z. Nasab, Y. Vaziri, and A. Ansari, "Electrochemical degradation of methylene blue dye using a graphite doped PbO_2 anode: Optimization of operational parameters, degradation pathway and improving the biodegradability of textile wastewater," *Arabian Journal of Chemistry*, vol. 13, no.8, pp. 6847-6864, 2020.

[31] J. A. Garrido-Cardenas, B. Esteban-García, A. Agüera, J. A. Sánchez-Pérez, and F. Manzano-Agugliaro, "Wastewater treatment by advanced oxidation process and their worldwide research trends," *International Journal of Environmental Research and Public Health*, vol. 17, no.1, pp. 170, 2020.

[32] N. Barhoumi, N. Oturan, H. Olvera-Vargas, E. Brillas, A. Gadri, S. Ammar, and M. A. Oturan, "Pyrite as a sustainable catalyst in electro-Fenton process for improving oxidation of sulfamethazine. Kinetics, mechanism and toxicity assessment," *Water Research*, vol. 94, 52-61, 2016.

[33] J. I. Martínez-Costa, J. Rivera-Utrilla, R. Leyva-Ramos, M. Sánchez-Polo, I. Velo-Gala, and A. J. Mota, "Individual and simultaneous degradation of the antibiotics sulfamethoxazole and trimethoprim in aqueous solutions by Fenton, Fenton-like and photo-Fenton processes using solar and UV radiations," *Journal of Photochemistry and Photobiology A: Chemistry*, vol. 360, 95-108, 2018.

[34] Q. Yu, Y. Dai, Z. Zhang, and B. Feng, "Photo-Fenton enhanced degradation of antibiotic by Fe single-atom material: Mechanism, performance and adaptability," *Separation and Purification Technology*, vol. 310, 123149, 2023.

[35] Y. Jiang, J. Ran, K. Mao, X. Yang, L. Zhong, C. Yang, X. Feng, and H. Zhang, "Recent progress in Fenton/Fenton-like reactions for the removal of antibiotics in aqueous environments," *Ecotoxicology and Environmental Safety*, vol. 236, 113464, 2022.

[36] Z. Ji, R. Cai, W. Ye, P. Lu, C.-L. Dong, Y.-C. Huang, X. She, D. S. Butenko, Y. Liu, Y. Zhu, and D. Yang, "Confined Fe single atomic sites on (100) plane of anatase TiO_2 nanofibers boost white LED driven Fenton-like norfloxacin degradation," *Journal of Cleaner Production*, vol. 382, 135161, 2023.

[37] M. Karaca, C. Karaca, Z. Eroğlu, M. Sevim, and S. Karaca, "Usage of $MnFe_2O_4$-rGO nanocomposite as efficient Fenton catalyst for Tetracycline removal by heterogeneous sono Fenton process: Characterizations, catalytic performance assessment, and mechanism," *Materials Chemistry and Physics*, vol. 309, 128379, 2023.

[38] B. Kakavandi, M. Ahmadi, J. Bedia, M. Hashamfirooz, A. Naderi, V. Oskoei, H. Yousefian, R. Rezaei Kalantary, P. Rasool, and R. Dewil, "Metronidazole degradation mechanism by sono-photo-Fenton processes using a spinel ferrite cobalt on activated carbon catalyst," *Chemosphere*, vol. 358, 142102, 2024.

[39] Y. Tian, M. Zhou, Y. Pan, X. Du, and Q. Wang, "MoS_2 as highly efficient co-catalyst enhancing the performance of Fe^0 based electro-Fenton process in degradation of sulfamethazine: Approach and mechanism," *Chemical Engineering Journal*, vol. 403, 126361, 2021.

[40] M. Qian, F. Zhuo, Y. Li, P. Yi, Y. Gao, W. Zhou, Y. Sun, J. Chen, and X.-L. Wu, "FeNC catalyst coated on carbon felt for efficient degradation of antibiotics via electro-Fenton process," *Applied Surface Science*, vol. 609, 155310, 2023.

[41] J. Gao, Y. Gao, Z. Sui, Z. Dong, S. Wang, and D. Zou, "Hydrothermal synthesis of BiOBr/$FeWO_4$ composite photocatalysts and their photocatalytic degradation of doxycycline," *Journal of Alloys and Compounds*, vol. 732, 43-51, 2018.

[42] T. Ge, Z. Jiang, L. Shen, J. Li, Z. Lu, Y. Zhang, and F. Wang, "Synthesis and application of Fe_3O_4/$FeWO_4$ composite as an efficient and magnetically recoverable visible light-driven photocatalyst for the reduction of Cr(VI)," *Separation and Purification Technology*, vol. 263, 118401, 2021.

[43] C. Liu, H. Lü, C. Yu, B. Ding, R. Ye, Y. Ji, B. Dai, and W. Liu, "Novel $FeWO_4$/WO_3 nanoplate with p–n heterostructure and its enhanced mechanism for organic pollutants removal under visible-light illumination," *Journal of Environmental Chemical Engineering*, vol. 8, no.5, pp. 104044, 2020.

[44] H. Boudghene Stambouli, F. Guenfoud, A. Benomara, M. Mokhtari, and M. Sönmez-Çelebi, "Synthesis of $FeWO_4$ heterogeneous composite by the sol–gel process: enhanced photocatalytic activity on malachite green," *Reaction Kinetics, Mechanisms and Catalysis*, vol. 133, no.1, pp. 563-578, 2021.

[45] D. Sun, N. Iqbal, W. Liao, Y. Lu, X. He, K. Wang, B. Ma, Y. Zhu, K. Sun, Z. Sun, and T. Li, "Efficient degradation of MB dye by 1D $FeWO_4$ nanomaterials through the synergistic effect of piezo-Fenton catalysis," *Ceramics International*, vol. 48, no.17, pp. 25465-25473, 2022.

[46] E. N. Zare, S. Iftekhar, Y. Park, J. Joseph, V. Srivastava, M. A. Khan, P. Makvandi, M. Sillanpaa, and R. S. Varma, "An overview on non-spherical semiconductors for heterogeneous photocatalytic degradation of organic water contaminants," *Chemosphere*, vol. 280, 130907, 2021.

[47] S. W. A. Shah, M. u. Rehman, M. Arslan, S. A. Abbasi, A. Hayat, S. Anwar, S. Iqbal, and M. Afzal, "Response surface methodology for optimization of operational parameters to remove ciprofloxacin from contaminated water in the presence of a bacterial consortium," *ACS Omega*, vol. 7, no.31, pp. 27450-27457, 2022.

[48] A. A. Najafpoor, O. N. Sani, H. Alidadi, M. Yazdani, A. A. N. Fezabady, and M. Taghavi, "Optimization of ciprofloxacin adsorption from synthetic wastewaters using γ-Al_2O_3 nanoparticles: an experimental design based on response surface methodology," *Colloid and Interface Science Communications*, vol. 33, 100212, 2019.

[49] Y. Ahmed, A. A. Siddiqua Maya, P. Akhtar, M. S. Alam, H. AlMohamadi, M. N. Islam, O. A. Alharbi, and S. M. Rahman, "A novel interpretable machine learning and metaheuristic-based protocol to predict and optimize ciprofloxacin antibiotic adsorption with nano-adsorbent," *Journal of Environmental Management*, vol. 370, 122614, 2024.

[50] Y. Ahmed, M. M. Rahman, M. S. Alam, M. I. Miah, M. S. H. Choudhury, O. A. Alharbi, P. Akhtar, and S. M. Rahman, "Harnessing neural network model with optimization for enhanced ciprofloxacin antibiotic adsorption from contaminated water: A transparent and objective framework," *Journal of Water Process Engineering*, vol. 65, 105724, 2024.

[51] E. A. Serna-Galvis, A. M. Botero-Coy, D. Martínez-Pachón, A. Moncayo-Lasso, M. Ibáñez, F. Hernández, and R. A. Torres-Palma, "Degradation of seventeen contaminants of emerging concern in municipal wastewater effluents by

sonochemical advanced oxidation processes," *Water Research*, vol. 154, 349-360, 2019.

[52] J. Jiang, X. Wang, Y. Liu, Y. Ma, T. Li, Y. Lin, T. Xie, and S. Dong, "Photo-Fenton degradation of emerging pollutants over Fe-POM nanoparticle/porous and ultrathin g-C_3N_4 nanosheet with rich nitrogen defect: Degradation mechanism, pathways, and products toxicity assessment," *Applied Catalysis B: Environmental*, vol. 278, 119349, 2020.

[53] L. Zhang, Z. Zhu, M. Zhao, J. He, X. Zhang, F. Hao, and P. Du, "Occurrence, removal, emission and environment risk of 32 antibiotics and metabolites in wastewater treatment plants in Wuhu, China," *Science of The Total Environment*, vol. 899, 165681, 2023.

[54] J. Guo, Y. Wang, Y. Ahmed, M. Jin, and J. Li, Control strategies to combat dissemination of antibiotic resistance in urban water systems, in *Antibiotic Resistance in the Environment : A Worldwide Overview*, C. M. Manaia, E. Donner, I. Vaz-Moreira, and P. Hong, Editors. Springer International Publishing: Cham. pp. 147-187,2020.

[55] J. Zhong, Y. Ahmed, G. Carvalho, Z. Wang, L. Wang, J. F. Mueller, and J. Guo, "Simultaneous removal of micropollutants, antibiotic resistant bacteria, and antibiotic resistance genes using graphitic carbon nitride under simulated solar irradiation," *Chemical Engineering Journal*, vol. 433, 133839, 2022.

[56] J. Zhong, Y. Ahmed, Z. Yu, J. F. Mueller, and J. Guo, "Synergistic combination of graphitic carbon nitride and peroxymonosulfate for efficient photocatalytic destruction of emerging contaminants under simulated solar irradiation," *ACS ES&T Water*, vol. 3, no.1, pp. 6-15, 2023.

[57] Y. Ahmed, J. Zhong, Z. Yuan, and J. Guo, "Roles of reactive oxygen species in antibiotic resistant bacteria inactivation and micropollutant degradation in Fenton and photo-Fenton processes," *Journal of Hazardous Materials*, vol. 430, 128408, 2022.

[58] Y.-M. Zhu, Y. Chen, H. Lu, K. Jin, Y. Lin, H. Ren, and K. Xu, "Simultaneous efficient removal of tetracycline and mitigation of antibiotic resistance genes enrichment by a modified activated sludge process with static magnetic field," *Water Research*, vol. 262, 122107, 2024.

[59] Z. Lu, G. Liu, H. Xie, Y. Zhai, and X. Li, "Advances and solutions in biological treatment for antibiotic wastewater with resistance genes: A review," *Journal of Environmental Management*, vol. 368, 122115, 2024.

[60] S. Li, N. Hofstra, M. G. M. van de Schans, J. Yang, Y. Li, Q. Zhang, L. Ma, M. Strokal, C. Kroeze, X. Chen, X. Chen, and F. Zhang, "Riverine antibiotics from animal production and wastewater," *Environmental Science & Technology Letters*, vol. 10, no.11, pp. 1059-1067, 2023.

[61] O.-o. L. Oharisi, S. Ncube, H. Nyoni, M. L. Madikizela, O. J. Olowoyo, and B. R. Maseko, "Occurrence and prevalence of antibiotics in wastewater treatment plants and effluent receiving rivers in South Africa using UHPLC-MS determination," *Journal of Environmental Management*, vol. 345, 118621, 2023.

[62] B. Wang, Z. Xu, and B. Dong, "Occurrence, fate, and ecological risk of antibiotics in wastewater treatment plants in China: A review," *Journal of Hazardous Materials*, vol. 469, 133925, 2024.

[63] P. Akhtar, Y. Ahmed, F. Islam, K. Alam, M. Mary, M. Z. Islam, M. M. H. Bhuiyan, and Z. Yaakob, "Efficiency of Effluent Treatment Plants and Threat to Human Health and Aquatic Environment in Bangladesh," *Asian Journal of Chemistry*, vol. 28, no.1, pp. 60-68, 2015.

[64] E. Brillas, "Progress of antibiotics removal from synthetic and real waters and wastewaters by persulfate-based advanced oxidation processes," *Journal of Environmental Chemical Engineering*, vol. 11, no.6, pp. 111303, 2023.
[65] Z. Honarmandrad, X. Sun, Z. Wang, M. Naushad, and G. Boczkaj, "Activated persulfate and peroxymonosulfate based advanced oxidation processes (AOPs) for antibiotics degradation – A review," *Water Resources and Industry*, vol. 29, 100194, 2023.
[66] Y. Zhang, Y.-G. Zhao, F. Maqbool, and Y. Hu, "Removal of antibiotics pollutants in wastewater by UV-based advanced oxidation processes: Influence of water matrix components, processes optimization and application: A review," *Journal of Water Process Engineering*, vol. 45, 102496, 2022.
[67] Z. Lu, Y. Ling, W. Sun, C. Liu, T. Mao, X. Ao, and T. Huang, "Antibiotics degradation by UV/chlor (am) ine advanced oxidation processes: A comprehensive review," *Environmental Pollution*, vol. 308, 119673, 2022.
[68] A. J. dos Santos, M. S. Kronka, G. V. Fortunato, and M. R. V. Lanza, "Recent advances in electrochemical water technologies for the treatment of antibiotics: A short review," *Current Opinion in Electrochemistry*, vol. 26, 100674, 2021.
[69] M.-f. Li, Y.-g. Liu, G.-m. Zeng, N. Liu, and S.-b. Liu, "Graphene and graphene-based nanocomposites used for antibiotics removal in water treatment: A review," *Chemosphere*, vol. 226, 360-380, 2019.
[70] X. Bai, W. Chen, B. Wang, T. Sun, B. Wu, and Y. Wang, "Photocatalytic degradation of some typical antibiotics: Recent advances and future outlooks," *International Journal of Molecular Sciences*, vol. 23, no.15, pp. 8130, 2022.
[71] Y. Ahmed, J. Lu, Z. Yuan, P. L. Bond, and J. Guo, "Efficient inactivation of antibiotic resistant bacteria and antibiotic resistance genes by photo-Fenton process under visible LED light and neutral pH," *Water Research*, vol. 179, 115878, 2020.
[72] F. Machado, A. C. S. C. Teixeira, and L. A. M. Ruotolo, "Critical review of Fenton and photo-Fenton wastewater treatment processes over the last two decades," *International Journal of Environmental Science and Technology*, vol. 20, no.12, pp. 13995-14032, 2023.
[73] Q. Wang, Y. Ma, and S. Xing, "Comparative study of Cu-based bimetallic oxides for Fenton-like degradation of organic pollutants," *Chemosphere*, vol. 203, 450-456, 2018.
[74] N. Wang, T. Zheng, G. Zhang, and P. Wang, "A review on Fenton-like processes for organic wastewater treatment," *Journal of Environmental Chemical Engineering*, vol. 4, no.1, pp. 762-787, 2016.
[75] H. Zeng, J. Li, W. Zhao, J. Xu, H. Xu, D. Li, and J. Zhang, "The current status and prevention of antibiotic pollution in groundwater in China," *International Journal of Environmental Research and Public Health*, vol. 19, no.18, pp. 11256, 2022.
[76] J. A. Galarza, L. Murphy, and J. Mappes, "Antibiotics accelerate growth at the expense of immunity," *Proceedings of The Royal Society B: Biological Sciences*, vol. 288, no.1961, pp. 20211819, 2021.
[77] K. C. Leung, Q. Huang, S. St-Hilaire, H. Liu, X. Zheng, K. B. Cheung, and I. M. Zwetsloot, "Fraudulent antibiotic products on the market for aquaculture use," *Preventive Veterinary Medicine*, vol. 181, 105052, 2020.
[78] K. Wang, T. Zhuang, Z. Su, M. Chi, and H. Wang, "Antibiotic residues in wastewaters from sewage treatment plants and pharmaceutical industries:

Occurrence, removal and environmental impacts," *Science of The Total Environment*, vol. 788, 147811, 2021.
[79] S. I. Polianciuc, A. E. Gurzău, B. Kiss, M. G. Ştefan, and F. Loghin, "Antibiotics in the environment: causes and consequences," *Medicine and Pharmacy Reports*, vol. 93, no.3, pp. 231, 2020.
[80] R. Wang, M. Ji, H. Zhai, Y. Guo, and Y. Liu, "Occurrence of antibiotics and antibiotic resistance genes in WWTP effluent-receiving water bodies and reclaimed wastewater treatment plants," *Science of The Total Environment*, vol. 796, 148919, 2021.
[81] J. Xue, D. Lei, X. Zhao, Y. Hu, S. Yao, K. Lin, Z. Wang, and C. Cui, "Antibiotic residue and toxicity assessment of wastewater during the pharmaceutical production processes," *Chemosphere*, vol. 291, 132837, 2022.
[82] N. Hassoun-Kheir, Y. Stabholz, J.-U. Kreft, R. de la Cruz, J. L. Romalde, J. Nesme, S. J. Sørensen, B. F. Smets, D. Graham, and M. Paul, "Comparison of antibiotic-resistant bacteria and antibiotic resistance genes abundance in hospital and community wastewater: A systematic review," *Science of The Total Environment*, vol. 743, 140804, 2020.
[83] R. Selvarajan, T. Sibanda, J. Pandian, and K. Mearns, "Taxonomic and functional distribution of bacterial communities in domestic and hospital wastewater system: Implications for public and environmental health," *Antibiotics*, vol. 10, no.9, pp. 1059, 2021.
[84] R. Anjali and S. Shanthakumar, "Insights on the current status of occurrence and removal of antibiotics in wastewater by advanced oxidation processes," *Journal of Environmental Management*, vol. 246, 51-62, 2019.
[85] M. Z. Akbari, Y. Xu, Z. Lu, and L. Peng, "Review of antibiotics treatment by advance oxidation processes," *Environmental Advances*, vol. 5, 100111, 2021.
[86] J. Wang and R. Zhuan, "Degradation of antibiotics by advanced oxidation processes: An overview," *Science of The Total Environment*, vol. 701, 135023, 2020.
[87] R. Pulicharla, S. K. Brar, T. Rouissi, S. Auger, P. Drogui, M. Verma, and R. Y. Surampalli, "Degradation of chlortetracycline in wastewater sludge by ultrasonication, Fenton oxidation, and ferro-sonication," *Ultrasonics Sonochemistry*, vol. 34, 332-342, 2017.
[88] X. Li, S. Chen, I. Angelidaki, and Y. Zhang, "Bio-electro-Fenton processes for wastewater treatment: Advances and prospects," *Chemical Engineering Journal*, vol. 354, 492-506, 2018.
[89] Q. Ouyang, F. Kou, P. E. Tsang, J. Lian, J. Xian, J. Fang, and Z. Fang, "Green synthesis of Fe-based material using tea polyphenols and its application as a heterogeneous Fenton-like catalyst for the degradation of lincomycin," *Journal of Cleaner Production*, vol. 232, 1492-1498, 2019.
[90] Z. Wan and J. Wang, "Ce-doped zero-valent iron nanoparticles as a Fenton-like catalyst for degradation of sulfamethazine," *RSC advances*, vol. 6, no.105, pp. 103523-103531, 2016.
[91] Q. Shi, N. A. Al-Dhabi, M. Cheng, Y. Liu, J. Wang, G. Wang, G. Zhang, L. Li, L. Du, H. Liu, S. Yang, and W. Tang, "Puissant synergistic effect between g-C_3N_4 and MIL-100(Fe) for highly stable enhanced activation of H_2O_2 to degrade antibiotic tetracycline hydrochloride," *Journal of Environmental Chemical Engineering*, vol. 12, no.3, pp. 112537, 2024.

[92] L. Clarizia, D. Russo, I. Di Somma, R. Marotta, and R. Andreozzi, "Homogeneous photo-Fenton processes at near neutral pH: A review," *Applied Catalysis B: Environmental*, vol. 209, 358-371, 2017.
[93] A. Babuponnusami and K. Muthukumar, "A review on Fenton and improvements to the Fenton process for wastewater treatment," *Journal of Environmental Chemical Engineering*, vol. 2, no.1, pp. 557-572, 2014.
[94] W. Baran and E. Adamek, "Degradation of veterinary antibiotics by Fenton process: Products identification and toxicity assessment," *Chemosphere*, vol. 341, 139854, 2023.
[95] C. Dong, W. Fang, Q. Yi, and J. Zhang, "A comprehensive review on reactive oxygen species (ROS) in advanced oxidation processes (AOPs)," *Chemosphere*, vol. 308, 136205, 2022.
[96] M. E. Sillanpää, T. A. Kurniawan, and W.-h. Lo, "Degradation of chelating agents in aqueous solution using advanced oxidation process (AOP)," *Chemosphere*, vol. 83, no.11, pp. 1443-1460, 2011.
[97] T. Oppenländer, "Mercury-free sources of VUV/UV radiation: application of modern excimer lamps (excilamps) for water and air treatment," *Journal of Environmental Engineering and Science*, vol. 6, no.3, pp. 253-264, 2007.
[98] G. Yang, Y. Liang, H. Zheng, X. Zhang, and J. Jia, "Fe-polyoxometalate nanodots decorated Bi_2MoO_6 nanosheets with dominant {010} facets for photo-Fenton degradation of antibiotics over a wide pH range: Mechanism insight and toxicity assessment," *Separation and Purification Technology*, vol. 310, 123167, 2023.
[99] W. He, H. Jia, Z. Li, C.-q. Miao, R. Lu, S. Zhang, and Z. Zhang, "Magnetic recyclable g-C_3N_4/Fe_3O_4@MIL-100(Fe) ternary catalyst for photo-Fenton degradation of ciprofloxacin," *Journal of Environmental Chemical Engineering*, vol. 10, no.6, pp. 108698, 2022.
[100] M. A. Oturan and J.-J. Aaron, "Advanced Oxidation Processes in Water/Wastewater Treatment: Principles and Applications. A Review," *Critical Reviews in Environmental Science and Technology*, vol. 44, no.23, pp. 2577-2641, 2014.
[101] H. Li, Y. Li, L. Xiang, Q. Huang, J. Qiu, H. Zhang, M. V. Sivaiah, F. Baron, J. Barrault, S. Petit, and S. Valange, "Heterogeneous photo-Fenton decolorization of Orange II over Al-pillared Fe-smectite: Response surface approach, degradation pathway, and toxicity evaluation," *Journal of Hazardous Materials*, vol. 287, 32-41, 2015.
[102] H. Qin, H. Cheng, H. Li, and Y. Wang, "Degradation of ofloxacin, amoxicillin and tetracycline antibiotics using magnetic core–shell $MnFe_2O_4$@C-NH_2 as a heterogeneous Fenton catalyst," *Chemical Engineering Journal*, vol. 396, 125304, 2020.
[103] M. A. Tony, P. J. Purcell, Y. Q. Zhao, A. M. Tayeb, and M. F. El-Sherbiny, "Photo-catalytic degradation of an oil-water emulsion using the photo-Fenton treatment process: Effects and statistical optimization," *Journal of Environmental Science and Health, Part A*, vol. 44, no.2, pp. 179-187, 2009.
[104] L. Hou, L. Wang, S. Royer, and H. Zhang, "Ultrasound-assisted heterogeneous Fenton-like degradation of tetracycline over a magnetite catalyst," *Journal of Hazardous Materials*, vol. 302, 458-467, 2016.
[105] E. De Bel, C. Janssen, S. De Smet, H. Van Langenhove, and J. Dewulf, "Sonolysis of ciprofloxacin in aqueous solution: Influence of operational parameters," *Ultrasonics Sonochemistry*, vol. 18, no.1, pp. 184-189, 2011.

[106] J.-K. Im, J. Yoon, N. Her, J. Han, K.-D. Zoh, and Y. Yoon, "Sonocatalytic-TiO_2 nanotube, Fenton, and CCl_4 reactions for enhanced oxidation, and their applications to acetaminophen and naproxen degradation," *Separation and Purification Technology*, vol. 141, 1-9, 2015.
[107] J. Liu, C. Dong, Y. Deng, J. Ji, S. Bao, C. Chen, B. Shen, J. Zhang, and M. Xing, "Molybdenum sulfide Co-catalytic Fenton reaction for rapid and efficient inactivation of *Escherichia coli*," *Water Research*, vol. 145, 312-320, 2018.
[108] T. Song, G. Li, R. Hu, Y. Liu, H. Liu, and Y. Gao, "Degradation of antibiotics via UV-activated peroxodisulfate or peroxymonosulfate: A Review," *Catalysts*, vol. 12, no.9, pp. 1025, 2022.
[109] P. Karaolia, I. Michael-Kordatou, E. Hapeshi, J. Alexander, T. Schwartz, and D. Fatta-Kassinos, "Investigation of the potential of a membrane bioreactor followed by solar Fenton oxidation to remove antibiotic-related microcontaminants," *Chemical Engineering Journal*, vol. 310, 491-502, 2017.
[110] M. Pirsaheb, N. Moradi, and H. Hossini, "Sonochemical processes for antibiotics removal from water and wastewater: A systematic review," *Chemical Engineering Research and Design*, vol. 189, 401-439, 2023.
[111] W. Yang, N. Oturan, J. Liang, and M. A. Oturan, "Synergistic mineralization of ofloxacin in electro-Fenton process with BDD anode: Reactivity and mechanism," *Separation and Purification Technology*, vol. 319, 124039, 2023.
[112] E. Adamek, E. Masternak, D. Sapińska, and W. Baran, "Degradation of the selected antibiotic in an aqueous solution by the Fenton process: Kinetics, products and ecotoxicity," *International Journal of Molecular Sciences*, vol. 23, no.24, pp. 15676, 2022.
[113] E. Gürtekin, M. Çelik, E. Aydın, and A. Celik, "Degradation of oxytetracycline and chlortetracycline by Fenton process," *Journal of the Institute of Science and Technology*, vol. 13, no.1, pp. 192-199, 2023.
[114] T. Kanti Das, M. R. Wati, and K. Fatima-Shad, "Oxidative Stress Gated by Fenton and Haber Weiss Reactions and Its Association With Alzheimer's Disease," *Archives of Neuroscience*, vol. 2, no.2, pp. e60038, 2015.
[115] Q. Yi, J. Ji, B. Shen, C. Dong, J. Liu, J. Zhang, and M. Xing, "Singlet oxygen triggered by superoxide radicals in a molybdenum cocatalytic Fenton reaction with enhanced REDOX activity in the environment," *Environmental Science & Technology*, vol. 53, no.16, pp. 9725-9733, 2019.
[116] Y. Liu and J. Wang, "Multivalent metal catalysts in Fenton/Fenton-like oxidation system: A critical review," *Chemical Engineering Journal*, vol. 466, 143147, 2023.
[117] R. Palominos, J. Freer, M. A. Mondaca, and H. D. Mansilla, "Evidence for hole participation during the photocatalytic oxidation of the antibiotic flumequine," *Journal of Photochemistry and Photobiology A: Chemistry*, vol. 193, no.2, pp. 139-145, 2008.
[118] H. J. H. Fenton, "LXXIII.—Oxidation of tartaric acid in presence of iron," *Journal of the Chemical Society, Transactions*, vol. 65, 899-910, 1894.
[119] E. Elmolla and M. Chaudhuri, "Optimization of Fenton process for treatment of amoxicillin, ampicillin and cloxacillin antibiotics in aqueous solution," *Journal of Hazardous Materials*, vol. 170, no.2, pp. 666-672, 2009.
[120] C. Rodrigues-Silva, M. G. Maniero, S. Rath, and J. R. Guimarães, "Degradation of flumequine by the Fenton and photo-Fenton processes: Evaluation of residual antimicrobial activity," *Science of The Total Environment*, vol. 445-446, 337-346, 2013.

[121] G. Rakhshandehroo, M. Salari, and M. Nikoo, "Optimization of degradation of ciprofloxacin antibiotic and assessment of degradation products using full factorial experimental design by Fenton homogenous process," *Global NEST Journal*, vol. 20, no.2, pp. 324-332, 2018.
[122] A. Gupta and A. Garg, "Degradation of ciprofloxacin using Fenton's oxidation: Effect of operating parameters, identification of oxidized by-products and toxicity assessment," *Chemosphere*, vol. 193, 1181-1188, 2018.
[123] Y.-Y. Lee and C. Fan, "Mechanistic exploration of the catalytic modification by co-dissolved organic molecules for micropollutant degradation during Fenton process," *Chemosphere*, vol. 258, 127338, 2020.
[124] S. Wang and J. Wang, "Comparative study on sulfamethoxazole degradation by Fenton and Fe(II)-activated persulfate process," *RSC Advances*, vol. 7, no.77, pp. 48670-48677, 2017.
[125] S. Wang and J. Wang, "Trimethoprim degradation by Fenton and Fe(II)-activated persulfate processes," *Chemosphere*, vol. 191, 97-105, 2018.
[126] Z. Fang, J. Chen, X. Qiu, X. Qiu, W. Cheng, and L. Zhu, "Effective removal of antibiotic metronidazole from water by nanoscale zero-valent iron particles," *Desalination*, vol. 268, no.1, pp. 60-67, 2011.
[127] S. K. Mondal, A. K. Saha, and A. Sinha, "Removal of ciprofloxacin using modified advanced oxidation processes: Kinetics, pathways and process optimization," *Journal of Cleaner Production*, vol. 171, 1203-1214, 2018.
[128] N. Zhang, J. Chen, Z. Fang, and E. P. Tsang, "Ceria accelerated nanoscale zerovalent iron assisted heterogenous Fenton oxidation of tetracycline," *Chemical Engineering Journal*, vol. 369, 588-599, 2019.
[129] H. Guo, Z. Li, Z. Xie, J. Song, L. Xiang, L. Zhou, C. Li, L. liuni, J. Li, and H. Wang, "Accelerated Fenton reaction for antibiotic ofloxacin degradation in discharge plasma system based on graphene-Fe_3O_4 nanocomposites," *Vacuum*, vol. 185, 110022, 2021.
[130] L. Liu, R. Yu, S. Zhao, X. Cao, X. Zhang, and S. Bai, "Heterogeneous Fenton system driven by iron-loaded sludge biochar for sulfamethoxazole-containing wastewater treatment," *Journal of Environmental Management*, vol. 335, 117576, 2023.
[131] M. Pourshaban-Mazandarani, M. Ahmadian, A. Nasiri, and A. Poormohammadi, "$CuCoFe_2O_4$@AC magnetic nanocomposite as a novel heterogeneous Fenton-like nanocatalyst for Ciprofloxacin degradation from aqueous solutions," *Applied Water Science*, vol. 13, no.9, pp. 179, 2023.
[132] J. Chen, C. Qin, Y. Mou, Y. Cao, H. Chen, X. Yuan, and H. Wang, "Linker regulation of iron-based MOFs for highly effective Fenton-like degradation of refractory organic contaminants," *Chemical Engineering Journal*, vol. 459, 141588, 2023.
[133] S. Zha, Y. Cheng, Y. Gao, Z. Chen, M. Megharaj, and R. Naidu, "Nanoscale zero-valent iron as a catalyst for heterogeneous Fenton oxidation of amoxicillin," *Chemical Engineering Journal*, vol. 255, 141-148, 2014.
[134] Z.-H. Diao, X.-R. Xu, D. Jiang, G. Li, J.-J. Liu, L.-J. Kong, and L.-Z. Zuo, "Enhanced catalytic degradation of ciprofloxacin with FeS_2/SiO_2 microspheres as heterogeneous Fenton catalyst: Kinetics, reaction pathways and mechanism," *Journal of Hazardous Materials*, vol. 327, 108-115, 2017.
[135] D. Huang, H. Luo, C. Zhang, G. Zeng, C. Lai, M. Cheng, R. Wang, R. Deng, W. Xue, X. Gong, X. Guo, and T. Li, "Nonnegligible role of biomass types and its compositions on the formation of persistent free radicals in biochar: Insight into

the influences on Fenton-like process," *Chemical Engineering Journal*, vol. 361, 353-363, 2019.
[136] S. Wu, H. Qin, H. Cheng, W. Shi, J. Chen, J. Huang, and H. Li, "A novel $MnFe_2O_4$-HSO_3 nanocatalyst for heterogeneous Fenton degradation of antibiotics," *Catalysis Communications*, vol. 171, 106522, 2022.
[137] Y. Lei, W. Chen, Q. Lin, F. Lin, X. Wang, and H. Zhu, "Synthesis of Fe(III)-doping Morchella-like porous magnesium hydroxide for the enhanced heterogeneous Fenton degradation of amphoteric antibiotics and anionic dyes," *Applied Surface Science*, vol. 606, 154970, 2022.
[138] H. He, Y. Wang, J. Li, S. Jiang, S. Sidra, W. Gong, Y. Tang, Y. Hu, R. Wei, D. Yang, X. Li, and Z. Zhao, "Confined conductive and light-adsorbed network in metal organic frameworks (MIL-88B(Fe)) with enhanced photo-Fenton catalytic activity for sulfamethoxazole degradation," *Chemical Engineering Journal*, vol. 427, 131962, 2022.
[139] J. H. Ramírez-Franco, L.-A. Galeano, and M.-A. Vicente, "Fly ash as photo-Fenton catalyst for the degradation of amoxicillin," *Journal of Environmental Chemical Engineering*, vol. 7, no.5, pp. 103274, 2019.
[140] Z. Xian, S. Liang, X. Jin, H. Tian, J. Ling, and C. Wang, "Application of FeIII-TAML/H_2O_2 system for treatment of fluoroquinolone antibiotics," *Journal of Environmental Sciences*, vol. 99, 110-118, 2021.
[141] H. Zhou, S. Wu, Y. Zhou, Y. Yang, J. Zhang, L. Luo, X. Duan, S. Wang, L. Wang, and D. C. W. Tsang, "Insights into the oxidation of organic contaminants by iron nanoparticles encapsulated within boron and nitrogen co-doped carbon nanoshell: Catalyzed Fenton-like reaction at natural pH," *Environment International*, vol. 128, 77-88, 2019.
[142] B. Huang, Z. Wu, H. Zhou, X. Wang, Y. Liu, H. Zhang, Z. Xiong, and B. Lai, "The structure-performance relationships in active center size-dependent Fenton-like catalysis: From nanoparticles to single atoms," *Applied Catalysis B: Environment and Energy*, vol. 355, 124157, 2024.
[143] B. Huang, Z. Wu, X. Wang, X. Song, H. Zhou, H. Zhang, P. Zhou, W. Liu, Z. Xiong, and B. Lai, "Coupled Surface-Confinement Effect and Pore Engineering in a Single-Fe-Atom Catalyst for Ultrafast Fenton-like Reaction with High-Valent Iron-Oxo Complex Oxidation," *Environmental Science & Technology*, vol. 57, no.41, pp. 15667-15679, 2023.
[144] Y. Gou, P. Chen, L. Yang, S. Li, L. Peng, S. Song, and Y. Xu, "Degradation of fluoroquinolones in homogeneous and heterogeneous photo-Fenton processes: A review," *Chemosphere*, vol. 270, 129481, 2021.
[145] J. H. F. de Jesus, K. V. L. Lima, P. Hammer, and R. F. P. Nogueira, "Wastewater sludge recycling: An efficient catalyst for photo-Fenton degradation of antibiotics and effluent disinfection," *Chemical Engineering Journal*, vol. 467, 143380, 2023.
[146] M. Nawaz, A. Shahzad, K. Tahir, J. Kim, M. Moztahida, J. Jang, M. B. Alam, S.-H. Lee, H.-Y. Jung, and D. S. Lee, "Photo-Fenton reaction for the degradation of sulfamethoxazole using a multi-walled carbon nanotube-$NiFe_2O_4$ composite," *Chemical Engineering Journal*, vol. 382, 123053, 2020.
[147] J. Hang, X.-H. Yi, C.-C. Wang, H. Fu, P. Wang, and Y. Zhao, "Heterogeneous photo-Fenton degradation toward sulfonamide matrix over magnetic Fe_3S_4 derived from MIL-100(Fe)," *Journal of Hazardous Materials*, vol. 424, 127415, 2022.

[148] H. He, Y. Li, C. Lai, J. Wu, L. Sun, M. Xu, and J. Wang, "In-situ formation of magnetic sodium ferric silicate/ferric oxide S-scheme heterojunction with efficiently removing tetracycline in photo-Fenton-like reaction," *Journal of Cleaner Production*, vol. 413, 137463, 2023.
[149] J. Li, Y. Li, M. Chen, X. Tang, N. Zhu, W. Li, Q. Mei, S. Yue, Y. Tang, and Q. Wang, "Construction of polynary systems by coupling Cd/CdS with magnetic recyclable $CuO/Fe_2O_3/CuFe_2O_4$ nanocomposite for enhancing photo-Fenton degradation of antibiotics," *Journal of Environmental Chemical Engineering*, vol. 11, no.5, pp. 111089, 2023.
[150] Z. Shan, F. Ma, S. You, L. Shan, D. Kong, H. Guo, and C. Cui, "Enhanced visible light photo-Fenton catalysis by lanthanum-doping $BiFeO_3$ for norfloxacin degradation," *Environmental Research*, vol. 216, 114588, 2023.
[151] H. Zhao, C. Tian, J. Mei, S. Yang, and P. K. Wong, "Faster electron injection and higher interface reactivity in $g\text{-}C_3N_4/Fe_2O_3$ nanohybrid for efficient photo-Fenton-like activity toward antibiotics degradation," *Environmental Research*, vol. 195, 110842, 2021.
[152] F. Xu, C. Lai, M. Zhang, D. Ma, L. Li, S. Liu, X. Zhou, H. Yan, N. Wang, M. Xu, L. Qin, and H. Yi, "Graphite carbon nitride coupled with high-dispersed iron (II) phthalocyanine for efficient oxytetracycline degradation under photo-Fenton process: Performance and mechanism," *Separation and Purification Technology*, vol. 308, 122829, 2023.
[153] J. Jiang, J. Gao, T. Li, Y. Chen, Q. Wu, T. Xie, Y. Lin, and S. Dong, "Visible-light-driven photo-Fenton reaction with $\alpha\text{-}Fe_2O_3$/BiOI at near neutral pH: Boosted photogenerated charge separation, optimum operating parameters and mechanism insight," *Journal of Colloid and Interface Science*, vol. 554, 531-543, 2019.
[154] L. Li, J. Gao, Y. Yuan, S. Zhang, M. Liang, and Y. Liu, "Study on $FeS_2/g\text{-}C_3N_4$ as a photo-Fenton heterojunction catalyst for tetracycline degradation with H_2O_2 under visible light irradiation," *Journal of the Taiwan Institute of Chemical Engineers*, vol. 126, 134-144, 2021.
[155] D. B. Hernández-Uresti, C. Alanis-Moreno, and D. Sanchez-Martinez, "Novel and stable Fe-$BiVO_4$ nanocatalyst by efficient dual process in the ciprofloxacin degradation," *Materials Science in Semiconductor Processing*, vol. 102, 104585, 2019.
[156] F. Wang, X. Yu, M. Ge, and S. Wu, "One-step synthesis of $TiO_2/\gamma\text{-}Fe_2O_3$/GO nanocomposites for visible light-driven degradation of ciprofloxacin," *Chemical Engineering Journal*, vol. 384, 123381, 2020.
[157] S. Sun, H. Yao, W. Fu, S. Xue, and W. Zhang, "Enhanced degradation of antibiotics by photo-Fenton reactive membrane filtration," *Journal of Hazardous Materials*, vol. 386, 121955, 2020.
[158] Y. Gou, L. Peng, H. Xu, S. Li, C. Liu, X. Wu, S. Song, C. Yang, K. Song, and Y. Xu, "Insights into the degradation mechanisms and pathways of cephalexin during homogeneous and heterogeneous photo-Fenton processes," *Chemosphere*, vol. 285, 131417, 2021.
[159] X. Zhang, G. Zhu, B. Xiao, J. Geng, Y. Yang, D. Wang, J. Li, J. Wang, and Y. Zhu, "Iron-based resin heterogeneous photo-self-Fenton system for efficient photocatalytic degradation of antibiotic wastewater," *Separation and Purification Technology*, vol. 330, 125338, 2024.
[160] X. Tian, X. He, Y. Nie, Z. Zhou, C. Yang, and Y. Wang, "Surface deep oxidation of ofloxacin and 2,4-dichlorophenol over ferrocene@sepiolite due to their

synergistic effect in visible light driven heterogeneous Fenton reaction process," *Environmental Science: Nano*, vol. 5, no.8, pp. 1943-1950, 2018.
[161] J. González-Rodríguez, L. Fernández, Z. Vargas-Osorio, C. Vázquez-Vázquez, Y. Piñeiro, J. Rivas, G. Feijoo, and M. T. Moreira, "Reusable Fe_3O_4/SBA_{15} nanocomposite as an efficient photo-Fenton catalyst for the removal of sulfamethoxazole and orange II," *Nanomaterials*, vol. 11, no.2, pp. 533, 2021.
[162] S. Xin, B. Ma, G. Liu, X. Ma, C. Zhang, X. Ma, M. Gao, and Y. Xin, "Enhanced heterogeneous photo-Fenton-like degradation of tetracycline over $CuFeO_2$/biochar catalyst through accelerating electron transfer under visible light," *Journal of Environmental Management*, vol. 285, 112093, 2021.
[163] C. Lai, F. Huang, G. Zeng, D. Huang, L. Qin, M. Cheng, C. Zhang, B. Li, H. Yi, S. Liu, L. Li, and L. Chen, "Fabrication of novel magnetic $MnFe_2O_4$/bio-char composite and heterogeneous photo-Fenton degradation of tetracycline in near neutral pH," *Chemosphere*, vol. 224, 910-921, 2019.
[164] J. H. F. de Jesus, K. V. L. Lima, and R. F. Pupo Nogueira, "Copper-containing magnetite supported on natural clay as a catalyst for heterogeneous photo-Fenton degradation of antibiotics in WWTP effluent," *Journal of Environmental Chemical Engineering*, vol. 10, no.3, pp. 107765, 2022.
[165] Lalmalsawmdawngliani, C. Lalhriatpuia, C. Jeon, and D. Tiwari, "Highly efficient novel heterojunction catalyst in the elimination of antibiotics under the photo-Fenton-like process," *Colloids and Surfaces A: Physicochemical and Engineering Aspects*, vol. 699, 134651, 2024.
[166] X. Lu, W. Qiu, J. Peng, H. Xu, D. Wang, Y. Cao, W. Zhang, and J. Ma, "A review on additives-assisted ultrasound for organic pollutants degradation," *Journal of Hazardous Materials*, vol. 403, 123915, 2021.
[167] X. Ma, Y. Cheng, Y. Ge, H. Wu, Q. Li, N. Gao, and J. Deng, "Ultrasound-enhanced nanosized zero-valent copper activation of hydrogen peroxide for the degradation of norfloxacin," *Ultrasonics Sonochemistry*, vol. 40, 763-772, 2018.
[168] F. Damiri, S. Dobaradaran, S. Hashemi, R. Foroutan, M. Vosoughi, S. Sahebi, B. Ramavandi, and D. Camilla Boffito, "Waste sludge from shipping docks as a catalyst to remove amoxicillin in water with hydrogen peroxide and ultrasound," *Ultrasonics Sonochemistry*, vol. 68, 105187, 2020.
[169] A. Keck, E. Gilbert, and R. Köster, "Influence of particles on sonochemical reactions in aqueous solutions," *Ultrasonics*, vol. 40, no.1, pp. 661-665, 2002.
[170] G. Yazdanpanah, M. R. Heidari, N. Amirmahani, and A. Nasiri, "Heterogeneous Sono-Fenton like catalytic degradation of metronidazole by Fe_3O_4@HZSM-5 magnetite nanocomposite," *Heliyon*, vol. 9, no.6, pp. 2023.
[171] H. B. Ammar, "Sono-Fenton process for metronidazole degradation in aqueous solution: Effect of acoustic cavitation and peroxydisulfate anion," *Ultrasonics Sonochemistry*, vol. 33, 164-169, 2016.
[172] Y. Sukhatskiy, M. Shepida, D. Lysak, Z. Znak, and P. R. Gogate, "Modified sono-Fenton process for oxidative degradation of chloramphenicol," *Environmental Science and Pollution Research*, vol. 31, no.42, pp. 54559-54573, 2024.
[173] N. Thi Mai, D. Van Thanh, N. Nhat Huy, D. Danh Bich, T. Thi Minh Hang, N. Huu Hao, and N. Manh Khai, "Red mud supported on rice husk biochar as sono-photo-Fenton catalysts for degradation of ciprofloxacin in water," *Separation and Purification Technology*, vol. 354, 129039, 2025.
[174] A. Y. Ghjair and A. H. Abbar, "Applications of advanced oxidation processes (electro-Fenton and sono-electro-Fenton) for COD removal from hospital

wastewater: Optimization using response surface methodology," *Process Safety and Environmental Protection*, vol. 169, 481-492, 2023.
[175] Z. Wang, M. Liu, F. Xiao, G. Postole, H. Zhao, and G. Zhao, "Recent advances and trends of heterogeneous electro-Fenton process for wastewater treatment-review," *Chinese Chemical Letters*, vol. 33, no.2, pp. 653-662, 2022.
[176] J. Yi, N. Abdullah Al-Dhabi, T. Hu, T.-O. Soyol-Erdene, O. Bayanjargal, E. Liu, and W. Tang, "Highly efficient degradation of antibiotic metronidazole by an environmental-friendly metal-free dual-cathode electro-Fenton system," *Chemical Engineering Journal*, vol. 492, 152447, 2024.
[177] Z. Zhang, G. Huang, Y. Li, Y. Yao, P. Zhang, X. Chen, S. Ren, Y. Luo, and Y. Zhang, "Antibiotic oxidation and fouling control of ceramic microfiltration membrane through effective heterogeneous electro-Fenton process based on nitrogen-doped carbon nanotubes and Cu-Fe bimetallic oxides," *Separation and Purification Technology*, vol. 354, 128834, 2025.
[178] C. M. Sánchez-Sánchez, E. Expósito, J. Casado, and V. Montiel, "Goethite as a more effective iron dosage source for mineralization of organic pollutants by electro-Fenton process," *Electrochemistry Communications*, vol. 9, no.1, pp. 19-24, 2007.
[179] I. Ouiriemmi, A. Karrab, N. Oturan, M. Pazos, E. Rozales, A. Gadri, M. Á. Sanromán, S. Ammar, and M. A. Oturan, "Heterogeneous electro-Fenton using natural pyrite as solid catalyst for oxidative degradation of vanillic acid," *Journal of Electroanalytical Chemistry*, vol. 797, 69-77, 2017.
[180] M. Luo, S. Yuan, M. Tong, P. Liao, W. Xie, and X. Xu, "An integrated catalyst of Pd supported on magnetic Fe_3O_4 nanoparticles: simultaneous production of H_2O_2 and Fe^{2+} for efficient electro-Fenton degradation of organic contaminants," *Water research*, vol. 48, 190-199, 2014.
[181] G. Pan, X. Sun, and Z. Sun, "Fabrication of multi-walled carbon nanotubes and carbon black co-modified graphite felt cathode for amoxicillin removal by electrochemical advanced oxidation processes under mild pH condition," *Environmental Science and Pollution Research*, vol. 27, no.8, pp. 8231-8247, 2020.
[182] E. Liu, T. Hu, N. A. Al-Dhabi, T.-O. Soyol-Erdene, O. Bayanjargal, Y. Zuo, J. Wang, and W. Tang, "MOF-derived Fe/Ni@C marigold-like nanosheets as heterogeneous electro-Fenton cathode for efficient antibiotic oxytetracycline degradation," *Environmental Research*, vol. 247, 118357, 2024.
[183] X. Du, W. Fu, P. Su, J. Cai, and M. Zhou, "Internal-micro-electrolysis-enhanced heterogeneous electro-Fenton process catalyzed by Fe/Fe_3C@PC core–shell hybrid for sulfamethazine degradation," *Chemical Engineering Journal*, vol. 398, 125681, 2020.
[184] M. Ghasemi, A. Khataee, P. Gholami, and R. D. Cheshmeh Soltani, "Template-free microspheres decorated with Cu-Fe-NLDH for catalytic removal of gentamicin in heterogeneous electro-Fenton process," *Journal of Environmental Management*, vol. 248, 109236, 2019.
[185] C. Droguett, R. Salazar, E. Brillas, I. Sirés, C. Carlesi, J. F. Marco, and A. Thiam, "Treatment of antibiotic cephalexin by heterogeneous electrochemical Fenton-based processes using chalcopyrite as sustainable catalyst," *Science of the Total Environment*, vol. 740, 140154, 2020.
[186] S. Campos, J. Lorca, J. Vidal, W. Calzadilla, C. Toledo-Neira, M. Aranda, S. Miralles-Cuevas, A. Cabrera-Reina, and R. Salazar, "Removal of contaminants of emerging concern by solar photo electro-Fenton process in a solar electrochemical

raceway pond reactor," *Process Safety and Environmental Protection*, vol. 169, 660-670, 2023.
[187] S. Bugueño-Carrasco, H. Monteil, C. Toledo-Neira, M. Sandoval, A. Thiam, and R. Salazar, "Elimination of pharmaceutical pollutants by solar photoelectro-Fenton process in a pilot plant," *Environmental Science and Pollution Research*, vol. 28, no.19, pp. 23753-23766, 2021.
[188] H. Olvera-Vargas, N. Oturan, M. A. Oturan, and E. Brillas, "Electro-Fenton and solar photoelectro-Fenton treatments of the pharmaceutical ranitidine in pre-pilot flow plant scale," *Separation and Purification Technology*, vol. 146, 127-135, 2015.
[189] K. Kowalska, M. Roccamante, A. Cabrera Reina, P. Plaza-Bolaños, I. Oller, and S. Malato, "Pilot-scale removal of microcontaminants by solar-driven photo-Fenton in treated municipal effluents: Selection of operating variables based on lab-scale experiments," *Journal of Environmental Chemical Engineering*, vol. 9, no.1, pp. 104788, 2021.
[190] E. Gualda-Alonso, P. Soriano-Molina, J. L. Casas López, J. L. García Sánchez, P. Plaza-Bolaños, A. Agüera, and J. A. Sánchez Pérez, "Large-scale raceway pond reactor for CEC removal from municipal WWTP effluents by solar photo-Fenton," *Applied Catalysis B: Environmental*, vol. 319, 121908, 2022.
[191] F. Bensaibi, M. Chabani, S. Bouafia, and H. Djelal, "Doxycycline removal by solar photo-Fenton on a pilot-scale composite parabolic collector (CPC) reactor," *Processes*, vol. 11, no.8, pp. 2363, 2023.
[192] P. Soriano-Molina, P. Plaza-Bolaños, A. Lorenzo, A. Agüera, J. L. García Sánchez, S. Malato, and J. A. Sánchez Pérez, "Assessment of solar raceway pond reactors for removal of contaminants of emerging concern by photo-Fenton at circumneutral pH from very different municipal wastewater effluents," *Chemical Engineering Journal*, vol. 366, 141-149, 2019.
[193] S. Arzate, J. L. García Sánchez, P. Soriano-Molina, J. L. Casas López, M. C. Campos-Mañas, A. Agüera, and J. A. Sánchez Pérez, "Effect of residence time on micropollutant removal in WWTP secondary effluents by continuous solar photo-Fenton process in raceway pond reactors," *Chemical Engineering Journal*, vol. 316, 1114-1121, 2017.
[194] R. A. Al-Juboori and N. Hilal, "Pharmaceuticals removal from wastewater: Ultrasound technology and its potential amalgamation with membrane processes," *Journal of Water Process Engineering*, vol. 53, 103810, 2023.
[195] E. A. Serna-Galvis, J. Silva-Agredo, A. M. Botero-Coy, A. Moncayo-Lasso, F. Hernández, and R. A. Torres-Palma, "Effective elimination of fifteen relevant pharmaceuticals in hospital wastewater from Colombia by combination of a biological system with a sonochemical process," *Science of The Total Environment*, vol. 670, 623-632, 2019.
[196] I. Basturk, G. Varank, S. Murat-Hocaoglu, S. Yazici-Guvenc, E. Can-Güven, E. E. Oktem-Olgun, and O. Canli, "Simultaneous degradation of cephalexin, ciprofloxacin, and clarithromycin from medical laboratory wastewater by electro-Fenton process," *Journal of Environmental Chemical Engineering*, vol. 9, no.1, pp. 104666, 2021.
[197] S. Garcia-Segura, E. B. Cavalcanti, and E. Brillas, "Mineralization of the antibiotic chloramphenicol by solar photoelectro-Fenton: From stirred tank reactor to solar pre-pilot plant," *Applied Catalysis B: Environmental*, vol. 144, 588-598, 2014.

[198] M. F. Murrieta, E. Brillas, J. L. Nava, and I. Sirés, "Photo-assisted electrochemical production of HClO and Fe^{2+} as Fenton-like reagents in chloride media for sulfamethoxazole degradation," *Separation and Purification Technology*, vol. 250, 117236, 2020.
[199] F. Ay and F. Kargi, "Advanced oxidation of amoxicillin by Fenton's reagent treatment," *Journal of Hazardous Materials*, vol. 179, no.1, pp. 622-627, 2010.
[200] O. Rozas, D. Contreras, M. A. Mondaca, M. Pérez-Moya, and H. D. Mansilla, "Experimental design of Fenton and photo-Fenton reactions for the treatment of ampicillin solutions," *Journal of Hazardous Materials*, vol. 177, no.1, pp. 1025-1030, 2010.
[201] A. A. Borghi, M. F. Silva, S. Al Arni, A. Converti, and M. S. A. Palma, "Doxycycline degradation by the oxidative Fenton process," *Journal of Chemistry*, vol. 2015, 492030, 2015.
[202] M. Salari, G. R. Rakhshandehroo, and M. R. Nikoo, "Degradation of ciprofloxacin antibiotic by homogeneous Fenton oxidation: Hybrid AHP-PROMETHEE method, optimization, biodegradability improvement and identification of oxidized by-products," *Chemosphere*, vol. 206, 157-167, 2018.
[203] N. S. Shah, A. D. Rizwan, J. A. Khan, M. Sayed, Z. U. H. Khan, B. Murtaza, J. Iqbal, S. U. Din, M. Imran, M. Nadeem, A. a. H. Al-Muhtaseb, N. Muhammad, H. M. Khan, M. Ghauri, and G. Zaman, "Toxicities, kinetics and degradation pathways investigation of ciprofloxacin degradation using iron-mediated H_2O_2 based advanced oxidation processes," *Process Safety and Environmental Protection*, vol. 117, 473-482, 2018.
[204] G. K. Turkay and H. Kumbur, "Investigation of amoxicillin removal from aqueous solution by Fenton and photocatalytic oxidation processes," *Kuwait Journal of Science*, vol. 46, no.2, pp. 2019.
[205] H. Titouhi and J.-E. Belgaied, "Removal of ofloxacin antibiotic using heterogeneous Fenton process over modified alginate beads," *Journal of Environmental Sciences*, vol. 45, 84-93, 2016.
[206] J. Li, L. Pan, G. Yu, S. Xie, C. Li, D. Lai, Z. Li, F. You, and Y. Wang, "The synthesis of heterogeneous Fenton-like catalyst using sewage sludge biochar and its application for ciprofloxacin degradation," *Science of The Total Environment*, vol. 654, 1284-1292, 2019.
[207] L. Xu, Y. Yang, W. Li, Y. Tao, Z. Sui, S. Song, and J. Yang, "Three-dimensional macroporous graphene-wrapped zero-valent copper nanoparticles as efficient micro-electrolysis-promoted Fenton-like catalysts for metronidazole removal," *Science of The Total Environment*, vol. 658, 219-233, 2019.
[208] B. Gokulakrishnan and G. Satishkumar, "Facilely prepared heterogeneous Fenton catalyst $Fe(Fe_{0.69}Al_{0.31})_2O_4$@C for catalytic wet peroxide oxidation of ciprofloxacin in batch and continuous reactor: Reaction intermediates and toxicity evaluation," *Separation and Purification Technology*, 125690, 2023.
[209] G. Yang, Y. Liang, J. Yang, X. Zhang, Z. Zeng, Z. Xiong, J. Jia, and K. Sa, "Fe-heteropolyoxometalate nanodots modified dominant {001} facet Bi_4TaO_8Cl nanosheets with oxygen vacancies for enhanced photocatalytic-Fenton degradation of fluoroquinolone antibiotics," *Journal of Environmental Chemical Engineering*, vol. 11, no.2, pp. 109328, 2023.
[210] S.-P. Sun, H.-Q. Guo, Q. Ke, J.-H. Sun, S.-H. Shi, M.-L. Zhang, and Q. Zhou, "Degradation of antibiotic ciprofloxacin hydrochloride by photo-Fenton oxidation process," *Environmental Engineering Science*, vol. 26, no.4, pp. 753-759, 2009.

[211] M. Pérez-Moya, M. Graells, G. Castells, J. Amigó, E. Ortega, G. Buhigas, L. M. Pérez, and H. D. Mansilla, "Characterization of the degradation performance of the sulfamethazine antibiotic by photo-Fenton process," *Water Research*, vol. 44, no.8, pp. 2533-2540, 2010.

[212] A. G. Trovó, V. A. B. de Paiva, A. E. H. Machado, C. A. de Oliveira, and R. O. Santos, "Degradation of the antibiotic chloramphenicol by photo-Fenton process at lab-scale and solar pilot plant: Kinetic, toxicity and inactivation assessment," *Solar Energy*, vol. 97, 596-604, 2013.

[213] M. Velásquez, I. P. Santander, D. R. Contreras, J. Yáñez, C. Zaror, R. A. Salazar, M. Pérez-Moya, and H. D. Mansilla, "Oxidative degradation of sulfathiazole by Fenton and photo-Fenton reactions," *Journal of Environmental Science and Health, Part A*, vol. 49, no.6, pp. 661-670, 2014.

[214] J. Wang, T. Zhou, J. Mao, and X. Wu, "Comparative study of sulfamethazine degradation in visible light induced photo-Fenton and photo-Fenton-like systems," *Journal of Environmental Chemical Engineering*, vol. 3, no.4, Part A, pp. 2393-2400, 2015.

[215] A. E. Sarrai, S. Hanini, N. K. Merzouk, D. Tassalit, T. Szabó, K. Hernádi, and L. Nagy, "Using central composite experimental design to optimize the degradation of tylosin from aqueous solution by photo-Fenton reaction," *Materials*, vol. 9, no.6, pp. 428, 2016.

[216] F. Cheng, P. Zhou, Y. Liu, X. Huo, J. Zhang, Y. Yuan, H. Zhang, B. Lai, and Y. Zhang, "Graphene oxide mediated Fe(III) reduction for enhancing Fe(III)/H_2O_2 Fenton and photo-Fenton oxidation toward chloramphenicol degradation," *Science of The Total Environment*, vol. 797, 149097, 2021.

[217] E. E. Hernández-Coronado, E. J. Ruiz-Ruiz, L. Hinojosa-Reyes, F. J. Beltrán, J. López-Gallego, M. Á. Gracia-Pinilla, and M. Villanueva-Rodríguez, "Effective degradation of cefuroxime by heterogeneous photo-Fenton under simulated solar radiation using α-Fe_2O_3-TiO_2," *Journal of Environmental Chemical Engineering*, vol. 9, no.6, pp. 106822, 2021.

[218] X. Zhang, B. Xu, S. Wang, X. Li, B. Liu, Y. Xu, P. Yu, and Y. Sun, "High-density dispersion of CuN_x sites for H_2O_2 activation toward enhanced photo-Fenton performance in antibiotic contaminant degradation," *Journal of Hazardous Materials*, vol. 423, 127039, 2022.

[219] P. Bansal and A. Verma, "Synergistic effect of dual process (photocatalysis and photo-Fenton) for the degradation of cephalexin using TiO_2 immobilized novel clay beads with waste fly ash/foundry sand," *Journal of Photochemistry and Photobiology A: Chemistry*, vol. 342, 131-142, 2017.

[220] T. Shi, J. Peng, J. Chen, C. Sun, and H. He, "Heterogeneous photo-Fenton degradation of norfloxacin with Fe_3O_4-multiwalled carbon nanotubes in aqueous solution," *Catalysis Letters*, vol. 147, no.6, pp. 1598-1607, 2017.

[221] Y. Xiang, Y. Huang, B. Xiao, X. Wu, and G. Zhang, "Magnetic yolk-shell structure of $ZnFe_2O_4$ nanoparticles for enhanced visible light photo-Fenton degradation towards antibiotics and mechanism study," *Applied Surface Science*, vol. 513, 145820, 2020.

[222] X. Li, X. Zhang, S. Wang, P. Yu, Y. Xu, and Y. Sun, "Highly enhanced heterogeneous photo-Fenton process for tetracycline degradation by Fe/SCN Fenton-like catalyst," *Journal of Environmental Management*, vol. 312, 114856, 2022.

[223] H. Rahmani, M. Gholami, A. Mahvi, M. Ali-Mohammadi, and K. Rahmani, "Tinidazol antibiotic degradation in aqueous solution by zero valent iron

nanoparticles and hydrogen peroxide in the presence of ultrasound radiation," *Journal of Water Chemistry and Technology*, vol. 36, 317-324, 2014.
[224] H. Wei, D. Hu, J. Su, and K. Li, "Intensification of levofloxacin sono-degradation in a US/H_2O_2 system with Fe_3O_4 magnetic nanoparticles," *Chinese journal of chemical engineering*, vol. 23, no.1, pp. 296-302, 2015.
[225] M. Gholami, K. Rahmani, A. Rahmani, H. Rahmani, and A. Esrafili, "Oxidative degradation of clindamycin in aqueous solution using nanoscale zero-valent iron/H_2O_2/US," *Desalination and Water Treatment*, vol. 57, no.30, pp. 13878-13886, 2016.
[226] A. Yazdani and M. H. Sayadi, "Sonochemical degradation of azithromycin in aqueous solution," *Environmental Health Engineering and Management Journal*, vol. 5, no.2, pp. 85-92, 2018.
[227] S. Dehghan, B. Kakavandi, and R. R. Kalantary, "Heterogeneous sonocatalytic degradation of amoxicillin using ZnO@Fe_3O_4 magnetic nanocomposite: Influential factors, reusability and mechanisms," *Journal of Molecular Liquids*, vol. 264, 98-109, 2018.
[228] T. J. Al-Musawi, H. Kamani, E. Bazrafshan, A. H. Panahi, M. F. Silva, and G. Abi, "Optimization the effects of physicochemical parameters on the degradation of cephalexin in sono-Fenton reactor by using Box-Behnken response surface methodology," *Catalysis Letters*, vol. 149, no.5, pp. 1186-1196, 2019.
[229] N. Geng, W. Chen, H. Xu, M. Ding, T. Lin, Q. Wu, and L. Zhang, "Insights into the novel application of Fe-MOFs in ultrasound-assisted heterogeneous Fenton system: Efficiency, kinetics and mechanism," *Ultrasonics Sonochemistry*, vol. 72, 105411, 2021.
[230] E. Aseman-Bashiz and H. Sayyaf, "Enhancement of tetracycline removal in aquatic environment by nano-pyrite/H_2O_2/ultrasound as a sono-Fenton process," *Journal of Water and Environmental Nanotechnology*, vol. 8, no.2, pp. 179-189, 2023.
[231] G. Ren, M. Zhou, P. Su, W. Yang, X. Lu, and Y. Zhang, "Simultaneous sulfadiazines degradation and disinfection from municipal secondary effluent by a flow-through electro-Fenton process with graphene-modified cathode," *Journal of Hazardous Materials*, vol. 368, 830-839, 2019.
[232] J. Zhang, C. Zheng, Y. Dai, C. He, H. Liu, and S. Chai, "Efficient degradation of amoxicillin by scaled-up electro-Fenton process: Attenuation of toxicity and decomposition mechanism," *Electrochimica Acta*, vol. 381, 138274, 2021.
[233] R. R. Kalantary, M. Farzadkia, M. Kermani, and M. Rahmatinia, "Heterogeneous electro-Fenton process by nano-Fe_3O_4 for catalytic degradation of amoxicillin: Process optimization using response surface methodology," *Journal of Environmental Chemical Engineering*, vol. 6, no.4, pp. 4644-4652, 2018.
[234] F. Görmez, Ö. Görmez, B. Gözmen, and D. Kalderis, "Degradation of chloramphenicol and metronidazole by electro-Fenton process using graphene oxide-Fe_3O_4 as heterogeneous catalyst," *Journal of Environmental Chemical Engineering*, vol. 7, no.2, pp. 102990, 2019.
[235] M. Ghasemi, A. Khataee, P. Gholami, R. D. C. Soltani, A. Hassani, and Y. Orooji, "In-situ electro-generation and activation of hydrogen peroxide using a CuFeNLDH-CNTs modified graphite cathode for degradation of cefazolin," *Journal of Environmental Management*, vol. 267, 110629, 2020.
[236] X. Jia, C. Li, X. Zhao, M. Xu, Y. Cai, J. Huang, and T. Wu, "Levofloxacin degradation in electro-Fenton system with Fe@Co/GF composite cathode,"

Journal of Chemical Technology & Biotechnology, vol. 98, no.7, pp. 1703-1712, 2023.

[237] D. Liu, D. Chen, L. Jiang, Z. Hao, R. Tan, B. Deng, Y. Wang, Y. Tian, L. Chen, and B. Jia, "Efficient degradation of sulfamethoxazole in heterogeneous Electro-Fenton process with CeO_2@MoS_2@GF modified cathode: Mechanism and degradation pathway," *Separation and Purification Technology*, vol. 320, 124212, 2023.

[238] Y. Li, Z. Yan, and Z. Sun, "Efficient electrocatalytic degradation of sulfamethoxazole with CuAl-LDO/HGF cathode in a neutral heterogeneous electro-Fenton process," *Journal of Environmental Chemical Engineering*, vol. 11, no.3, pp. 109762, 2023.

[239] I. Michael, E. Hapeshi, C. Michael, A. R. Varela, S. Kyriakou, C. M. Manaia, and D. Fatta-Kassinos, "Solar photo-Fenton process on the abatement of antibiotics at a pilot scale: Degradation kinetics, ecotoxicity and phytotoxicity assessment and removal of antibiotic resistant enterococci," *Water Research*, vol. 46, no.17, pp. 5621-5634, 2012.

[240] P. Kubelka, "Ein beitrag zur optik der farbanstriche," *Z. tech. Phys*, vol. 12, 593-601, 1931.

[241] Y. Feng, S. Lin, S. Huang, S. Shrestha, and G. Conibeer, "Can Tauc plot extrapolation be used for direct-band-gap semiconductor nanocrystals?," *Journal of Applied Physics*, vol. 117, no.12, pp. 2015.

[242] P. H. Chang, B. Juhrend, T. M. Olson, C. F. Marrs, and K. R. Wigginton, "Degradation of extracellular antibiotic resistance genes with UC_{254} treatment," *Environmental Science & Technology*, vol. 51, no.11, pp. 6185-6192, 2017.

[243] Q. Gao and Z. Liu, "$FeWO_4$ nanorods with excellent UV–Visible light photocatalysis," *Progress in Natural Science: Materials International*, vol. 27, no.5, pp. 556-560, 2017.

[244] J. N. Sharma, D. K. Pattadar, B. P. Mainali, and F. P. Zamborini, "Size determination of metal nanoparticles based on electrochemically measured surface-area-to-volume ratios," *Analytical Chemistry*, vol. 90, no.15, pp. 9308-9314, 2018.

[245] S. Dolabella, A. Borzì, A. Dommann, and A. Neels, "Lattice strain and defects analysis in nanostructured semiconductor materials and devices by high-resolution X-ray diffraction: Theoretical and practical aspects," *Small Methods*, vol. 6, no.2, pp. 2100932, 2022.

[246] P. Debye and P. Scherrer, "Interference on inordinate orientated particles in x-ray light. III," *Physikalische Zeitschrift*, vol. 18, 291-301, 1917.

[247] U. Holzwarth and N. Gibson, "The Scherrer equation versus the 'Debye-Scherrer equation'," *Nature Nanotechnology*, vol. 6, no.9, pp. 534-534, 2011.

[248] I. Ahmad, Y. Zou, J. Yan, Y. Liu, S. Shukrullah, M. Y. Naz, H. Hussain, W. Q. Khan, and N. R. Khalid, "Semiconductor photocatalysts: A critical review highlighting the various strategies to boost the photocatalytic performances for diverse applications," *Advances in Colloid and Interface Science*, vol. 311, 102830, 2023.

[249] J. Xiong, J. Di, J. Xia, W. Zhu, and H. Li, "Surface defect engineering in 2D nanomaterials for photocatalysis," *Advanced Functional Materials*, vol. 28, no.39, pp. 1801983, 2018.

[250] A. K. Chakraborty, S. Akter, S. Ganguli, M. A. Haque, A. S. M. Nur, and M. A. Sabur, "Design of $FeWO_4$@N-TiO_2 nanocomposite and its enhanced

photocatalytic activity in decomposing methylene blue and phenol under visible light," *Environmental Technology & Innovation*, vol. 33, 103536, 2024.
[251] S. Rajagopal, D. Nataraj, O. Y. Khyzhun, Y. Djaoued, J. Robichaud, and D. Mangalaraj, "Hydrothermal synthesis and electronic properties of $FeWO_4$ and $CoWO_4$ nanostructures," *Journal of Alloys and Compounds*, vol. 493, no.1, pp. 340-345, 2010.
[252] S. Guan, R. Li, X. Sun, T. Xian, and H. Yang, "Construction of novel ternary Au/$LaFeO_3$/Cu_2O composite photocatalysts for RhB degradation via photo-Fenton catalysis," *Materials Technology*, vol. 36, no.10, pp. 603-615, 2021.
[253] X. Li, J. Wan, Y. Ma, J. R. Zhao, and Y. Wang, "Mesopores octahedron GCNOX/Cu_2O@ C inhibited photo-corrosion as an efficient visible-light catalyst derived from oxidized g-C_3N_4/HKUST-1 composite structure," *Applied Surface Science*, vol. 510, 145459, 2020.
[254] M. Ahsan, M. M. Rahman, A. E. Alsafrani, M. A. Aziz, A. Almahri, H. M. Marwani, M. M. Rahman, and M. A. Hasnat, "Immobilization of poly(o-aminophenol) film on Pt surface: A robust sensor for detecting As(III) in an acidic medium," *Surfaces and Interfaces*, vol. 39, 102976, 2023.
[255] D. Liao, R. Wang, Y. Zheng, J. Ma, J. Sun, Q. Yang, and G. Zhou, "In-situ growth of small-size Fe_3O_4 nanoparticles on N-doped hollow carbon spheres for electrochemical high-efficiency determination of ofloxacin-contaminated water," *Microchemical Journal*, vol. 191, 108927, 2023.
[256] Y. Ahmed, J. Zhong, Z. Wang, L. Wang, Z. Yuan, and J. Guo, "Simultaneous removal of antibiotic resistant bacteria, antibiotic resistance genes, and miicropollutants by FeS_2@GO-based heterogeneousphoto-Fenton process," *Environmental Science & Technology*, vol. 56, no.21, pp. 15156-15166, 2022.
[257] H. Qin, Y. Yang, W. Shi, and Y. She, "Heterogeneous Fenton degradation of ofloxacin catalyzed by magnetic nanostructured $MnFe_2O_4$ with different morphologies," *Environmental Science and Pollution Research*, vol. 28, no.21, pp. 26558-26570, 2021.
[258] G. Wu, S. Bian, J. Wang, F. Wu, W. Sun, Y. Pan, C. Zhao, W. Xing, and Y. Huang, "Construction of biochar modified multi-morphologies Fe_2O_3 for efficient boosting photo-Fenton organic antibiotic pollutants degradation: Mechanism and toxicity evaluation in degradation pathways," *Industrial Crops and Products*, vol. 222, 119726, 2024.
[259] D. M. Montoya-Rodríguez, E. A. Serna-Galvis, F. Ferraro, and R. A. Torres-Palma, "Degradation of the emerging concern pollutant ampicillin in aqueous media by sonochemical advanced oxidation processes - Parameters effect, removal of antimicrobial activity and pollutant treatment in hydrolyzed urine," *Journal of Environmental Management*, vol. 261, 110224, 2020.
[260] E. A. Serna-Galvis, J. Silva-Agredo, J. Lee, A. Echavarría-Isaza, and R. A. Torres-Palma, "Possibilities and limitations of the sono-Fenton process using mid-high-frequency ultrasound for the degradation of organic pollutants," *Molecules*, vol. 28, no.3, pp. 1113, 2023.
[261] E. Basturk and M. Karatas, "Advanced oxidation of reactive blue 181 solution: A comparison between Fenton and sono-Fenton Process," *Ultrasonics Sonochemistry*, vol. 21, no.5, pp. 1881-1885, 2014.
[262] F. Bashiri, S. M. Khezri, R. R. Kalantary, and B. Kakavandi, "Enhanced photocatalytic degradation of metronidazole by TiO_2 decorated on magnetic reduced graphene oxide: Characterization, optimization and reaction mechanism studies," *Journal of Molecular Liquids*, vol. 314, 113608, 2020.

[263] S. Ding, J. Wan, Y. Wang, Z. Yan, and Y. Ma, "Activation of persulfate by molecularly imprinted Fe-MOF-74@SiO_2 for the targeted degradation of dimethyl phthalate: Effects of operating parameters and chlorine," *Chemical Engineering Journal*, vol. 422, 130406, 2021.
[264] X. Li, J. Xu, and Z. Yang, "Efficient catalytic degradation of alkanes in soil by a novel heterogeneous Fenton catalyst of functionalized magnetic biochar," *Chemosphere*, vol. 301, 134693, 2022.
[265] B. Krishnakumar, K. Selvam, R. Velmurugan, and M. Swaminathan, "Influence of operational parameters on photodegradation of Acid Black 1 with ZnO," *Desalination and Water Treatment*, vol. 24, no.1-3, pp. 132-139, 2010.
[266] W. Chu, W. K. Choy, and T. Y. So, "The effect of solution pH and peroxide in the TiO_2-induced photocatalysis of chlorinated aniline," *Journal of Hazardous Materials*, vol. 141, no.1, pp. 86-91, 2007.
[267] A. Al Mayyahi and H. A. A. Al-Asadi, "Advanced oxidation processes (AOPs) for wastewater treatment and reuse: A brief review," *Asian Journal of Applied Science Technology*, vol. 2, 18-30, 2018.
[268] A. Raja, P. Rajasekaran, K. Selvakumar, M. Arunpandian, K. Kaviyarasu, S. Asath Bahadur, and M. Swaminathan, "Visible active reduced graphene oxide-$BiVO_4$-ZnO ternary photocatalyst for efficient removal of ciprofloxacin," *Separation and Purification Technology*, vol. 233, 115996, 2020.
[269] S. A. C. Carabineiro, T. Thavorn-Amornsri, M. F. R. Pereira, and J. L. Figueiredo, "Adsorption of ciprofloxacin on surface-modified carbon materials," *Water Research*, vol. 45, no.15, pp. 4583-4591, 2011.
[270] S. Subramanian, J. Noh, and J. Schwarz, "Determination of the point of zero charge of composite oxides," *Journal of Catalysis*, vol. 114, no.2, pp. 433-439, 1988.
[271] A. Azizi, M. R. Alavi Moghaddam, R. Maknoon, and E. Kowsari, "Investigation of enhanced Fenton process (EFP) in color and COD removal of wastewater containing Acid Red 18 by response surface methodology: evaluation of EFP as post treatment," *Desalination and Water Treatment*, vol. 57, no.30, pp. 14083-14092, 2016.
[272] R. Zhang, H. You, and D. Wu, "Advanced treatment of coking wastewater by heterogeneous photo-Fenton technology with Cu/Fe oxide catalysts," *Desalination and Water Treatment*, vol. 57, no.26, pp. 12010-12018, 2016.
[273] P. Ji, L. Wang, S. Chen, Q. Wen, J. Wu, G. Meng, J. Hou, Z. Liu, and X. Guo, "Enhanced photo-Fenton activity of γ-Fe_2O_3/Bent modified with $BiVO_4$ under visible light," *Chemical Physics Letters*, vol. 786, 138987, 2022.
[274] F. C. Drumm, P. Grassi, J. Georgin, D. P. Franco, D. Tonato, E. L. Foletto, G. L. Dotto, and S. L. Jahn, "Applicability of amethyst mining rejects as a novel photo-fenton catalyst for the abatement of an emerging pollutant in water," *Applied Geochemistry*, vol. 136, 105136, 2022.
[275] Z. Chen, H. Ma, J. Xia, J. Zeng, J. Di, S. Yin, L. Xu, and H. Li, "Ionic liquid-induced strategy for $FeWO_4$ microspheres with advanced visible light photocatalysis," *Ceramics International*, vol. 42, no.7, pp. 8997-9003, 2016.
[276] Y. Zhu, Q. Xie, R. Zhu, Y. Lv, Y. Xi, J. Zhu, and J. Fan, "Hydrothermal carbons/ferrihydrite heterogeneous Fenton catalysts with low H_2O_2 consumption and the effect of graphitization degrees," *Chemosphere*, vol. 287, 131933, 2022.
[277] H. Wang, C. Wang, X. Cui, L. Qin, R. Ding, L. Wang, Z. Liu, Z. Zheng, and B. Lv, "Design and facile one-step synthesis of $FeWO_4$/Fe_2O_3 di-modified WO_3 with

super high photocatalytic activity toward degradation of quasi-phenothiazine dyes," *Applied Catalysis B: Environmental*, vol. 221, 169-178, 2018.
[278] I. García-Fernández, M. I. Polo-López, I. Oller, and P. Fernández-Ibáñez, "Bacteria and fungi inactivation using Fe^{3+}/sunlight, H_2O_2/sunlight and near neutral photo-Fenton: A comparative study," *Applied Catalysis B: Environmental*, vol. 121-122, 20-29, 2012.
[279] S. Giannakis, "Analogies and differences among bacterial and viral disinfection by the photo-Fenton process at neutral pH: A mini review," *Environmental Science and Pollution Research International*, vol. 25, no.28, pp. 27676-27692, 2018.
[280] S. Giannakis, M. I. Polo López, D. Spuhler, J. A. Sánchez Pérez, P. Fernández Ibáñez, and C. Pulgarin, "Solar disinfection is an augmentable, in situ-generated photo-Fenton reaction—Part 1: A review of the mechanisms and the fundamental aspects of the process," *Applied Catalysis B: Environmental*, vol. 199, 199-223, 2016.
[281] S. Giannakis, T. M. Le, J. M. Entenza, and C. Pulgarin, "Solar photo-Fenton disinfection of 11 antibiotic-resistant bacteria (ARB) and elimination of representative AR genes. Evidence that antibiotic resistance does not imply resistance to oxidative treatment," *Water Research*, vol. 143, 334-345, 2018.
[282] Y. Zhang, Y. Zhuang, J. Geng, H. Ren, K. Xu, and L. Ding, "Reduction of antibiotic resistance genes in municipal wastewater effluent by advanced oxidation processes," *Sci Total Environ*, vol. 550, 184-191, 2016.
[283] S. Giannakis, S. Watts, S. Rtimi, and C. Pulgarin, "Solar light and the photo-Fenton process against antibiotic resistant bacteria in wastewater: A kinetic study with a Streptomycin-resistant strain," *Catalysis Today*, vol. 313, 86-93, 2018.
[284] E. A. Serna-Galvis, E. Vélez-Peña, P. Osorio-Vargas, J. N. Jiménez, L. Salazar-Ospina, Y. M. Guaca-González, and R. A. Torres-Palma, "Inactivation of carbapenem-resistant Klebsiella pneumoniae by photo-Fenton: Residual effect, gene evolution and modifications with citric acid and persulfate," *Water Research*, vol. 161, 354-363, 2019.